THE
PHYSICAL REVIEW
A Journal of Experimental and Theoretical Physics Established by E. L. Nichols in 1893
VOL. 52, NO. 10 NOVEMBER 15, 1937 SECOND SERIES

The Radioactive Isotopes of Bromine: Isomeric Forms of Bromine 80

ARTHUR H. SNELL*
Radiation Laboratory, Physics Department, University of California, Berkeley, California
(Received August 3, 1937)

A study of the radioactive isotopes of bromine has been carried out by cross checking a number of nuclear reactions induced by bombarding the elements arsenic, selenium, bromine, krypton and rubidium with neutrons, deuterons, and electrically accelerated α-particles. The results indicate that the active isotope bromine 80 exists in two isomeric forms, from which it decays with the respective periods of 18 minutes and 4.5 hours. An example of two successive β-transitions is found to occur in the active isotopes selenium 83 and bromine 83, and a new type of transmutation is observed in which the emission of two neutrons apparently follows deuteron capture, the reaction in this case being Se^{82} $(D, 2n)$ Br^{82}. The discovery of a number of new radioactive isotopes and the identification of isotopes which carry some of the already-known activities have led to results which may be summarized in the following table of decay periods:

Arsenic 78:	65 ± 3 min.
Selenium 83:	17 ± 5 min.
Selenium 79 or 81:	57 ± 1 min.
Bromine 78:	6.4 ± 0.1 min. (positron emitter)
Bromine 80:	18.5 ± 0.5 min. and 4.54 ± 0.10 hrs.
Bromine 82:	33.9 ± 0.3 hr.
Bromine 83:	2.54 ± 0.10 hr.
Krypton:	74 ± 2 min., 4.5 ± 0.1 hrs. and 18 ± 2 hrs.
Rubidium 86 and 88:	18 ± 2 min., 18 ± 1 days (not necessarily respectively).

All of these activities emit negative electrons except bromine 78 and possibly the krypton 18-hr. activity, which is very weak. Absorption measurements for the β-rays of the bromine isotopes have given the following values for their maximum energy: Br^{78} (6.4 min.) 2.3 Mev; Br^{80} (18 min.) 2.2 Mev; Br^{80} (4.5 hrs.) 2.0 Mev; Br^{82} (33.9 hrs.) 0.4 Mev; Br^{83} (2.45 hrs.) 1.3 Mev. The emission of γ-rays accompanies the activity of Br^{78}, Br^{80} (18 min.) and Br^{82}, but is not found with Br^{80} (4.5 hrs.) nor Br^{83}.

IN 1935 Fermi and his collaborators[1] bombarded bromine with neutrons, and discovered two induced activities which emitted negative electrons, and decayed with periods of 18 min. and 4.5 hrs., respectively. It was shown chemically that these belonged to isotopes of bromine, and it was accordingly surmised that they were due to bromine 80 and 82, formed by simple neutron capture from the two stable bromine isotopes 79 and 81. Later Kourchatow, Kourchatow, Myssowsky and Roussinow[2] found that a third activity also is induced by the action of neutrons upon bromine; this activity emitted soft β-particles, and had a decay period of 35 hrs. It also was found to be chemically inseparable from bromine. This third activity was found also by Johnson and Hamblin.[3] Meanwhile Blewett[4] made a search with the mass spectrograph for a third stable isotope, the presence of which would account for the existence of one of the bromine radioactivities. His results indicated that no other isotope (excluding bromine 78, 80 and 82, which if stable would be of no assistance in explaining the extra induced activity) could be present to an extent greater than 1/3000 of the equally abundant isotopes 79 and 81. Therefore,

* 1851 Exhibition Scholar, McGill University, Montreal.
[1] Amaldi, D'Agostino, Fermi, Pontecorvo, Rasetti and Segrè, Proc. Roy. Soc. **A149**, 522 (1935).
[2] Kourchatow, Kourchatow, Myssowsky and Roussinow, Comptes rendus **200**, 1201 (1935).
[3] Johnson and Hamblin, Nature **138**, 504 (1936).
[4] Blewett, Phys. Rev. **49**, 900 (1936).

if one of the activities resulted from neutron capture by a third, rare stable isotope, the effective cross section for capture must be very large—a possibility which at the time could not be definitely excluded, in view of the large cross sections known to be possessed by a few elements for slow neutron capture. A different solution was proposed both by Kourchatow, Kourchatow, Myssowski and Roussinow and by Johnson and Hamblin, who suggested that one of the activities might be due to bromine 78, formed from bromine 79 by neutron capture followed by the expulsion of two neutrons according to the reaction $Br^{79}(n, 2n)Br^{78}$.

The present investigation was undertaken in an attempt to clarify the situation by bombarding bromine and its adjacent elements with deuterons, neutrons and artificially accelerated α-particles. It was hoped that some light could be thrown on the problem if bromine 78, 80 or 82 could be formed independently by transmutations from arsenic, selenium, krypton, or rubidium. The experiments led to the conclusion that the only satisfactory explanation of the occurrence of the three bromine activities lies in ascribing two activities to bromine 80. These are the 18-min. and the 4.5-hr. activities; the 35-hr. activity appears to belong to bromine 82. During the course of the work evidence has been obtained for two other interesting phenomena; *viz.* the emission of two neutrons following deuteron capture, and the growth of a radioactive bromine from a radioactive selenium. The latter discovery is interesting mainly insofar as it is one of the first examples of successive β-transformations found in the field of induced radioactivity.[5] Two new radio-bromines have been discovered, as well as some new active isotopes of arsenic, selenium, krypton and rubidium. The latter are merely mentioned, in anticipation of their fuller study later. These results were presented at the Washington Meeting of the American Physical Society,[6] and with respect to the isomeric forms of bromine 80 they are in agreement with the photodisintegration results briefly noted by Bothe and Gentner[7] near the conclusion of the present investigation.

Experimental

The Berkeley cyclotron[8] served as a source of the deuterons, α-particles and neutrons used in activating the various samples. Except when otherwise stated, the neutrons were made by the deuteron-beryllium reaction. The deuteron beam had an energy of about 5.5 Mev, and amounted usually to between 10 and 20 microamperes. The α-particle beam was usually easily resolvable (by means of the magnetic field control) from the deuteron beam arising from residual deuterium contamination of the helium in the accelerating chamber, and the freedom of the samples from deuteron-induced activities attested its purity. Usually it amounted to 0.2μA at 11 Mev.

Arsenic and selenium were bombarded in the metallic form, and bromine was used in the form of bromides of lead, potassium and sodium. Ammonium bromide was used for neutron activation, but is not suitable for direct deuteron bombardment; this was found to be true also for lithium bromide, but the latter has the added disadvantage of being hydroscopic. All targets were chemically pure. A quartz-fiber electroscope was used to follow the decay of the samples and also to obtain absorption curves of the β-rays. The activities of the samples are here given in the arbitrary units of "electroscope divisions per second," but their absolute activities can be roughly gauged from the estimate that a fall through one electroscope division corresponds to a total emission of about 10^4 β-particles from the sample. The sign of the emitted particles was measured with a crude but adequate magnetic deflector used in air in conjunction with the electroscope: whenever necessary the results were checked by means of the cloud chamber.

Chemical separations of arsenic, selenium, bromine and krypton were accomplished in more than one way. When a separation was required from an activated bromine sample, the sample was usually dissolved in hot water,

[5] Cork and Thornton (Phys. Rev. **51**, 608 (1937)) have recently described another case found in cadmium and indium.

[6] April 29, 1937. For abstract see Phys. Rev. **51**, 1011 (1937).

[7] Bothe and Gentner, Naturwiss. **25**, 284 (1937) (April 30), and Zeits. f. Physik **106**, 235 (1937).

[8] Lawrence and Cooksey, Phys. Rev. **50**, 1131 (1936).

to which traces of ammonium selenite and arsenious anhydride had previously been added. The selenium was then precipitated in the metallic form by the addition of hydrazine sulphate. Boiling accelerated this precipitation, and also drove off any active krypton which might have been present. The bromine was next removed as AgBr, and finally the arsenic was taken out by a sulphide separation. When selenium was activated, the procedure was slightly different, but either of the two following methods was found to be adequate: (1) the sample was dissolved in boiling, concentrated nitric acid, to which a little lead bromide and arsenic had been added, and the evolved gases were passed through an ammoniacal solution of silver nitrate. Neutralization of this solution caused the complete precipitation of the bromine in the form of AgBr. The selenium in the acid solution was then precipitated by neutralizing the solution and adding hydrazine sulphate, and the arsenic was brought down with H_2S. (2) The selenium was fused with sodium peroxide and dissolved in water. The solution was neutralized with HNO_3 and the separation proceeded as above. If the bromine fraction was required before the selenium, the solution was acidified, and the bromine was precipitated by adding $AgNO_3$. The acid prevented the simultaneous precipitation of the selenium in the form of silver selenite. In most of this work the major interest lay in the bromine and selenium fractions; when it is desired to study the arsenic fraction more closely methods of separation which are more specific for arsenic undoubtedly will have to be used.

Bromine 78

As noted above, it has been suggested that one of the three neutron-induced bromine activities might be attributed to bromine 78, formed according to the reaction $Br^{79}(n, 2n)Br^{78}$. It seemed attractive to test this hypothesis by preparing bromine 78 in a different way, and a very direct method which suggested itself was to bombard arsenic with α-particles in the hope of inducing the reaction $As^{75}(\alpha, n)Br^{78}$. (This is reaction (1) as given in the isotope scheme given of Fig. 10.) The chances of obtaining a conclusive answer to the question were unusually good, because arsenic has only one stable isotope, and unless a reaction of a novel kind were to take place, bromine 78 should be the only unstable transmutation product formed.

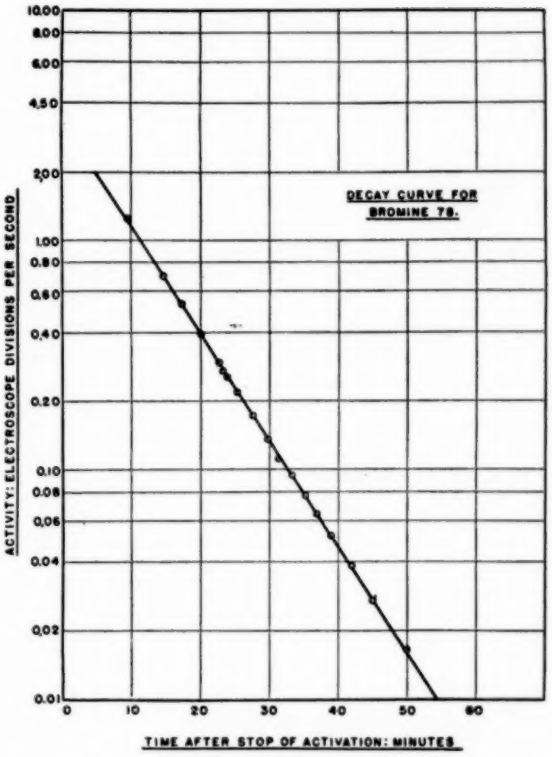

Fig. 1. Decay curve for bromine 78, made by α-particle bombardment of arsenic. Positive electrons are emitted, the decay period being 6.4 ± 0.1 minutes.

Metallic arsenic was bombarded with a beam of 0.2μA of 11 Mev α-particles. The sample showed an activity which was fairly strong compared to other activities which have been induced in this laboratory with α-particles, and it was possible to follow the decay for six half-lives. The decay curve of the sample (see Fig. 1) showed that a single radioactive isotope was formed, but unlike any of the familiar bromine activities, it had a half-life of 6.4 ± 0.1 minutes. Observation of the particles in the cloud chamber, and by means of a Thibaud magnetic focusing device, indicated that 95 percent or more were positives.[9] Absorption measurements were made, the results of which are given in Fig. 2. The end-point for transmission of the

[9] I am indebted to J. R. Richardson and E. M. Lyman for help in these experiments.

positrons is seen to occur at an absorber thickness of about 4.1 mm of aluminum. According to Feather's[10] empirical formula "range in grams per $cm^2 = 0.511$ (energy in Mev) $- 0.091$," this means that they had an upper energy limit of about 2.3 Mev. The γ-ray background indicated in the figure was due, in part at least, to the annihilation radiation from the positive electrons.

A simple chemical separation was carried out to make sure that the activity was due to an isotope of bromine. Arsenic trioxide[11] was activated in the cyclotron, and then dissolved in sodium hydroxide solution, to which a little KBr had previously been added. The solution was made slightly acid with HNO_3, and the bromine was precipitated as AgBr. All of the activity separated with the precipitate. The arsenic was later precipitated with hydrogen sulphide, and was found to be inactive; this indicated that there were a negligible number of deuterons in the beam, for otherwise, the 26-hr. period of arsenic 76 would have been present. The experiments appeared to give a definite identification of bromine 78.

Since it might be expected that bromine 78 could also be made by the transmutation $Se^{77}(D, n)Br^{78}$ (reaction 2 of Fig. 10), it was possible to carry out a confirmatory experiment by activating selenium with deuterons for a short time. Fig. 3 gives the decay curve of a bromine separation from a sample of selenium metal which had been bombarded with deuterons for 5 minutes. Subtraction of the longer-lived activity (shown later to be due to bromine 83, simultaneously made from other selenium isotopes) showed that a period of 6.2 ± 0.2 minutes was indeed present, and the emission of positive electrons was confirmed by magnetic deflection. The strengths of the activities, corrected to infinite activation time, were 1.5 div. per sec. for the short period, and 3.2 div. per sec. for the longer period.

[10] N. Feather, Phys. Rev. **35**, 1559 (1930).

[11] Oxygen has given no detectable radioactive product when bombarded with α-particles in this laboratory.

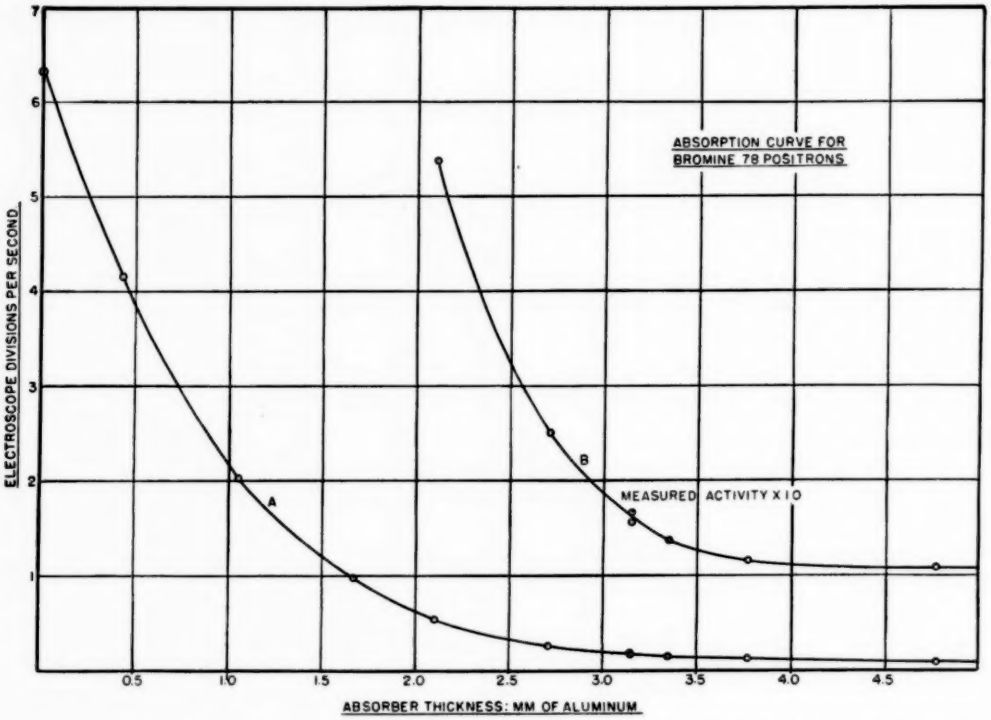

FIG. 2. Absorption curve for the positrons emitted from bromine 78. *A* is the complete curve, but in order to show the end-point clearly the flattening part of the curve has been replotted in *B*, using ten times the vertical scale of *A*. The end-point is seen to occur at an absorber thickness of about 4.1 mm of aluminum which shows that the positrons have a maximum energy of about 2.3 Mev.

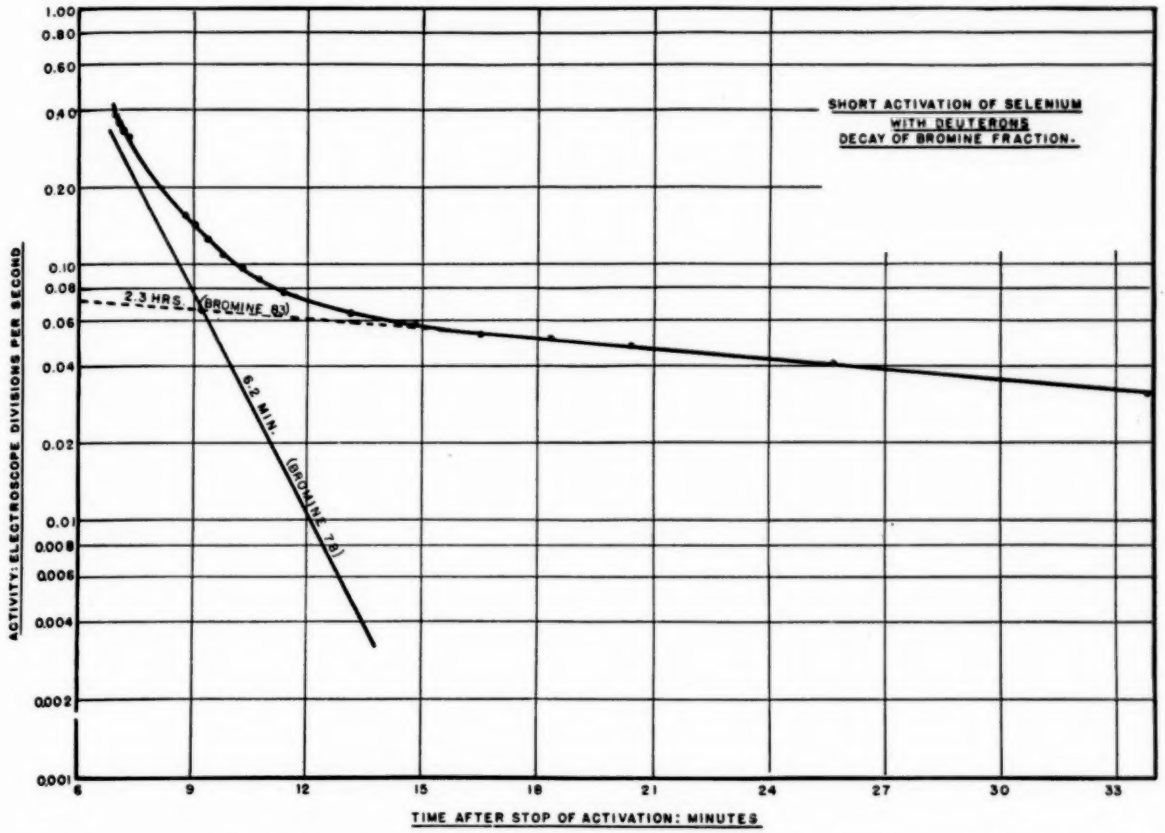

FIG. 3. Decay curve of a bromine separation from a sample of selenium which had been activated for 5 minutes with deuterons. The short periods only are shown. The 6.2-minute period belongs to bromine 78, and the 2.4-hour period to bromine 83.

During the course of this work notes from other laboratories[12, 13] have appeared, reporting the formation of bromine 78 by bombardment of bromine with energetic γ-rays (reaction $Br^{79}(\gamma, n)Br^{78}$), and with very fast neutrons (reaction $Br^{79}(n, 2n)Br^{78}$). In all of these reports the value of decay period is quoted as 5 minutes, and the sign of the emitted particles is not given. It seemed worth while to repeat the second of these experiments, to see if closer agreement could be obtained with the results of the arsenic and selenium activations just described. Accordingly, a sample of sodium bromide was activated for $3\frac{1}{2}$ minutes with neutrons from the (Li+D) reaction. The presence of a short-period activity was immediately apparent. The decay curve was followed into the 18-minute and 4.5-hour periods before the sample became too weak to measure; subtraction of these two activities then gave for the shortest period a value of 6.4 minutes. The presence of positive electrons with the short-lived activity was confirmed. The agreement of the results of all of these experiments upon bromine 78 is therefore very satisfactory. As indicated in Fig. 10, the substance has now been made in a total of four different ways, its identification is definite, and it has radioactive properties different from any of the three activities first formed by the action of neutrons upon bromine.

[12] Heyn, Nature **139**, 842 (1937).
[13] Chang, Goldhaber and Sagane, Nature **139**, 962 (1937).

BROMINE 83

The decay curve of Fig. 3 has already been referred to; it was taken from a bromine separation from selenium activated for a short time with deuterons. In addition to the short period attributed to bromine 78, a period of about $2\frac{1}{2}$ hrs. is seen to be present. This bromine activity has been studied more closely, and

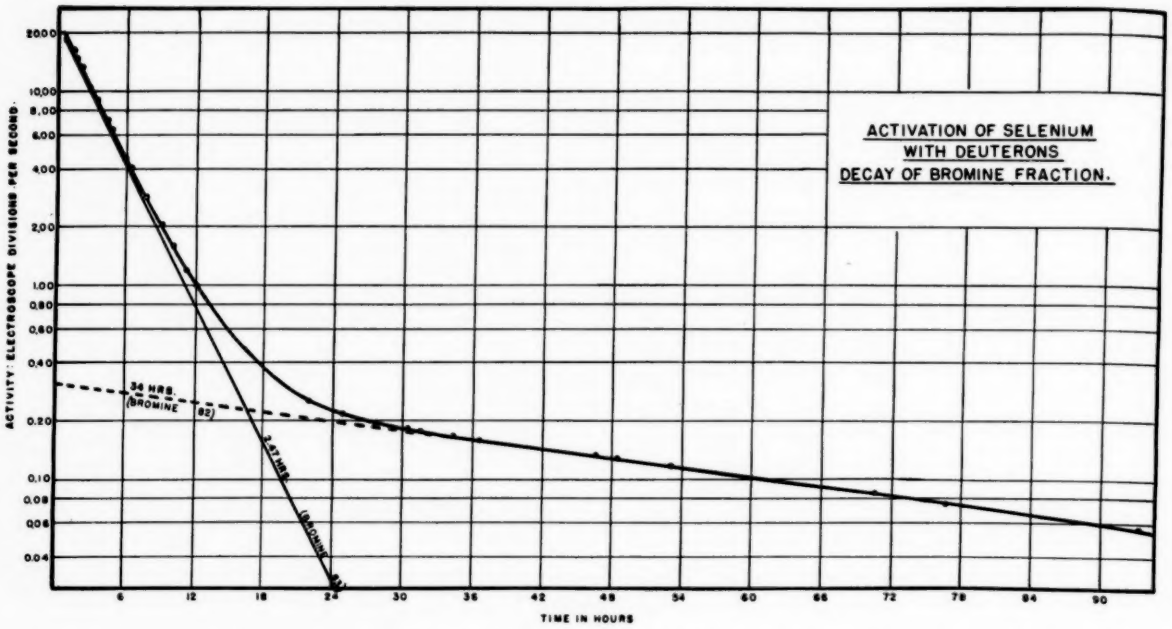

FIG. 4. Decay curve of bromine separation from selenium activated with deuterons; long periods. The 2.4-hr. period of bromine 83 shown in Fig. 3 reappears here, and is accompanied by the 34-hr. period of bromine 82.

Fig. 4 gives the decay curve of a bromine separation from selenium which had been given a much longer bombardment with deuterons (beam, 4μA; time of exposure, 1 hr.). The short bromine 78 activity had disappeared by the time this sample reached the electroscope, and therefore does not show in this decay curve. However, two other activities are present; their decay periods are 2.45$\pm$0.10 hrs. and 34 hrs., and their saturation strengths are, respectively, 92 and 15 divisions per sec. The 34-hr. period is one of the three original neutron-induced activities; its presence here has special significance which will be referred to later. The 2.45-hr. activity is new. It is accompanied by the emission of negative electrons, with no γ-rays.

Figure 5 gives absorption curves taken from one of these samples. In this figure, curve *A* includes the effects due to both the 2.45-hr. and the 34-hr. activities; the latter is partly responsible for the very rapid initial fall of the curve, because its β-particles are low in energy, and it also contributes the relatively weak γ-ray background. Curve *B* shows the absorption of the high energy β-particles in greater detail. To obtain this curve, the 34-hr. γ-ray effect was measured a day later, corrected for decay, and subtracted from the electroscope readings. The differences were then corrected for the decay of the sample while the absorption measurements were being taken, on the assumption of a half-life of 2.45 hrs. These differences were very small, and were multiplied by 100 for the purpose of plotting. As the 34-hr. β-rays are absorbed by less than a millimeter of aluminum (see Fig. 8), curve *B* applies to the β-rays of the 2.45-hr. activity alone. The limit of absorption occurs at about 2.1 mm of aluminum, and this corresponds to an upper energy limit of 1.3 Mev, according to Feather's rule.

The existing isotopes of selenium and bromine leave bromine 83 as the only possible carrier of this new activity. Since it is unlike any of the bromine activities so far discovered, it is not due to bromine 78, 80 or 82, and since it emits negative electrons it probably is not due to bromine 77. It is apparent that if this identification is correct, then there is a possibility that the substance was being made in two ways:

(a) By direct transmutation, according to the reaction Se^{82} (D, n) Br^{83};

(b) By growth from a hitherto unknown selenium 83; i.e., the bromine 83 would be the second member in a pair of successive β-emitters, the reactions being Se^{82} (D, p) Se^{83}, $Se^{83} \rightarrow Br^{83} + \epsilon^-$, $Br^{83} \rightarrow Kr^{83} + \epsilon^-$.

There was evidence for the second process in the decay curves of the selenium fractions obtained in the experiments, and it appeared that the selenium 83 had a half-life of 17 ± 5 minutes. The two following experiments were then carried out, which established without doubt the presence of a pair of successive β-transformations.

1. Selenium was activated with deuterons, and selenium, bromine and arsenic were separated chemically. Decay readings were started on the bromine and arsenic fractions, and part of the selenium. The remainder of the selenium was thoroughly washed, and 3 hours later it was redissolved, and bromine was again extracted from it. This second extraction showed a weak activity, which decayed with the expected period of 2.4 hrs.

2. Selenium was activated for one hour with *slow neutrons*. There was therefore no possibility of a direct transmutation to bromine, and selenium 83 was made (along with some other active selenium isotopes) initially unaccompanied by bromine 83. The selenium was dissolved, and three fractions were taken from the solution, in the following order: (1) part of the selenium, immediately after activation; (2) the remainder of the selenium, half an hour later; (3) bromine, immediately after (2).

The decay curves of the three fractions are given in Fig. 6. The bromine was active, and showed the expected decay period. The selenium curves showed a mixture of periods, due mostly to other selenium isotopes. (Other experiments have shown that none of these has a period as long as 2.45 hrs. The strongest and longest-lived selenium activity induced by neutrons or deuterons has a half-life of 57 minutes.) The fact that the two curves are not parallel shows that the selenium samples were not identical in radioactive composition. The second sample had so much less of the long-lived constituent that its decay curve fell quickly and crossed that for the first sample. This is in agreement with the supposition that the 2.45-hr. activity was growing in the selenium samples after their separation, and was much stronger in the first sample

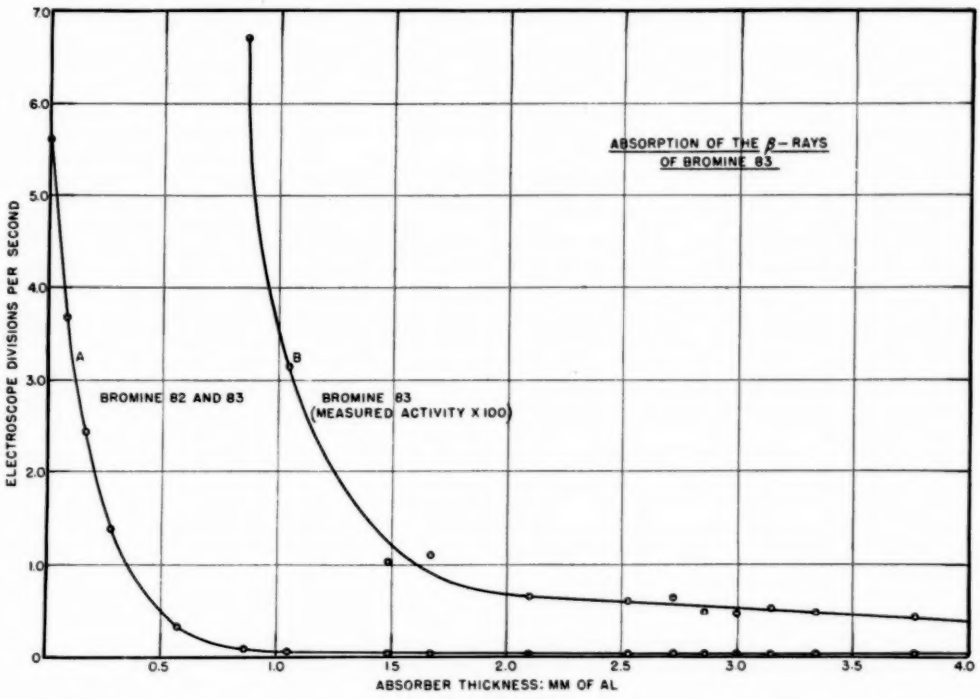

FIG. 5. Absorption curves for the β-rays of bromine 83. Curve *A* shows the absorption of the radiations from a mixture of bromine 83 (2.4 hrs.) and bromine 82 (34 hrs.); the γ-ray background is due to the latter activity. Curve *B* gives the absorption of the high-energy particles of bromine 83 alone, for the γ-ray effect has been subtracted, and the bromine 82 β-rays do not penetrate this far into the aluminum. Note that the true ordinates for curve *B* are 1/100 of the figures given at the left.

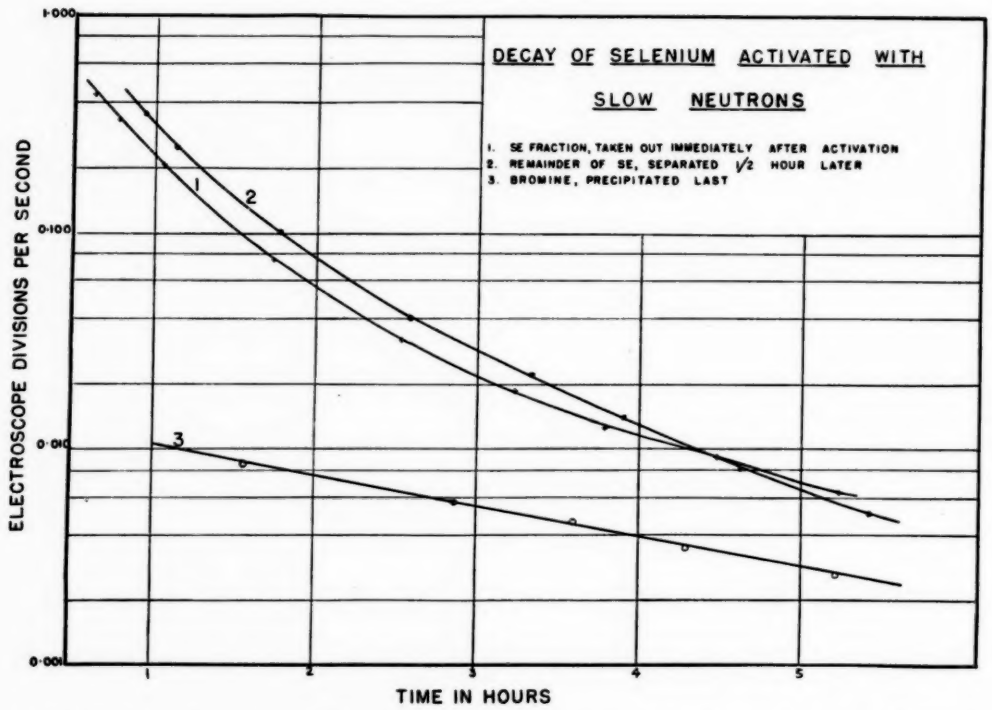

FIG. 6. These decay curves show that active bromine 83 (2.4 hrs.) results from the decay of active selenium 83 (17 min.). The selenium was activated with slow neutrons, and therefore the fact that the bromine fraction was active (curve 3) shows that a double β-transition must take place. The rate of decay shown by curve 3 corresponds to a half-life of 2.4 hrs. The selenium decay curves 1 and 2 slope off toward the 2.4-hr. bromine 83 period, because this substance has grown in the samples, and it lasts longer than any of the selenium active isotopes. The long period (bromine 83) is stronger in curve 1 than in curve 2, because the former sample, being removed first, had in it much more selenium 83 (17 min.) from which the bromine 83 subsequently grew.

because there was more selenium 83 present in the mother liquor when the first sample was taken out. The absolute activity of all of these samples was much less than that obtained by deuteron activation.

The establishment of these two successive β-transformations leaves no doubt as to the correctness of attributing the 2.45-hr. activity to bromine 83. Evidently this isotope is not connected in any way with the three original bromine activities, and if a third stable isotope is responsible for one of them, one can now say that it must be lighter than bromine 77 or heavier than bromine 83.

BROMINE 80 AND 82

A substantial contribution to the study of the bromine activities resulted from the activation of bromine with deuterons. The element was bombarded in the form of various bromides, and three activities resulted which decayed with the same half-lives as result from slow neutron activation. All three activities again followed the chemistry of bromine, and the absorption curves of the β-rays for each activity were the same as those obtained from neutron-activated samples. Therefore it seems quite definite that the same three activities are induced by deuterons as are induced by neutrons. The values of the decay periods, taken from a selection of the best decay curves obtained from both neutron- and deuteron-activated samples, are respectively 18.5 $\pm$0.5 minutes, 4.54$\pm$0.10 hours, and 33.9$\pm$0.3 hours. Since the only known (or easily conceivable) reaction whereby bombardment of bromine with 5 Mev deuterons would give active bromine isotopes is $Br^{79, 81}(D, p)Br^{80, 82}$ (both of which would probably take place according to the process suggested by Oppenheimer and Phillips[14]) these results joined with the results

[14] J. R. Oppenheimer and M. Phillips, Phys. Rev. **48**, 500 (1935).

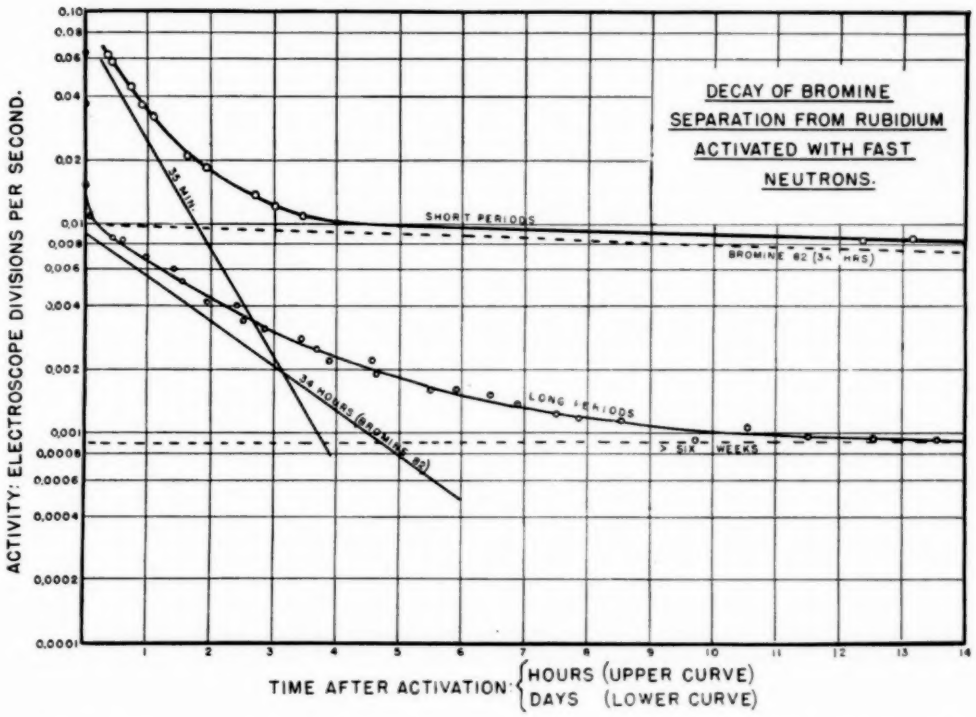

FIG. 7. Decay curve for bromine separation from rubidium nitrate activated for 4 hours with (Li+D) neutrons. The sample was weak, but three decay periods were present, *viz.* 35±3 min., 34±3 hrs. and a long period of more than 6 weeks. The second of these is one of the periods found in neutron and deuteron activated bromine, and its presence here identifies it as belonging to bromine 82 (reaction 12, Fig. 10). Whether or not one of the others belongs to bromine 84 is not yet certain, because of the possible presence of impurities.

of neutron activation in giving a very strong indication that all three activities must arise from the two isotopes bromine 80 and 82. The assumption of the existence of a very rare third stable isotope must now be finally abandoned, because the activities were all strong in the deuteron-activated samples; furthermore, tests with activation by neutrons of various energies have shown that none of the activities is a specifically slow neutron effect.

There remained the problem of finding how the three activities are distributed between the two active isotopes. In the last section it was mentioned that the 34-hour period was present in the bromine separation from selenium activated with deuterons, and the fact that it was unaccompanied by either the 18-minute or the 4.5-hour period might be taken as evidence that it alone belongs to one active isotope. More direct evidence was obtained, however, in two different ways, *viz.* by bombarding rubidium with fast neutrons, and by a study of the relative strengths of the three bromine activities when induced under varying conditions.

Since rubidium has two isotopes, with mass-numbers 85 and 87, it was expected that bombardment with fast neutrons might lead to the expulsion of an α-particle, giving bromine 82 and 84 according to the reactions $Rb^{85,\,87}(n, \alpha)Br^{82,\,84}$. (The first of these is reaction 12 in Fig. 10.) In order to test this possibility, a sample of about 25 grams of rubidium nitrate was given an intense bombardment with fast neutrons. After activation, the sample was dissolved in warm water, a drop of bromine water was added, and AgBr was precipitated from the solution by adding silver nitrate. Only an exceedingly weak activity resulted from bombardments of this kind when (Be+D) neutrons were used, but when the experiment was repeated using (Li+D) neutrons, the activity in the bromine fraction was strengthened sufficiently to enable the decay to be followed with some certainty. The decay curve (Fig. 7) shows a short period of 35±3

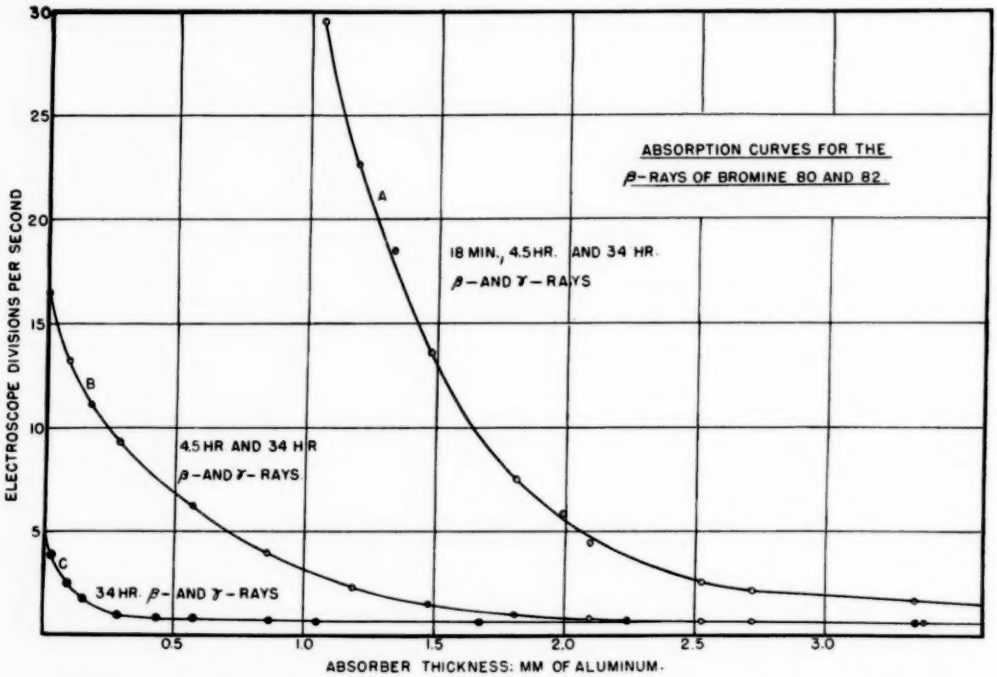

FIG. 8. Absorption curves showing the changes in the character of the radiations emitted by an aging deuteron activated bromine sample. Curve *A* was taken immediately after activation, when the 18-minute period accounted for most of the activity. Curve *B* was taken four hours later, when only the 4.5-hour and the 34-hour activities were present. Curve *C* was taken when only the 34-hour activity was left, and it has been corrected back to the time of curve *B*. It will be noticed that the 34-hour activity accounts for all of the γ-ray ionization present after the 18-minute activity had decayed.

minutes, an intermediate period of 34 ± 3 hours, and a long-lived, very weak activity with a decay period of at least six weeks. For this discussion the presence of the 34 ± 3 hour activity is very important; the other two will be considered later. Here the 34-hour bromine activity has apparently been again produced independently of the 18-minute and 4.5-hour activities, and the manner in which it was made shows that it belongs to bromine 82, and not to bromine 80. Although the sample was weak, a few points on the absorption curve of its β-rays were obtained while it was decaying with the 34-hour half-life, and the agreement with the absorption curve (Fig. 8, curve *C*) for the long period particles from activated bromine was excellent.

The study of the relative strengths of the three activities when induced in bromine by different methods lent support to the ascription of the 34-hour activity to bromine 82, and it also gave good evidence for attributing both the 18 minute and the 4.5-hour activities to bromine 80.

In these experiments the active samples were dissolved after activation, and the bromine was precipitated as AgBr. The precipitate was then spread in a thin layer upon a piece of metal, and this type of source was used for the electroscope measurements. It was important to make the samples as uniform as possible; otherwise wide variations in the self-absorption of the β-rays in the source might occur, because of the great difference between the energy of the 34 hour β-particles and those emitted with the shorter periods. The conditions of activation of the samples and the relative strengths of the

TABLE I. *Conditions of activation and relative strengths of the three activities.*

Details of Activation			Relative Intensities		
Sample	Agent	Substance surrounding sample	18 min.	4.5 hr	34 hr.
1	(Be+D) neutrons	Paraffin	2.3	1	0.6
2	(Be+D) neutrons	Cadmium	2.7	1	0.8
3	(Li+D) neutrons	Boron	1.7	1	0.3
4	(Li+D) neutrons	KBr and cadmium	0.8	1	0.2
5	Deuterons	—	2.1	1	1.6

three activities are given in Table I. The intensities have been corrected to infinite activation time, and to facilitate comparisons the strength of the 4.5-hour period in each sample has been taken as unity.

The relative strengths of the 18 minute and 4.5-hour activities do not show wide variations except in the case of sample 4, which was surrounded by KBr. Here the 18-minute activity was weaker, probably because of the absorption in the KBr of the resonance neutrons known to exist for this activity,[15] some of which undoubtedly were present about the cyclotron. (Nothing is known about the existence of resonance levels for the other two periods; the results of sample 4 must therefore be treated with caution.) The variations in the intensities of the 34-hour activity are greater, and extend over a factor of eight. Deuterons (sample 5) emphasize this activity to a great extent, but no reason for this is as yet known. On the other hand the very fast neutrons from the (Li+D) reaction reduce its relative intensity by a factor of about 3 (samples 3 and 4) as compared to the (Be+D) neutrons (samples 1 and 2). This is significant, because neutrons having these high energies are known to be effective in expelling two neutrons from many nuclei (for bromine the reactions would be $Br^{79,\,81}(n, 2n)Br^{78,\,80}$), and bromine 81 nuclei struck by such neutrons would increase the numbers of active bromine 80 nuclei at the expense of bromine 82. Even though unknown resonance effects may have influenced the results of sample 4, the relative intensities of sample 3 therefore point to the conclusion that both of the shorter-lived activities belong to bromine 80. In this respect the evidence of Bothe and Gentner[7] is conclusive in showing that neither of the shorter periods belongs to bromine 82, because they both appear in the photodisintegration of bromine according to the reactions $Br^{79,\,81}(\gamma, n)Br^{78\ 80}$; moreover, the remote possibility that one of them belongs to bromine 78 must be excluded for many reasons given in this paper.

An experiment was performed to test the effectiveness of group *C* (thermal-energy) neutrons in inducing the three activities in bromine. Two equal and similarly-shaped samples of lead bromide were exposed simultaneously to the action of neutrons by placing them side by side between two large paraffin blocks. One of the samples was wrapped in sheet cadmium, and the other was simply wrapped in paper. An exposure lasting half an hour induced activities with the following measured intensities, corrected to the time of stop of activation:

Period	*Cadmium-wrapped Sample*	*Sample without Cadmium*
18 min.	14.5 div./sec.	51 div./sec.
4.5 hrs.	0.62	2.4
34 hrs.	0.04	0.12

It is seen that the cadmium reduced the intensity of all three activities by a factor of about 3.5. It can be concluded that all three bromine activities can be induced by the action of neutrons having thermal energies.

The assumption of the existence of the two isomeric forms of bromine 80 is seen to explain all of these results and there seems to be no contradictory experimental evidence whatever. Until recently, the only definitely established example of nuclear isomerism has been the case of the natural radioactive substances UX_2 and UZ, both of which, according to Hahn,[16] must belong to the isotope of atomic number 91 and mass 234. With the current progress in the study of the induced radioactivities, however, there are already indications[17] that the phenomenon may be quite common. Weizsäcker[18] has recently given some theoretical considerations which indicate that it is possible to understand the occurrence of lifetimes of minutes or hours for low lying excited states in nuclei, without having to assume unreasonably large angular momentum differences from the ground level. Considerations of this kind are of course intimately connected with the energies of the β- and γ-rays emitted by the pair of nuclear isomers.

The β- and γ-rays of bromine 80 and 82

Although an accurate study of the radiations emitted by bromine 80 has not yet been made, absorption measurements made with the electroscope have given some information about their

[15] von Halban and Preiswerk, J. de phys. **8**, 29 (1937); Goldsmith and Rasetti, Phys. Rev. **50**, 328 (1936).

[16] Hahn Zeits. f. physik. Chemie **103**, 461 (1922).

[17] Meitner, Hahn and Strassmann, Zeits. f. Physik **106**, 249 (1937), and McMillan, Kamen and Ruben, Phys. Rev. **52**, 375 (1937).

[18] Weizäcker, Naturwiss. **24**, 813 (1936).

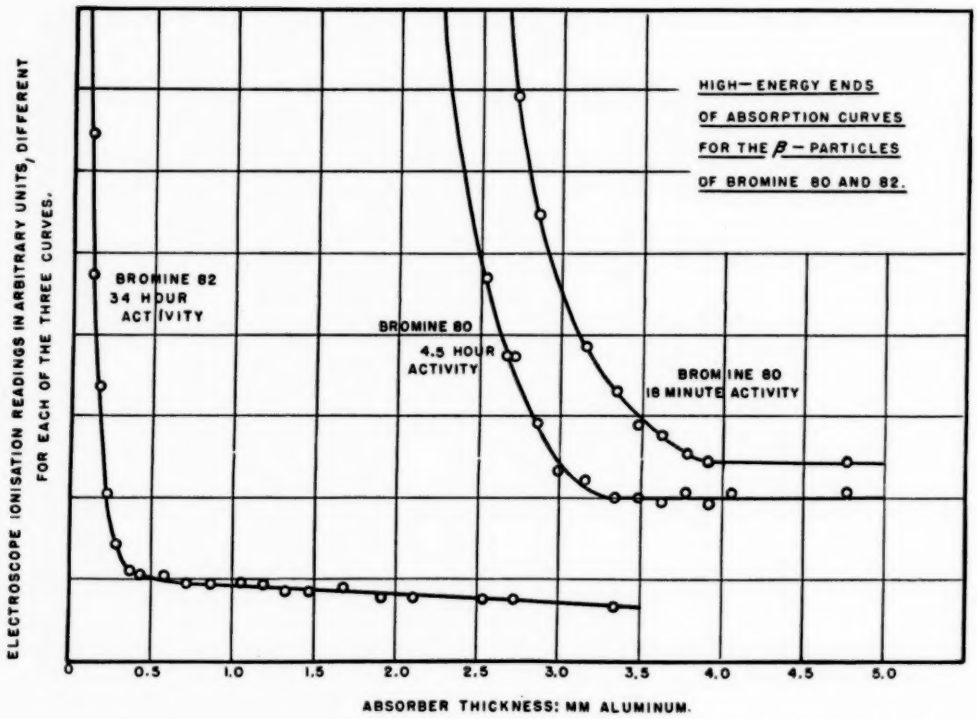

FIG. 9. The high energy ends of β-ray absorption curves taken from three different bromine samples, activated in such a way as to separate the 18-min., 4.5-hr. and 34-hr. activities. The curves are not to be compared with one another with respect to the scale of ordinates, and are intended only to show the positions of the end-points for the penetration of the β-rays. A slight difference is apparent in the energies of the β-rays emitted by the two isomeric forms of bromine 80.

general character which is worth reporting here. The 34-hour activity of bromine 82 was always present in the activated bromine samples, and it therefore came quite naturally under consideration at the same time.

The γ-ray decay curves of the neutron and deuteron activated samples were obtained with the electroscope by interposing sufficient absorber to stop all the β-rays. These decay curves showed a direct change from the 18-minute period to the 34-hour period, indicating that no appreciable γ-rays are emitted by the 4.5-hour activity. As measured in the electroscope, the γ-ray ionization arising from the 18-minute activity is weak, and that of the 34-hour activity is strong. Absorption measurements of the 18-minute γ-rays have shown that they are low in energy (undoubtedly less than 0.5 Mev) while the 34-hour γ-rays are more energetic. Kourchatow, Kourchatow, Myssousky and Roussinow[2] have given the value 0.65 Mev for the energy of the 34-hour γ-rays.

Negative electrons are emitted by the three activities of bromine 80 and 82. No positives have been observed. Absorption measurements of the β-rays, taken at different times during the decay of the sample, are reproduced in Fig. 8. These curves were taken from a sample of lead bromide which had been activated for 70 minutes with deuterons. The readings of curve *A* were obtained immediately after the stop of activation, and the curve shows the absorption of the β-rays (due predominantly to the 18-minute activity) together with a background which originates from a combination of the 18-minute and the 34-hour γ-rays. While the readings were being taken, the sample was decaying with a half-life of very nearly 18 minutes, and the corrections for decay were made on this basis. The activity for zero absorber was 110 divisions per second. Curve *B* was taken four hours later, after the 18-minute β- and γ-rays had disappeared, and accordingly shows a combination of the effects due to the 4.5-hour and the 34-hour periods. Curve *C* was taken 36 hours later still, and gives the absorption of the 34-hour

radiations alone. The experimental points of curves B and C were both corrected to a time four hours after the stop of activation, assuming decay periods of 4.5 hours and 34 hours, respectively; the two curves can therefore be compared directly without further allowance for decay.

It is seen that nearly all of the β-ray ionization of curve B is due to the 4.5-hour activity, but the γ-ray background arises entirely from the 34-hour period. In curve C the softness of the 34-hour β-rays is quite apparent, and this accounts partly for the fact that the β-ray ionization is unusually weak in comparison with that due to γ-rays, for the sample used in these measurements was quite thick. To obtain a better comparison of the relative strengths of the β- and γ-ray ionization, an active silver bromide precipitate was on one occasion spread thinly upon a piece of metal, and an absorption curve for the 34-hour activity was taken from this source. The ratio of the $(\beta+\gamma)$-ray ionization (i.e., the ionization measured with zero absorber) to that arising from the γ-rays alone was found with this sample to be 10. This is still small compared to the values obtained for many other radioactive isotopes, (values of about 50 for this ratio are more usual) and it may indicate that bromine 82 emits more than one γ-quantum per β-particle.

The high energy ends of the β-ray absorption curves for the three activities were examined more closely, in order to learn more about the maximum energies of the respective groups of β-rays. For this purpose it was necessary to isolate each of the three activities fairly completely from the others. This was accomplished by studying the 18-minute activity from samples which had been given a short slow neutron activation (lasting about 3 minutes), the 4.5-hour activity from longer slow neutron activations, and the 34-hour activity from either neutron or deuteron activated samples. Deuteron activation was not used for studying the shorter lived activities, because it increases the relative strength of the long period activity to an inconvenient extent. The high energy ends of three such absorption curves are reproduced in Fig. 9. They have been plotted to an enlarged vertical scale for the purpose of showing the end-points clearly. Since these curves were taken from three different samples, they are not to be compared with one another except with regard to the positions of the end-points of transmission of the β-rays. These end-points are given in Table II, together with the corresponding maximum energy of the β-rays as obtained from Feather's formula.

For purposes of comparison the values obtained by Alichanow, Alichanian and Dzelepow[19] with the magnetic spectrograph have been added, and also the value obtained by Kourchatow, Kourchatow, Myssowsky and Roussinow[2] for the maximum energy of the bromine 82 β-rays. The agreement in the figures is moderately good, but fails in what is perhaps the most interesting detail; *viz.* the maximum energies of the two groups of bromine 80 β-rays. The absorption measurements indicate that the 18-minute β-rays are slightly more energetic than the 4.5-hour β-rays and the clearness of this result may be judged from the curves of Fig. 9. However, Alichanow, Alichanian and Dzelepow failed to find this difference. Further measurements of both the β-rays and the γ-rays of the bromine activities are needed, and it is hoped that they soon will be obtained. As far as the present information goes, however, it is in agreement with the picture of a low lying metastable state in bromine 80, from which the nuclei decay with a half-life of 18 minutes by the emission either of a β-particle or a low energy γ-quantum, together with a ground level from which decay

[19] Alichanow, Alichanian and Dzelepow, Physik. Zeits. Sowjetunion **10**, 78 (1936).

TABLE II. *End-points of β-ray transmission from radioactive bromine together with the corresponding maximum energy as obtained from Feather's formula.*

Active Isotope	Decay Period	End-point of Transmission of β-rays	Maximum Energy of β-rays	Alichanow, Etc.	Kourchatow, Etc.
Bromine 80	18 min.	3.9 mm of Al	2.2 Mev	2.00±0.10 Mev	—
"	4.5 hrs.	3.4 " " "	2.0	2.05±0.10	—
Bromine 82	34 hrs.	0.5 " " "	0.4	0.85±0.20	0.6 Mev

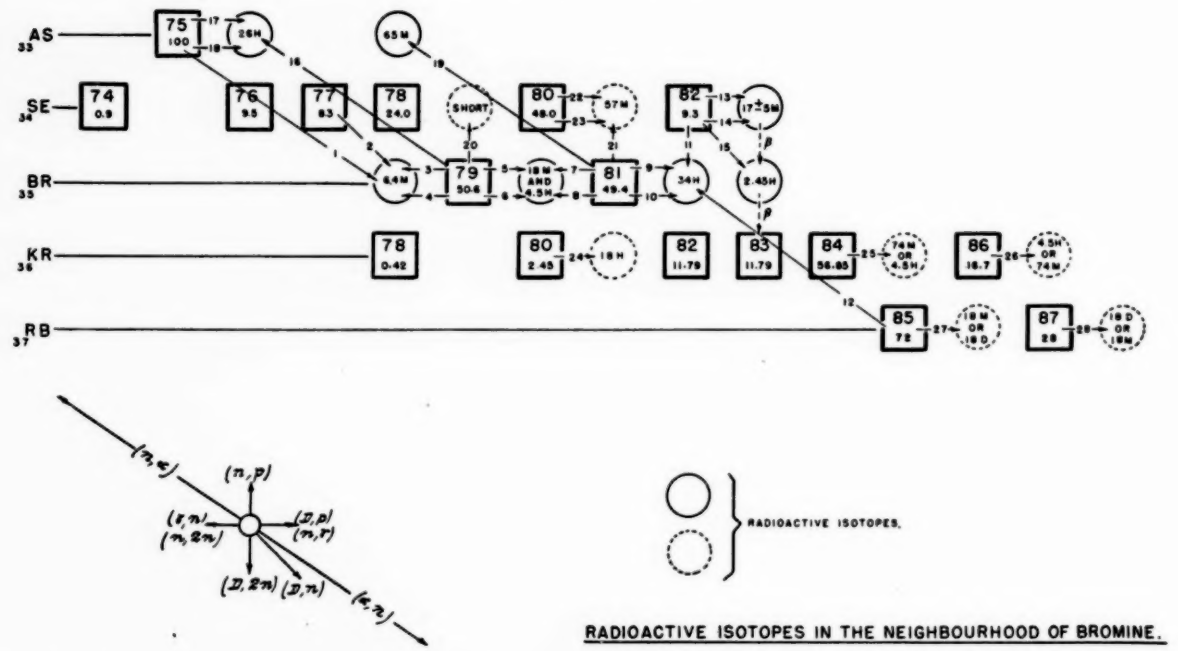

FIG. 10. This diagram gives a summary of all of the transmutations described in this paper. For convenience in reading, a square array has been chosen in which atomic number is plotted against atomic mass. The stable isotopes (squares) are given with their percentage abundance in small figures. Radioactive isotopes are given in circles, which are dotted when there is still some ambiguity as to their exact identification. The numbered arrows indicate transmutations which have been observed, and the reactions describing them are as follows:

1. $As^{75}(\alpha, n)\ Br^{78}$
2. $Se^{77}(D, n)\ Br^{78}$
3. $Br^{79}(n, 2n)\ Br^{78}$
4. $Br^{79}(\gamma, n)\ Br^{78}$ (Bothe and Gentner)
5. $Br^{79}(n, \gamma)\ Br^{80}$
6. $Br^{79}(D, p)\ Br^{80}$
7. $Br^{81}(n, 2n)\ Br^{80}$
8. $Br^{81}(\gamma, n)\ Br^{80}$ (Bothe and Gentner)
9. $Br^{81}(n, \gamma)\ Br^{82}$
10. $Br^{81}(D, p)\ Br^{82}$
11. $Se^{82}(D, 2n)\ Br^{82}$
12. $Rb^{85}(n, \alpha)\ Br^{82}$
13. $Se^{82}(n, \gamma)\ Se^{83}$
14. $Se^{82}(D, p)\ Se^{83}$
15. $Se^{82}(D, n)\ Br^{83}$
16. $Br^{79}(n, \alpha)\ As^{76}$
17. $As^{75}(n, \gamma)\ As^{76}$
18. $As^{75}(D, p)\ As^{76}$ (Thornton)
19. $Br^{81}(n, \alpha)As^{78}$
20. $Br^{79}(n, p)\ Se^{79}$
21. $Br^{81}(n, p)\ Se^{81}$
22. $Se^{78, 80}(n, \gamma)\ Se^{79, 81}$
23. $Se^{78, 80}(D, p)\ Se^{79, 81}$
24. $Kr^{80}(D, p)\ Kr^{81}$
25. $Kr^{84}(D, p)\ Kr^{85}$
26. $Kr^{86}(D, p)\ Kr^{87}$
27. $Rb^{85}(n, \gamma)\ Rb^{86}$
28. $Rb^{87}(n, \gamma)\ Rb^{88}$

by β-emission takes place with a half-life of 4.5 hours. The product nucleus in each case is krypton 80, and presumably it is formed in its ground state.[20]

BROMINE 75, 77 AND 84

It might be expected that deuteron bombardment of selenium would lead to the formation of bromine 75 and 77 from selenium 74 and 76, by the (D, n) type of reaction. However, neither of these isotopes has been found. That bromine 75 was not observed probably was due to the rareness of selenium 74. The absence from the decay curves of any activity which might be attributed to bromine 77 indicates that either (1) its half-life is less than a minute or greater than roughly two months (a very long lived activity has not been looked for); or (2) selenium 76 is not so susceptible to the (D, n) transmutation as are some of the other selenium isotopes.

The bombardment of rubidium with fast neutrons should yield bromine 84 in addition to bromine 82, according to the reactions $Rb^{85, 87}(n, \alpha)Br^{82, 84}$. As a matter of fact, when this experiment was tried the decay curve (Fig. 7) of the bromine separation did show activities other than that of bromine 82, but it is not yet certain whether either of them belongs to bromine 84. A 35 ± 2-minute activity is present, but it might be the 37-minute activity due to

[20] Alternatively, one may account for the experimental results by supposing that the 18-min. β-rays originate in a transition from a metastable state in bromine 80 to an excited state in krypton 80, which then emits the 18-min. γ-ray in going to the ground level. The 4.5-hr. β-rays would correspond to a transition from normal bromine 80 to the ground level of krypton 80, and the energy of excitation of the metastable state of bromine 80 would be given by the sum of the energy of the 18 min. γ-ray and the 0.2 Mev difference in energy of the two β-rays.

chlorine 36 or 38, made from possible potassium impurity in the rubidium by the reactions $K^{39, 41}(n, \alpha)Cl^{36, 38}$—the chlorine then separating chemically with the bromine. A long period also is present, but there is a possibility here of confusion with the 18-day rubidium activity, since it is conceivable that the chemical separation was not complete.* Larger samples of rubidium and stronger neutron activations will greatly facilitate a closer study of these possibilities.

Formation of Bromine 82 from Selenium

As has already been mentioned, a 34±1-hr. activity was present in the bromine separation from selenium activated with deuterons. It occurred in addition to the shorter lived activities of bromine 78 and 82, and it could be made sufficiently strong to follow for more than a week. Its β-ray absorption curve was obtained and found to be identical with that of the bromine 82 34-hr. period as given in Fig. 8. The γ-rays also were present. Apparently, therefore, bromine 82 can be made by deuteron bombardment of selenium.

Reference to the scheme of stable isotopes (Fig. 10) shows, however, that none of the reactions heretofore encountered in nuclear transmutations can account for a transmutation yielding this product. A reaction of the common type "deuteron in, neutron out" will indeed lead from selenium to bromine (as probably occurs in the case of bromine 78 and 83) but such a reaction is of no assistance here because a stable selenium isotope of mass 81 would be required, and this isotope does not exist in sufficient abundance to be detected by the mass-spectrograph. Radiative capture of the deuteron according to the reaction $Se^{80}(D, \gamma)Br^{82}$ would appear to be a possible solution according to a naïve inspection of the isotope scheme, but for theoretical reasons such a process must be regarded as very improbable. The bromine 82 nucleus would be formed with an excitation energy about twice as great as the individual binding energies of the constituent protons and neutrons, and this is regarded as an excessive amount of energy to be thrown off as γ-radiation. A more satisfying explanation, first suggested to the writer by Professor Bohr, lies in the supposition that selenium 82 captures the deuteron and emits two neutrons (reaction $Se^{82}(D, 2n)Br^{82}$, shown as number 11 in Fig. 10). No other reaction of this type has so far been established, but the comparative ease with which neutrons can be expelled from the nucleus has been demonstrated by current experiments upon disintegration with γ-rays and neutrons of high energy, and it is in good accordance with the Bohr picture of nuclear transmutation. The fact that the apparent reaction $Se^{82}(D, 2n)Br^{82}$ is observed to take place unaccompanied by the parallel reaction $Se^{80}(D, 2n)Br^{80}$ (which presumably would yield the 18-min. and 4.5-hr. bromine activities) may be understood from the lower binding energy of the neutrons in the heavier isotopes, and the consequent greater facility with which the extra neutron could escape.

Other Transmutations

Although primarily intended to be a study of the radioactive isotopes of bromine, this work has inevitably spread to the neighboring elements arsenic, selenium, krypton and rubidium. Some new activities have been discovered in these elements, and they are graphically summarized in Fig. 10 together with the transmutations by which they have been produced. Only a few of these new isotopes have yet been studied closely, but it might be well to describe briefly how they were found. Except for bromine 78 (and possibly one krypton isotope) all of these activities are accompanied by the emission of negative electrons.

Reactions 1 to 15 of Fig. 10 have already been described in the paper.

Reactions 17 and 18 are taken from the original work of Fermi[1] and Thornton.[21]

Reactions 16, 19, 20 and 21 resulted from an activation of a large sample of ammonium bromide with (Be+D) neutrons. After a chemical separation, the arsenic fraction showed activities having decay periods of 26±1 hours and 65±3 minutes, with intensities of 0.53 and

* *Noted added October 9:* Further aging of the samples has shown that the decay period is greater than six weeks, so that this possibility must be ruled out.

[21] R. L. Thornton, Phys. Rev. **49**, 207 (1936).

0.05 divisions per sec. respectively. (All intensities of activities given here have been corrected to infinite time of activation.) The first of these is the familiar period of arsenic 76, and it probably originates from bromine 79, being made by α-particle expulsion according to reaction 16. The second activity is new, and it has been attributed to arsenic 78, presumably made by a parallel reaction (number 19) from the other bromine isotope. It has not been cross checked by an independent transmutation. The selenium fraction showed a clear-cut 57 ± 1 minute activity (intensity 1.3 divisions per sec.) with no evidence of a longer period; there was, however, a slight indication of a shorter period of less than 5 minutes having an intensity of 0.1 divisions per sec. or less. These two active isotopes probably are made from the two stable bromine isotopes by the (n, p) reactions 20 and 21. The 57-minute period has been observed by Heyn,[12] and has been found by the writer in samples which have been activated with deuterons and slow neutrons (reactions 22 and 23). It is not yet certain whether it belongs to selenium 79 or to selenium 81.

Reactions 24, 25 and 26 resulted from activations of krypton gas with deuterons. Activities with decay periods of 74 ± 2 minutes (intensity 3.6 divisions per sec.) 4.5 ± 0.1 hours (2.1 divisions per sec.) and 18 ± 2 hours (0.018 divisions per sec.) were observed, and they can be considered to be identified as belonging to krypton isotopes, because any atomic rubidium or bromine formed in the bombardment would have stuck to the copper walls of the container or to the inside of the slender copper tubing used in handling the gas. The weakness of the 18-hour activity has so far prevented an observation of the charge of the emitted particles, and it may indicate that the activity belongs to krypton 79 or 81, which would be made from one of the rarer isotopes 78 or 80. This supposition is supported by the observation that the strong 74-minute and 4.5-hour activities emit negatives, which shows that they probably belong to krypton 85 and 87. The appearance of a decay period of 4.5 hours in krypton as well as in bromine appears to be fortuitous, because an absorption curve of the krypton 4.5-hour β-rays has shown that they are much lower in energy than the bromine 4.5-hour β-rays.

Reactions 27 and 28 refer to the activation of rubidium nitrate by neutrons. The two activities with 18 ± 2 minute and 18 ± 1 day half-lives appeared in the chemically separated rubidium fraction; they probably belong to rubidium 86 and 88, but lack of cross checks has as yet prevented any closer identification. The strengths of the activities in the small portion of the sample which was used for the electroscope measurements were: for the 18-minute activity, 0.77 divisions per sec., and for the 18-day activity, 4.2 divisions per sec. A weak rubidium activity with a period of "about 100 minutes" has been mentioned in the literature;[22] probably it is the 18-minute period found here with stronger samples. Experimentally, there is no possibility of confusion of this 18-minute activity with the 18-minute activity of bromine 80.

It is a pleasure to thank Professor E. O. Lawrence and the staff of the Radiation Laboratory for the cooperation and interest that they have shown during the progress of this work. The writer wishes also to acknowledge the support given by the Royal Commission for the Exhibition of 1851. The work has been aided by grants from the Chemical Foundation, the Research Corporation, and the Josiah Macy Jr. Foundation.

[22] Pontecorvo, Nuovo Cimento **12**, 223 (1935).

The Scattering and Absorption Cross Section of Neutrons in Cobalt

N. E. Bradbury, F. Bloch, H. Tatel and P. A. Ross
Department of Physics, Stanford University, California

(Received August 7, 1937)

A low voltage neutron source is described which employs the deuteron-deuteron reaction with a continuously renewable target of ND_4Cl. Such a target is formed by subliming ND_4Cl on a metal target cooled with solid CO_2. Neutrons so obtained have been used to study the absorption and scattering cross sections of cobalt. The sum of the absorption and scattering cross sections for cobalt is $26.1\pm2.6\times10^{-24}$ cm², and the scattering cross section alone, is for *C* neutrons $5.6\pm1.8\times10^{-24}$ cm², and for *D* neutrons $3.7\pm1.8\times10^{-24}$ cm². The anomalously large scattering cross sections of iron and nickle are thus seen to be independent of their ferromagnetism since the cobalt cross section is essentially normal in magnitude.

THE deuteron-deuteron reaction for the production of neutrons has frequently been suggested[1] for those laboratories desiring a relatively simple source of neutrons but which do not possess very high voltage equipment nor access to suitable radioactive materials. Such a low voltage neutron source has been constructed in this laboratory and has been used initially for the study of the absorption and scattering of neutrons in cobalt.

Description of Apparatus

The essential features of the apparatus are shown in Fig. 1. Since the laboratory supply of high voltage furnishes 100 kv above and below ground, it is necessary to work with both target and gun at high potential. A heavy porcelain tube *P* carries a metal end plate through which passes a $1\frac{1}{2}''$ steel tube at the end of which is the ion gun *G*. The target *T* is cooled from behind with a mush of CO_2 and alcohol and is mounted on the end of a flanged glass tube *A*. The tube *A* carries a thin walled side neck *S* which contains approximately 1 gram of ND_4Cl and is surrounded by a heating coil. By passing current through this coil, ND_4Cl may be sublimed upon the target *T*. The tube *A* itself is mounted at the end of a long brass tube *C* which is attached to the main structure of the apparatus *F* by a sylphon bellows *B*. It is thus possible to move the tube *C* so as to bring the ion beam from *G* into the center of the target.

Two three-inch dibutylphthalate pumps trapped with CO_2 and backed by a small Langmuir steel pump and a Cenco Megavac are used for evacuation. Since normal gas flow through the gun is approximately 15 cc per hour, this pumping system is ample and no trouble has been experienced with gaseous breakdown in the tube. The pumps are at ground potential and are insulated from the main structure of the apparatus by 12″ sections of Pyrex pipe.

The "howitzer" *H* is a cubical block of paraffin cast in a wooden frame and divided centrally into four parts for easy removal from around the target. On the four outer walls of this block is a 5 cm layer of a half-and-half borax and paraffin mixture. This mixture is easily made by mixing borax in melted paraffin and effectively screens the source for slow neutrons. These walls are then grounded with metal shields and any measuring apparatus at ground potential may be brought as close as

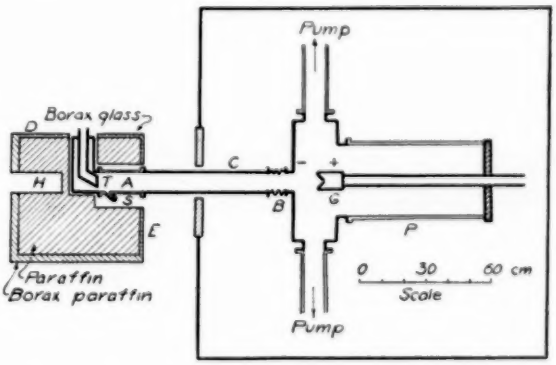

FIG. 1. General plan of apparatus. *P*, Porcelain tube to withstand 200 kv; *G*, ion gun; *B*, sylphon bellows; *C*, three-inch brass tube; *A*, two-inch glass tube; *S*, side neck containing ND_4Cl; *T*, target; *H*, paraffin howitzer.

[1] Oliphant, Harteck, and Rutherford, Proc. Roy. Soc. **A144**, 692 (1934); Slack and Ehrke, R. S. I. **8**, 193 (1937).

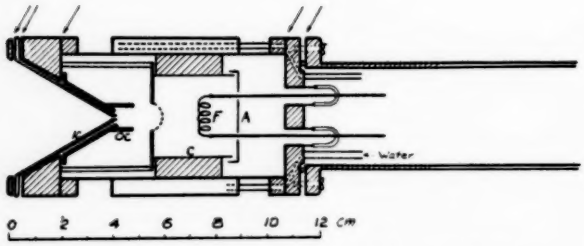

FIG. 2. Details of ion gun. *F*, Oxide coated filament; *A*, anode; *C*, secondary cathode; *IC* and *OC*, focusing electrodes.

desired. Since this mixture unfortunately does not have the insulating properties of paraffin, on the sides of the cube *D* and *E* where high insulation is imperative, an equivalent amount of borax was melted into borax glass and cast in thin slabs for these sides. A small side hole (not shown) was cut in the howitzer through the borax-paraffin to permit measurement of the yield of the source during a run.

The entire apparatus is made vacuum tight by means of the fuse wire gasket type of joint developed in this laboratory. For protection against x-rays which may be formed by secondary electrons from the target, the apparatus is housed in a $\frac{1}{4}''$ lead shield. This lead is replaced by an equivalent amount of lead rubber at the point where the target tube emerges.

The detailed features of the ion gun are shown in Fig. 2. The type of discharge employed is basically similar to that developed by Lamar and Luhr.[2] The filament *F* is of 0.010″ tungsten wire spirally wrapped with 0.008″ nickel and oxide coated. A potential of approximately 50 volts is maintained between the filament *F* and the anode *A* with an arc current of 0.5 to 1.0 ampere. The auxiliary cathode *C* is maintained at a potential of 140 volts negative to the filament. Under the action of this field, ions diffuse out through the hemispherical grid in *C*. The inner cone *IC* is made strongly negative with respect to the auxiliary cathode *C* by about 1200 volts thus strongly pulling positive ions towards its apex which contains a small hole 0.75 mm in diameter. The outer cone *OC* may then be used to *focus* the positive ions on *IC* by making it slightly *positive* with respect to *C*. The amount of positive potential needed depends upon the various voltages in the gun, but is of the order of 75–150 volts. As *OC* is made increasingly positive, the current passing through the hole in *IC* increases and the current *received* by *IC* decreases. If *OC* is made too positive, however, the current through *IC* rapidly drops. It is thus possible to find a potential for *OC* such that a maximum current is transmitted by the hole in *IC*. This device makes it possible to use a small hole in *IC* and consequently higher pressures in the arc chamber. The details of the operation of this type of arc at pressures from 0.1 to 0.5 mm have been studied by Lamar and Luhr.

The arc is cooled by a water jacket as shown through which water may be circulated at high potential by means of a small belt driven pump. Surrounding the gun is a smooth rounded brass shield to prevent cold emission. The arc electrodes are connected to metal-to-glass seals, only two of which are shown in the figure. The insulation of the two cones is of mica and glass. The arc chamber may be disassembled at any one of the points indicated by arrows for coating or replacing the filament or for inspection. The arc electrodes are of stainless steel, save for the focusing cones, which are of brass. The potentials necessary for operation of the arc are obtained by rectification of the current from an insulation transformer which supplies 110 volts at 100 kv. All potentials may be adjusted while the arc is under operation at high voltage.

With a gas pressure in the arc of 0.2 mm and 0.5 ampere arc current the total positive ion current measured at the target is of the order of 100–200μa. Of this current a rather crude magnetic analysis showed about 40 percent to be protonic. While this is a somewhat lower percentage than that obtained by Lamar and Luhr, it is nevertheless sufficiently high to justify operation without resorting to difficult and complicated magnetic analysis at high potentials. The arc is extremely stable in operation and easy to start and the focusing, once adjusted, remains constant unless the arc potentials are seriously altered.

It has not been possible as yet to compare the strength of this neutron source with a standard radioactive source under identical geometrical

[2] Lamar and Luhr, Phys. Rev. **46**, 87 (1934).

conditions. However, a rough estimate indicates a radium equivalent of 0.5–1.0 gram.*

Detection of the Neutrons

A conventional scale of sixteen Wynn-Williams counter is used with either a BF_3 ionization chamber and linear amplifier, or with a thin-window Geiger counter. The constancy of the source during a measurement is determined by means of a LiF lined Lauritsen electroscope which is lead shielded against x-rays and placed near the small side hole cut in the howitzer. The deflection of this instrument held in a constant position is directly proportional to the available number of neutrons. Precautions of this sort are essential since it can never be assumed that the yield has remained constant over any great period of time. This is mostly due to the fact that, after a short period of running, the efficiency of the target decreases considerably. To have a target which can be easily renewed in the vacuum at any time is apparently an essential feature of this type of experiment. This is accomplished in the present instance simply by increasing the heating current around S to a suitable value. Initially the use of LiD as a target substance was attempted, but was abandoned because of low yields and the difficulty of renewal. The exact cause of the low yield from this type of target is not understood, but may be due to surface contamination or to instability under ion bombardment.

Scattering of Slow Neutrons in Cobalt

The source described above has been used to study the scattering and absorption of slow neutrons in cobalt. This problem is of interest for two reasons; first, it might be possible that cobalt is better suited than iron for obtaining highly polarized neutron beams, and second, it appears from the scattering cross sections of many elements as given by Mitchell, Murphy, and Whitaker[3] that those of the iron group which have been measured, namely Fe and Ni, have anomalously high values. Although the reason for this behavior cannot be explained by any simple mechanism, it is of interest to verify whether it is a property inherent in all ferromagnetic substances or purely accidental.

A. Transmission

Cobalt metal was melted and cast in a hydrogen atmosphere in the form of blocks about 5 mm thick and 35 mm square. These were then surrounded with a tightly fitting block of the borax-paraffin mixture and the transmission measured as a function of thickness using the BF_3 ionization chamber. Similar pieces of iron were cut and their transmission measured under identical geometrical conditions. It may be noted that placing a 1 mm sheet of cadmium in front of the ionization chamber reduced the counts to 0.1 of the unshielded value. Hence these transmission experiments are almost entirely for C neutrons. The curves obtained in these two experiments are shown in Fig. 3.

From the slope of these curves the sum of the scattering and absorption cross sections for iron was found to be $10.2\pm0.8\times10^{-24}$ cm². This is in agreement with the result given by Mitchell of 10.6×10^{-24}. For cobalt the corresponding value was found to be $26.1\pm2.6\times10^{-24}$ cm². Since

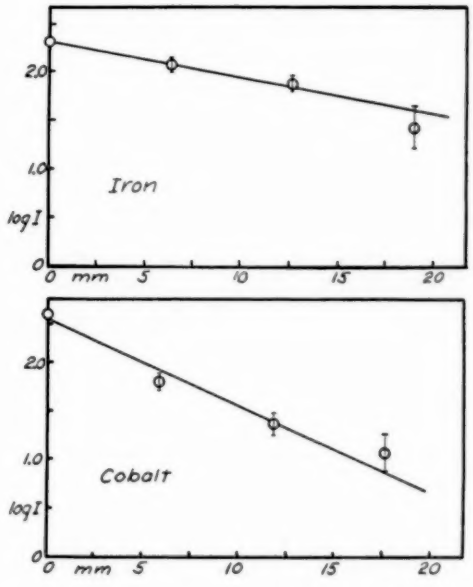

Fig. 3. Transmission of iron and cobalt for slow neutrons as a function of thickness.

* *Note added in proof:* Through the kindness of Dr. W. F. Libby and the University of California Hospital we have been able to compare our source with a 145 mC Rn-Be source under identical geometrical conditions. The results indicate a strength of our source of about 0.7 curies Rn-Be.

[3] Mitchell, Murphy, and Whitaker, Phys. Rev. **50**, 133 (1936).

early experiments of Fermi and Amaldi[4] have shown that a considerable fraction of this cross section must be due to absorption, it was necessary to separate the effects of scattering and absorption by another type of experiment.

B. Scattering

Some preliminary experiments of the relative number of neutrons scattered out of a beam by geometrically identical blocks of iron and cobalt made it seem probable that the scattering cross section of cobalt was noticeably lower than that of iron. Accordingly measurements were undertaken to compare it with that of zinc which has been shown by Mitchell to have a scattering cross section of 3.7×10^{-24} cm^2. This was done in the following way. A zinc plate 8 cm square and 0.6 cm thick was cast which contained as an alloy a suitable amount of cadmium so as to make its absorption for C neutrons closely equal to that of an identical plate of cobalt. The scattering of neutrons by these plates was measured by means of the activation of a rhodium disc 1.5 cm diameter in the following way: A 4 cm block of paraffin was placed behind the source, and the slow neutrons emerging from it were scattered back onto the rhodium disc with and without Cd screening. The rhodium was also screened from direct activation by screens of borax glass 1 cm thick and 1 mm cadmium. The rhodium was activated with (*a*) no scattering material; (*b*) the zinc-cadmium alloy plate; and (*c*) the cobalt plate behind it, and the activity determined with the Geiger counter. By this means it was possible to separate the relative number of C and D neutrons scattered under identical geometrical conditions for both cobalt and zinc. The results are shown in Table I.

TABLE I. *Relative numbers of scattered C and D neutrons.*

	C NEUTRONS	*D* NEUTRONS
Zinc	8.3 ± 3	7.2 ± 3
Cobalt	14.7 ± 3	5.5 ± 3

The scattering cross section of cobalt relative to that for C neutrons in zinc may be at once obtained from these data together with a knowledge of the transmission of the two plates for C and D neutrons. This was also determined by activation of the rhodium disks with and without Cd screening for the disk directly behind the plates. Correcting for the comparatively small differences in the transmission data by linear interpolation permits the scattering cross section of cobalt to be calculated accepting the value of the cross section of zinc given by Mitchell. In this way the scattering cross section of cobalt was found to be: for C neutrons $5.6\pm1.8\times10^{-24}$ cm^2, and for D neutrons $3.7\pm1.8\times10^{-24}$ cm^2.

Despite the relatively high inaccuracy of these results, nevertheless it appears at once that the scattering cross section of cobalt is considerably lower than that of iron or nickel, and, in fact, does not differ greatly from that of most other elements. We thus come to the conclusion that the high scattering cross sections of iron and nickel have nothing to do with their ferromagnetic properties since cobalt does not display this character. While its low scattering cross section might make it a desirable medium for polarization experiments, its high absorption unfortunately precludes this use.

We wish to express our thanks to Professor Fermi for helpful suggestions during the course of these experiments.

[4] Amaldi, D'Agostino, Fermi, Pontecorvo, Rasetti, Segrè, Proc. Roy. Soc. **A149**, 522 (1935).

Note on the Validity of Methods Used in Nuclear Calculations

DANA T. WARREN AND HENRY MARGENAU
Yale University, New Haven, Connecticut

(Received August 19, 1937)

A study has been made of several of the methods used to approximate the solutions of nuclear problems, especially the Schrödinger perturbation scheme and the linear variation method. The advantages of individual particle coordinates and relative coordinates are considered, the latter being more accurate. The methods are evaluated chiefly by application to the deuteron, where the possibility of an exact solution permits a check on the rapidity of convergence of the methods employed. The second Schrödinger approximation has been summed for this case, and the convergence is found to be rapid. However, the degree of approximation obtained is poorer than that readily obtainable from the linear variation scheme, using the same functions. This has been verified also for H^3 and He^4. For H^2 the Schrödinger scheme is found to be improved by decreasing the scale parameter (increasing the width) of the exponential functions from 0.60 to 0.45. For the linear variation method, this is not the case, at least if the functions are limited to those of double and quadruple excitation.

THE function that has been most frequently used for variational calculations of nuclear energies is a simple quadratic exponential ("error function") of the coordinates of the particles considered.[1, 2] This has a number of advantages, in that it is readily integrated using a similar form of potential energy (interaction) function, the function is readily separable into center of gravity and relative coordinate functions, respectively, and the function is applicable to any number of particles. It has, however, the serious difficulty of being quite inaccurate, as pointed out in detail by Bethe and Bacher.[3]

For this reason, the error function has been very widely used as the starting point for a large number of variational calculations, which are carried further by the use of various refinements. The most important refinements may be classified as follows. The first method will be called the equivalent two-body method.[1–3] A second method, also employed by Feenberg,[2] is the use of an additional variation function obtained by operating with the Hamiltonian on the original variation function. This function will be referred to as $H\psi_0$, H being the Hamiltonian and ψ_0 the error function. The third method makes use of the fact that the error function, ψ_0, is the zero-order wave function of a number of simple harmonic oscillators in the same coordinates. Hence the Schrödinger perturbation scheme can be applied, using the excited oscillator functions as a complete system of zero-order approximation functions. This method has been applied to light nuclei by Inglis.[4] There have also been variational calculations using complete sets of linear variation functions including work by Present and Rarita[5] and the authors.[6]

Before adopting this last method of calculation we made a considerable study of the various applicable methods. Since then, the criticism of the usual values for the interaction parameters[4, 5] has made it of some interest to present a comparison of these methods and a study of the validity of the results obtained.

In addition to the various methods possible, there are also several different systems of coordinates that have been employed. The simplest system is that of the rectangular coordinates of the individual particles involved.[7] The use of oscillator functions in such coordinates keeps the particles tied to a fictitious center, as in the Hartree method. These Hartree coordinates can be improved on by the use of the relative coordinates $\mathbf{r}_{ij}=\mathbf{r}_i-\mathbf{r}_j$. These are the coordinates that enter the expression for the potential energy,

[1] E. Wigner, Phys. Rev. **43**, 252 (1933).
[2] E. Feenberg, Phys. Rev. **47**, 850 (1935); E. Feenberg and J. K. Knipp, Phys. Rev. **48**, 906 (1935); E. Feenberg and S. S. Share, Phys. Rev. **50**, 253 (1936).
[3] H. Bethe and H. Bacher, Rev. Mod. Phys. **8**, 55 (1936).
[4] D. R. Inglis, Phys. Rev. **51**, 531 (1937).
[5] R. D. Present, Phys. Rev. **50**, 635 (1936); W. Rarita and R. D. Present, Phys. Rev. **51**, 788 (1937).
[6] H. Margenau and D. T. Warren, Phys. Rev. **52**, 790 (1937).
[7] W. Heisenberg, Zeits. f. Physik **96**, 473 (1935).

and the expression for the Hamiltonian is correspondingly simplified. However, for all problems dealing with more than two particles, there are more relative coordinates than degrees of freedom ($\mathbf{r}_{ij}-\mathbf{r}_{jk}=\mathbf{r}_{ik}$), and the use of corresponding functions does not give an orthogonal set. For this reason normal coordinates were adopted, consisting of linearly independent combinations of the relative coordinates so chosen as to permit differentiation between like-particle and unlike-particle interactions. In addition to these coordinate systems, Present[5] has used the Hylleraas system for H^3.

Comparison of Methods[8]

In discussing the various methods used in refining the calculations, it might be pointed out that, as suggested above, so long as quadratic exponential functions are used, the results are equivalent in the first approximation. This is true independently of the coordinate system used. In central coordinates, all particles enter on a nearly equal footing, and there is little advantage in distinguishing like-particle and unlike-particle interactions. Even for H^3 the distinction between the proton and neutrons only lowers the first approximation from -6.15 to -6.19. Relative and normal coordinates permit the distinction between interactions of like and unlike particles. However, the change in resulting energy is small, and analytically the result is otherwise the same.

Table I. *Convergence of second Schrödinger approximation to the energy[8] of H^2 for different values of the exponential scale parameter $\sigma=qa^2$. Note the shift in minimizing value of σ as successive excited functions are added. The true value is $E(H^2)=-2.15$ Mev.*

Excitation \ σ	0.30	0.35	0.40	0.45	0.50	0.55	0.60
$E^{(1)}$	− .13	− .26	− .38	− .480	− .548	− .590	− .614
$E_{D^{(2)}}$				− .020	− .010	− .003	0
$E_{Q^{(2)}}$				− .626	− .611	− .599	− .561
$E_{S^{(2)}}$				− .232	− .212	− .191	− .170
$E_{O^{(2)}}$				− .092	− .079	− .067	− .055
$E_{D,Q,S,O^{(2)}}$				− .970	− .912	− .860	− .786
$E_{\text{all}^{(2)}}$	−1.15	−1.15	−1.12	−1.043	− .954	− .875	− .807
$E^{(1)}+E_{\text{all}}(2)$	−1.28	−1.41	−1.503	−1.523	−1.502	−1.465	−1.421

[8] The calculations quoted in this paper use the following sets of constants. For H^2, the preliminary values $a=2.00\times10^{-13}$ cm, $A=42.8$ Mev, $E(H^2)=-2.15$ Mev were used. For H^3 and He^4, the more probable values $a=2.25\times10^{-13}$ cm, $A=35.60$ Mev, $g=0.20$ were adopted. A few calculations on H^2 using the second set of values indicate that the results are not very different.

Table II. *Summary of variational calculations[8] for H^2, using $\sigma=0.60$. The calculations are for the Gaussian form of interaction and symmetrized oscillator variation functions in relative (=normal) coordinates.*

No. of functions	Degree of excitation	Resulting energy
1	0	−0.614
2	0,2	−0.614
3	0,4	−1.544
4	0,2,4	−1.67
7	0,2,4,6	−1.68
7	0,4,8	−1.74
8	0,2,4,8	−1.805
∞	all	−2.15

(Bethe and Bacher's[3] formulae 118 and 119, with $p=1$, or p adjustable.)

After we had found that all variation functions gave us the same result in the first approximation, we turned to a consideration of the Schrödinger perturbation scheme, and tried it first on the deuteron in relative (here equivalent to normal) coordinates. This has the advantage that the integrals of the "perturbing potential" $-\text{Be}^{-r^2/a^2}-(\hbar^2/2M)qr^2$ are readily expressed analytically. Moreover, it was found possible to sum the second Schrödinger approximation for all excited states. (See Appendix.) The results are shown in Table I.

It is found that successive contributions (beyond the first) diminish rapidly, approaching quickly to a value within a few percent of the total. This agrees with the findings of Inglis[4] and suggests that his results may be close to the limit of the second perturbation calculation. However, we find that the optimum value of the scale parameter σ varies with stage of excitation included over quite a wide range. This is due to the occurrence of the factor σ in the denominator of the second perturbation energy (diagonal unperturbed energy) and especially to increasing powers of $\sigma+1$ in the denominators of $V_{i,0}$ of excited states, making the more highly excited states more important for smaller values of σ. The difference between this result and that of Inglis for He^4 may possibly be due to his limitation of excited states to sextuple excitation, and to his narrow range of variation of σ.

It is further found that the second perturbation calculation gives values very far from the true limit of the energy. Indeed, for H^2, the use of only two quadruply excited linear variation functions gives a lower energy than any obtainable by

the second perturbation (cf. Table II). The poorness of the Schrödinger perturbation scheme is due, of course, to the large difference between the energies of excited states in first approximation and zero approximation, as well as to the large diagonal and nondiagonal elements that occur in the perturbation energy matrix. The error of 0.6 or 0.7 Mev for the second Schrödinger approximation in H^2 may be expected to be increased by a small factor when more terms enter the Hamiltonian, as is the case with other nuclei.

We have also studied the variation method as applied to H^2 with two purposes in view. The first was to determine the rapidity of convergence of our functions toward the true limit. For this purpose we used first symmetrized functions of successive excited states in relative (normal) coordinates. As always, it is found that the doubly excited states contribute negligibly to the energy if the variation parameters are properly adjusted for the first approximation. However, in combination with the quadruply excited states, the doubly excited function contributes 0.13 Mev. Again, it is found that the octuply excited states contribute more to the result than the sextuply excited states. The results are summarized in Table II. They show that the contribution of a function may change appreciably when the companion functions are changed. Further they show that the highly excited states contribute appreciably to the true energy. In spite of the fact that the three sextuply excited states contribute all together only 0.01 Mev or less, it would be misleading to suppose that the true convergence limit is being approached. It seems clear that great caution must be exercised in interpreting apparent convergence of the linear variation method.

We have further used the deuteron to investigate the dependence of the energy obtained in different approximations on the variation parameter $\sigma = qa^2$ which represents the scale of the Hermitean functions. The results have already been presented for the summed second perturbation. There it is found that a decrease of the scale improves the result. However, this is not the case with the variational method applied to a few functions as shown in Table III. We conclude that variation of the scale parameters is not necessary beyond the first approximation.

We have also tried the use of the variation function $H\psi_0$ in addition to a few of our complete set. As might be expected of such a completely independent function varying in the correct manner, it contributes a fairly constant fraction (3/5) of the difference between the true energy and that obtained without its use. ($E^{(O,\,D,\,Q)} = -1.67$, $E^{(O,\,D,\,Q,\,H\psi_0)} = -1.96$, $E(H^2) = -2.15$). For this reason it is suggested that the use of such a function in addition to the functions from the complete set will furnish a much better indication of the true convergence limit than any possibly deceptive appearance of convergence in the functions themselves. Feenberg[2] has already used it in this way as a check on his equivalent two-body method.

Comparison of Coordinate Systems

The Hylleraas coordinate system, though excellent for the treatment of the three-body problem, is not readily tested by the deuteron. However, we have applied individual particle central field coordinates to the two-, three-, and four-body problems. These coordinates have the advantage of simplicity of integration, the near equivalence of all particles permitting a good approximation with the use of a single scale parameter σ for all coordinates. Then a single integration gives the interaction between all particles.

However, the individual particle coordinate system has a number of disadvantages. For one thing, it requires the use of a larger number of functions. This is partly because of the use of an excess number of coordinates, partly because states with two particles excited an odd number of times give a nonvanishing matrix element.

Table III. *Dependence of calculated variational energy[8] of H^2 on scale parameter σ. The second column gives the first approximation using a single unexcited function ($E^{(O)} = H_{0,0}$). The third column gives the energy using four functions including all of zero, double, and quadruple excitation. The last column gives the contribution of the three excited functions. $E(H^2) = 2.15$ Mev.*

σ	$E^{(O)}$	$E^{(O,\,D,\,Q)}$	Difference
0.40	−0.38	−1.45	−1.07
.50	− .55	−1.62	−1.07
.55	− .59	−1.66	−1.07
.60	− .61	−1.68	−1.07
.70	− .55	−1.65	−1.10

Also, the individual particle coordinate system gives a worse approximation than the relative or normal coordinate system for the same degree of excitation, even with a larger number of functions.

It is also well to remember that the individual particle coordinates cannot be used to determine excited states. This is because the ground state is infinitely degenerate in these coordinates. Hence, any function used to approximate an excited state, even though orthogonal to some *one* ground state, may contain an unknown portion of some other ground state function. Hence a low energy may be due to the ground state and not to any excited state. As an example, we may cite the first "P state" for He^4 (function $\frac{1}{2}(\phi_{100}(1)\phi_{000}(2)\phi_{000}(3)\phi_{000}(4)+$permutations)). This gives an energy identical with that of the ground state, and differs from it only in being multiplied by a function $(X+Y+Z)$ of the center of gravity coordinates. Since the Hamiltonian is independent of these, the resulting energy will of course be the same as that of the ground state.

The use of relative coordinates is even simpler than that of individual particle coordinates for the deuteron. For this case, all the integrals required are easily evaluated algebraically in terms of a single summation by the use of the generating function. However, for more than two particles, relative coordinates are too numerous, and to obtain a complete orthogonal set of functions for the perturbation scheme or the variation method, it is necessary to use normal coordinates. These are identical with relative coordinates for H^2, but are more complicated for other nuclei.

These normal coordinates have the advantage of giving a wave function which is different in like-particle and unlike-particle relative coordinates, permitting a specific adaptation to the difference in the two types of interaction. On the other hand, this lack of symmetry makes the integrations more difficult. The use of two or more different parameters (p and σ, or q_1 and q_2) complicates the calculations considerably.

However, these coordinates give an appreciably better approximation than the individual particle coordinates do. For the deuteron, using doubly and quadruply excited states, the energy is -1.67 Mev as compared to -1.48 Mev obtained with individual particle coordinates for the same degree of excitation. For H^3, the energy beyond the first approximation is only 7/10 as much with individual particle coordinates.[6] For this reason, we believe the normal coordinate system to be more useful than the individual particle coordinate system.

These considerations apply immediately only to light nuclei. The difficulties arising from the use of functions in individual particle coordinates in connection with heavier nuclei are well known.[7]

Appendix

Summation of second Schrödinger perturbation for H^2

The second Schrödinger approximation gives

$$\Delta E^{(2)}=-\sum_i{}' \frac{V_{i,0}{}^2}{E_i-E_0}$$

with $$V=U-\frac{\hbar^2}{M}q^2r^2=-Be^{-r^2/a^2}-\frac{\hbar^2}{M}q^2r^2.$$

We take the oscillator functions

$$\psi_{i,\,j,\,k}=N_{i,\,j,\,k}H_i(q^{\frac{1}{2}}x)H_j(q^{\frac{1}{2}}y)H_k(q^{\frac{1}{2}}z)e^{-qr^2/2},$$

giving $E_{i,\,j,\,k}=[3+2(i+j+k)](\hbar^2/M)q$. Since V is even in x, y, and z, it is only necessary to consider functions $\psi_{2l,\,2m,\,2n}$ with even excitation in each coordinate. Of these, only the three doubly excited functions include any contribution from the second term in V. The matrix elements of the first term are

$$U_{2l,\,2m,\,2n;\,0,\,0,\,0}=L_{2l}L_{2m}L_{2n},$$

where

$$L_k=(-1)^{1+k/2}\frac{B^{1/3}}{(k/2)\,!}\left(\frac{k\,!\sigma}{\sigma+1}\right)^{\frac{1}{2}}\left[\frac{1}{2(\sigma+1)}\right]^{k/2},\qquad \sigma=qa^2.$$

Hence the second approximation, exclusive of the second term in V, becomes

$$-\sum_{l,\,m,\,n=0}{}'\frac{(L_{2l}L_{2m}L_{2n})^2}{(4\hbar^2/Ma^2)(l+m+n)\sigma}$$

$$=-\frac{Ma^2B^2}{4\hbar^2\sigma}\frac{(u-2)^3}{u^3}\sum_{l,\,m,\,n=0}{}'\frac{(2l)\,!(2m)\,!(2n)\,!}{l\,!^2m\,!^2n\,!^2}\frac{u^{-2(l+m+n)}}{(l+m+n)}\qquad(1)$$

with $u=2(\sigma+1)$, and the prime indicating that the term with $l=m=n=0$ is to be omitted.

To perform this summation, we first consider the series formed by omitting the factor $(l+m+n)$ in the denominator of each term. This series is

$$\sum_{l,\,m,\,n=0}{}'\frac{(2l)\,!(2m)\,!(2n)\,!}{l\,!^2m\,!^2n\,!^2}u^{-2(l+m+n)}$$

$$=\frac{1}{B^2}\left(\frac{u}{u-2}\right)^3\left\{\sum_{l,\,m,\,n=0}^{\infty}|U_{2l,\,2m,\,2n;\,0,\,0,\,0}|^2-B^2\left(\frac{u-2}{u}\right)^3\right\}.$$

But U is a matrix and the sum of the indicated elements is merely the diagonal element $(U^2)_{0,0}$ of the product matrix. The integration is readily performed, giving $(U^2)_{0,0}=[(u-2)/(u+2)]^{\frac{1}{2}}B^2$. Hence this series is

$$\sum_{l,m,n=0}{}' \frac{(2l)!(2m)!(2n)!}{l!^2 m!^2 n!^2} u^{-2(l+m+n)} = \frac{u^3}{(u^2-4)^{\frac{1}{2}}} - 1. \quad (2)$$

In order to obtain the series (1) for $\Delta E^{(2)}$ from this series just summed, we multiply each term by $2du/u$ and integrate from u to ∞. Applying the same process to the sum, Eq. (2), we obtain

$$-\frac{Ma^2B^2}{2\hbar^2\sigma}\left(\frac{u-2}{u}\right)^3\int_u^\infty \frac{2}{u}\left(\frac{u^3}{(u^2-4)^{\frac{1}{2}}}-1\right)du = -\frac{Ma^2B^2}{2\hbar^2\sigma}\left(\frac{u-2}{u}\right)^3 \times\left[\log 2 - 1 + \frac{u}{(u^2-4)^{\frac{1}{2}}} - \log\left(1+\frac{(u^2-4)^{\frac{1}{2}}}{u}\right)\right].$$

To this expression must be added, first the contribution from the second term in V, which turns out to be

$$-\frac{3}{8}\frac{\hbar^2\sigma}{Ma^2}+\frac{3B}{4(\sigma+1)}\left(\frac{\sigma}{\sigma+1}\right)^{\frac{1}{2}},$$

second the result of the first Schrödinger approximation:

$$\frac{3}{2}\frac{\hbar^2\sigma}{Ma^2}-B\left(\frac{\sigma}{\sigma+1}\right)^{\frac{1}{2}}.$$

When expressed in terms of σ, this gives the final result

$$E^{(1+2)}=\frac{9}{8}\frac{\hbar^2\sigma}{Ma^2}-B\left[1-\frac{3}{4(\sigma+1)}\right]\left[1-\frac{1}{\sigma+1}\right]^{\frac{1}{2}} - \frac{Ma^2B^2}{2\hbar^2}\frac{\sigma^2}{(\sigma+1)^3}\left\{\frac{\sigma+1}{[\sigma(\sigma+2)]^{\frac{1}{2}}} - \log\left[1+\frac{\{\sigma(\sigma+2)\}^{\frac{1}{2}}}{\sigma+1}\right]-0.30685\right\}.$$

The dependence of this expression on σ is shown in the last row of Table I.

NOVEMBER 15, 1937 PHYSICAL REVIEW VOLUME 52

The Disintegration of Beryllium and the Masses of the Beryllium Isotopes

JOHN H. WILLIAMS, ROBERT O. HAXBY AND WILLIAM G. SHEPHERD
University of Minnesota, Minneapolis, Minnesota

(Received September 4, 1937)

The following disintegrations have been studied up to bombarding energies of 250 Kv.

$$Be^9+H^1\rightarrow\begin{pmatrix}Be^8+H^2\\Li^6+He^4\end{pmatrix}, \quad (1)$$
$$Be^9+H^2\rightarrow Li^7+He^4+Q_2, \quad (2)$$
$$Be^9+H^2\rightarrow Be^8+H^3+Q_3, \quad (3)$$
$$Be^9+H^2\rightarrow Be^{10}+H^1+Q_4. \quad (4)$$

Efficiency curves for the four reactions are smooth and regular. Absolute yields from a thick target are given. Range measurements of the disintegration products determine the values of Q_2, Q_3, Q_4 as 6.95, 4.32, and 4.44 Mev respectively and the masses of Be^8, Be^9, Be^{10} as 8.0081, 9.0150 and 10.0168.

INTRODUCTION

PREVIOUS work[1,2] in this laboratory on the disintegration of light elements by protons and deuterons has been extended to include beryllium. In view of the anamolous scattering of 130 to 190 Kv protons by beryllium found by Dymond,[3] the efficiency curves for the proton-beryllium disintegration in this energy range should be of some interest. Furthermore, a consistent set of range measurements of the products of disintegrations by deuterons provides an opportunity to evaluate the masses of the beryllium isotopes.

We have investigated the following reactions with the use of the 250 Kv apparatus and the experimental method previously described.[2]

$$Be^9+H^1\rightarrow\begin{pmatrix}Be^8+H^2\\Li^6+He^4\end{pmatrix}, \quad (1)$$
$$Be^9+H^2\rightarrow Li^7+He^4+Q_2, \quad (2)$$
$$Be^9+H^2\rightarrow Be^8+H^3+Q_3, \quad (3)$$
$$Be^9+H^2\rightarrow Be^{10}+H^1+Q_4. \quad (4)$$

Oliphant, Kempton and Rutherford[4] have studied these disintegrations at 550 Kv and

[1] Williams, Wells, Tate and Hill, Phys. Rev. **51**, 434 (1937).
[2] Williams, Shepherd and Haxby, Phys. Rev. **52**, 390 (1937).
[3] Dymond, Proc. Roy. Soc. **A157**, 302 (1936).
[4] Oliphant, Kempton and Rutherford, Proc. Roy. Soc. **A150**, 241 (1935).

Allen[5] has investigated the efficiency curve for (1) up to 125 Kv.

Efficiency Measurements

Efficiency curves for the four disintegrations were obtained from thick targets by comparing, with the technique previously described,[2] the yield at a given voltage to the yield at an arbitrarily chosen standard voltage, 212 Kv. The results are shown in Fig. 1. It is seen that there is a marked similarity between these curves and that they are quite smooth and regular, showing no signs of any resonance process such as had been found for boron.[1]

The thick target yield curves are also compared by integrated Gamow plots[6] in Fig. 2. The experimental points are well fitted by straight lines and indicate the similarity between the excitation functions. It may be concluded, as in the case of lithium,[2] that for these deuteron energies the Oppenheimer-Phillips process does not contribute appreciably to the disintegration probability of (4).

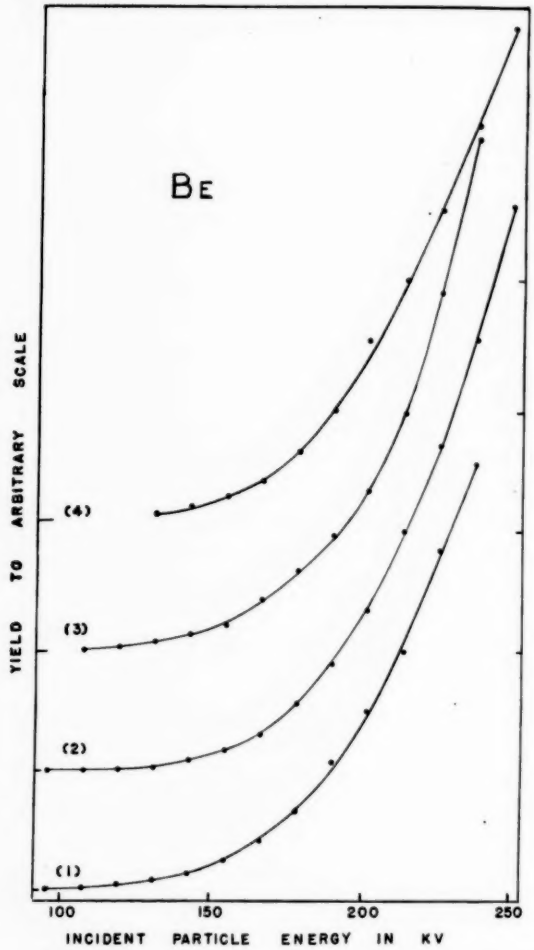

Fig. 1. Thick target yield curves for Be. The curves are displaced and plotted to the scale of unit yield at 212 Kv.

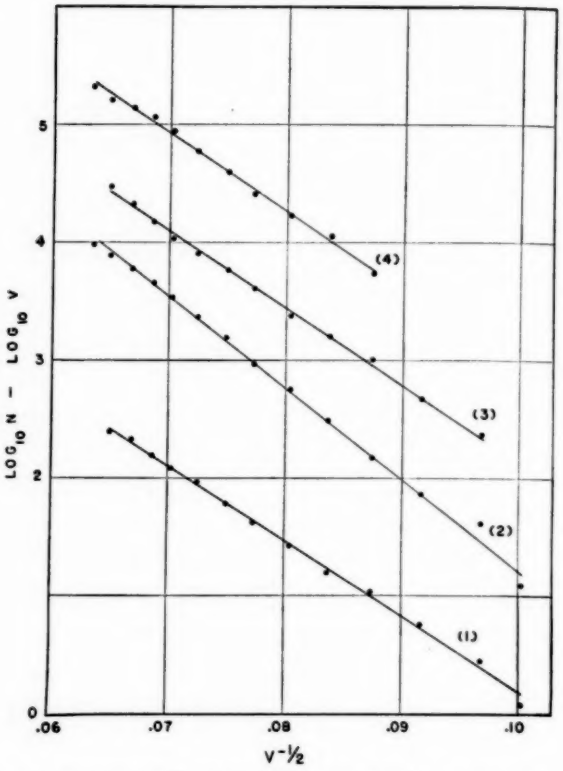

Fig. 2. Integrated Gamow plots from the thick target data shown in Fig. 1. The curves are displaced vertically.

The absolute yields from a thick target of beryllium per incident ion of 212 Kv energy are: (1) 4×10^{-7}, (2) 1×10^{-9}, (3) 2×10^{-10}, (4) 2×10^{-11}. These yields are based on reasonable assumptions of the solid angle employed, the deuteron concentration in the mass two spot and isotropic angular distribution of the disintegration particles. The estimated accuracy is ±50 percent. At 125 Kv our measured yields are approximately four times those of Allen. Oliphant, Kempton and Rutherford give a ratio of 10 : 45 : 45 for (2) : (3) : (4) at 550 Kv deuteron energy. Extrapolating the straight lines of Fig. 2 to this voltage leads to a value for the ratio of 90 : 9 : 1.

Range Measurements

In order to study the distribution in range of the particles from the deuteron reactions we have

[5] Allen, Phys. Rev. **51**, 182 (1937).
[6] Henderson, Phys. Rev. **43**, 98 (1933).

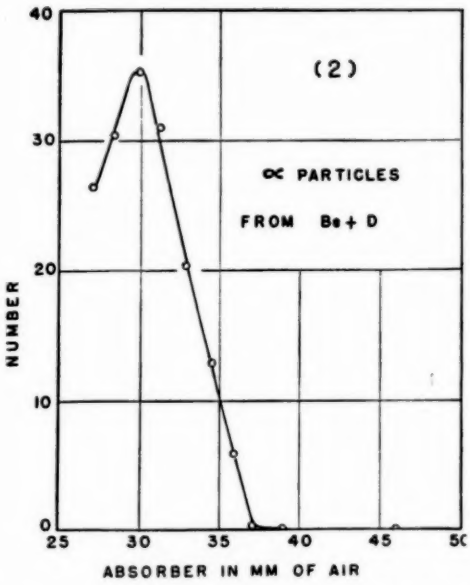

FIG. 3. Differential range number curve of the alpha-particles from reaction (2). The range scale shown should be increased by 0.6 mm.

made use of a differential ionization chamber and a variable bias counter so that only particle ionization kicks greater than a selected magnitude would be recorded. To vary the amount of absorbing material in the path of the particles we have used mica windows and an adjustable pressure air absorption tube which limited the particles observed to $90\pm5°$ with respect to the direction of the incident deuteron beam. The residual range of the mica windows and air absorption tube was calibrated with alpha-particles from a clean Th C+C′ source replacing the beryllium target.

A typical curve of the number of alpha-particles from (2) *vs.* absorbing material in cm of air at 15°C is shown in Fig. 3. By comparison with the Th C+C′ alpha-particles under identical detecting conditions we conclude that the mean range is 2.92 ± 0.02 cm at zero deuteron energy. This value agrees with the range of 3.0 cm given by Oliphant, Kempton and Rutherford.

When we substitute Bonner's values for the masses of Li^7, He^4, and H^2, we obtain for Be^9 a mass of 9.0150 which agrees within the accuracy of the mass data with Bonner's value of 9.0149 and with Bainbridge and Jordan's value of 9.01516 ± 0.0002.

The process of calibrating the range of the H^3 particles from (3) by comparison with alpha-particles from Th C′ is open to question. Since the variation of the specific ionization with residual range of an alpha-particle and a H^3 nucleus may be quite different we have adopted the following procedure. Differential numbers *vs.* range curves of approximately the same width were obtained by adjusting the detecting apparatus to record only those particles whose specific ionization was more than an arbitrarily large amount. Such a curve is shown for the H^3 particles from (3) in Fig. 4.

A direct comparison of the specific ionization curves of protons and alpha-particles has been made by Schmidt and Stetter and Stetter and Jentschke.[7] They showed that the alpha-particles had a maximum specific ionization when 4.6 mm from end of range and protons at 3.9 mm from end of range. If one assumes that the variation of specific ionization of a singly charged particle is a function of velocity alone, one can construct a Bragg curve for H^3 from the H^1 curve of Schmidt and Stetter. The peak of this Bragg curve should then be three times as far removed from the end

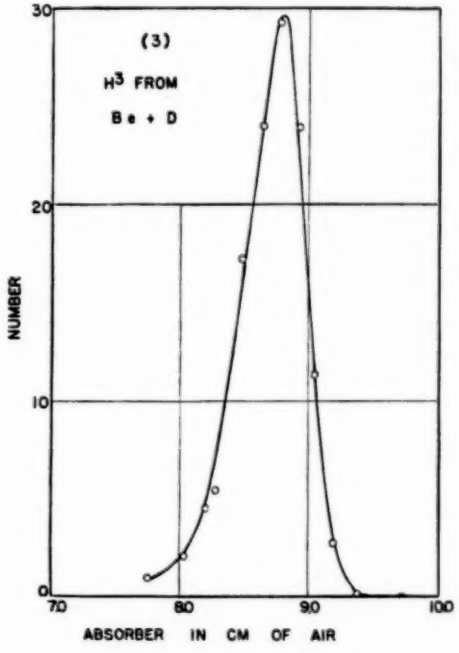

FIG. 4. Differential range number curve of the H^3 particles from reaction (3). The range scale shown should be increased by 1.4 mm.

[7] Schmidt and Stetter, Wiener Ber. **139**, 123 (1930). Stetter and Jentschke, Physik. Zeits. **36**, 441 (1935).

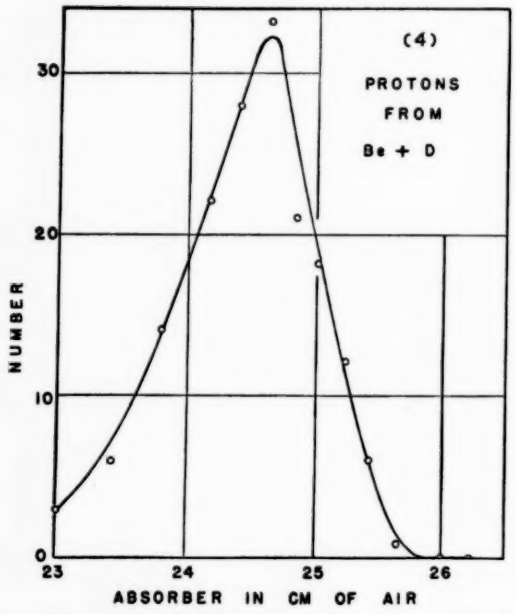

FIG. 5. Differential range number curve of the protons from reaction (4). The range scale shown should be increased by 8.0 mm.

of range, i.e., 11.7 mm, as in the case of protons, since the peak occurs at a range position corresponding to equal velocities of the particles. On the basis of these measurements we should calibrate our range scale by adding the difference between the alpha-particle and H^3 particle residuals to our direct comparison of the differential peaks.

On the other hand the recent measurements of Parkinson, Herb, Bellamy and Hudson[8] shown in curve VI of their Fig. 5 indicate that the maximum of the specific ionization curve for protons is not more than 10 Kv from the end of range, corresponding to about 0.2 mm range. One is therefore inclined to question the validity of the measurements of Schmidt and Stetter where the ionization from recoil protons is measured in a deep ionization chamber. Measurements on alpha-particles which may be compared directly to the above results[8] for protons are not available. It therefore seemed only possible to assume that the H^3 and alpha-particle differential peaks of approximately the same width may be compared directly to establish the range scale for the former and to realize that future experiments with artificially accelerated alpha-particles, deutrons and protons will make possible a method of correcting range calibrations with alpha-particles.

TABLE I.

REACTION	PARTICLE	Q IN MEV	MASS OF BE ISOTOPE
(2)	He^4	6.95	$Be^9 = 9.0150$
(3)	H^3	4.32	$Be^8 = 8.0081$
(4)	H^1	4.44	$Be^{10} = 10.0168$

[8] Parkinson, Herb, Bellamy and Hudson, Phys. Rev. **52**, 75 (1937).

On the basis of these considerations, the H^3 particles from (3) shown in Fig. 4 have a mean range of 8.94 ± 0.10 cm at 225 Kv deuteron energy. The stated error is purely experimental and makes no allowance for uncertainty in the above assumptions. If we set $Be^9 = 9.0150$ and use Bonner's masses for H^2 and H^3 we obtain for the mass of Be^8 a value of 8.0081 with an error of 0.00005 from the *experimental* range determination. This is to be compared to the mass of two alpha-particles, 8.0080, and Bonner's value of 8.0078. The range determination is to be compared to Oliphant, Kempton and Rutherford's value of 8 cm.

For the case of the protons from reaction (4), differential range *vs.* number curves were taken with the same air absorption tube. A typical curve is shown in Fig. 5. Additional mica foils were interposed in the path of the protons. These foils were of approximately 5 cm air equivalent and were separately calibrated with Th C′ alpha-particles which first passed through the mica and then through an adjustable distance of air. By comparison with the data of Mano[9] on the relative stopping power of mica and air for protons, we conclude that the mean range of the protons from (4) is 25.4 ± 0.3 cm of air. Oliphant, Kempton and Rutherford's value is 26 cm. Substituting the mass-energy data in (4) we obtain for the mass of Be^{10}, 10.0168 ± 0.0001, compared to Bonner's value of 10.0163. The nucleus should then be unstable with respect to B^{10} of mass 10.0160.

The range and mass data are shown in Table I.

We wish to express our sincere thanks to Professor E. L. Hill for his discussion of range calibrations and to Professor John T. Tate for his continued interest and support. This research was supported in part by a grant from the Graduate School.

[9] Mano, J. de phys. et rad. **5**, 628 (1934).

The Energy Losses of Fast Electrons

L. JACKSON LASLETT* AND D. G. HURST†
Radiation Laboratory, Department of Physics, University of California, Berkeley, California
(Received August 24, 1937)

The energy losses experienced by electrons of energies from 1.5 to 4.5 Mev in traversing thin laminae of carbon and of lead were investigated with a hydrogen-filled cloud chamber. The carbon absorber had almost the same calculated stopping power as the lead and was used to provide a check on the method in regard to such factors as straggling, and scattering of the electrons by the gas of the chamber. As a source of electrons activated chlorine was used, the electrons being admitted through a thin mica window mounted on the periphery of the chamber. A comparison was made between the average energy loss per g/cm² of absorber found as the result of the measurements and the values for this quantity predicted on the basis of current theory. As the experimental rate of loss in lead was markedly greater than that theoretically expected, the attempt was made to account for this difference on the basis of the obliquity of the electron paths in the absorber; this attempt, however, was unsuccessful, so that the results indicate a higher rate of absorption in lead of electrons with the energies studied than is predicted by theory. A further comparison was made with theory in regard to the absolute probability of large energy losses—losses of approximately half the initial energy. Here a very large discrepancy was found, which indicates that the difference found in the computation of the average rate of energy loss is due to the probability of large (radiative?) losses being considerably greater in lead than is expected from theory.

INTRODUCTION

SEVERAL authors have investigated the energy losses which electrons with kinetic energies of a few million electron volts experience in traversing matter. The experiments have been performed with either heavy gases[1,2] or thin laminae[2,3] in a cloud chamber. In all cases, the losses have been found higher for *heavy* elements than expected on the basis of current theory, although the latest results of Turin and Crane[3] on the average energy loss for lead absorbers can be brought to near agreement with theory by making use of not unreasonable assumptions regarding the obliquity of the electron paths in the lead foil. If the frequency of large losses—of the order of half the initial kinetic energy—is compared with the theoretical value for radiative losses of this magnitude, the disagreement is much greater.

In view of this situation it was felt that some results which we have obtained, using electrons of energies between 1.5 and 4.5 Mev and thin (approximately 1/7 g/cm²) foils stretched across a cloud chamber, would be of interest. By using foils as thin as these, the measurement of *ionization* losses becomes necessarily inaccurate, but, under these conditions, large energy losses would be expected to arise only from other processes, presumably from single radiative processes which theoretically begin to become of importance for electrons of these energies in elements of high atomic number. Although our chief interest in this paper will be with the data obtained with a lead absorber, measurements were also made with a carbon absorber of thickness such that approximately the same ionization loss would be expected as in the lead; the scarcity of large energy losses in the carbon indicated that when they appeared in the lead absorber they could in general be ascribed to mechanisms other than ionization.

APPARATUS

The cloud chamber was of the pressure operated sylphon type, being, except for a few modifications, that used by Kurie, Richardson and Paxton[4] for studies of β-ray distributions. The sensitive volume was 16 cm in diameter and approximately 1 cm high. The chamber was in all cases filled with tank hydrogen at a pressure between 100 and 110 cm and with a mixture of ethyl alcohol and water to provide the con-

* Now at the Institute for Theoretical Physics, Copenhagen.
† 1851 Exhibition Scholar, now at the Cavendish Laboratory, Cambridge.
[1] H. Klarmann and W. Bothe, Zeits. f. Physik **101**, 489 (1936).
[2] L. Leprince-Ringuet, Ann. de physique **7**, 5 (1937).
[3] J. J. Turin and H. R. Crane, Phys. Rev. **52**, 63 (1937).
[4] F. N. D. Kurie, J. R. Richardson, and H. C. Paxton, Phys. Rev. **49**, 368 (1936).

densable vapor. The selection of hydrogen as the permanent gas with which to fill the chamber is of importance because the distortions of electron tracks due to nuclear scattering become more serious in heavier gases.

Coils above and below the chamber provided a magnetic field of approximately 700 oersteds. To avoid overheating, current was passed through these only for short intervals during which the expansions took place; the value of the current was observed for each expansion.

The tracks were illuminated by a shorted carbon arc and photographed with a single Sept camera having a $f:2$ lens. Their curvatures were determined by reprojecting the photographs to their original size and fitting circles drawn on white Bristol board to the images of the tracks. The angles of incidence and deviation were found by first measuring the angles for chords of a fixed length (5 cm) and later correcting for the angles between the chords and tangents at the lamina.

Several series of expansions were taken, some with a carbon absorber and the rest with a lead absorber. The runs with carbon were interposed between two series of runs with lead. Pictures were measured in the same order as they were taken. The carbon absorber had a surface density of 0.130 g/cm^2 (volume density$=1.52$ g/cm^3); the lead had a surface density of 0.158 g/cm^2. From theory, losses of 0.44 mc^2 in the carbon and 0.33 mc^2 in the lead are to be expected. This value for lead does not include the expected mean radiation loss, which amounts to 0.09 mc^2.

The electrons were those emitted by active chlorine (half-life 37.5 min.) produced by deuteron bombardment of silver chloride in the Berkeley cyclotron. The active sample was placed outside the chamber at a distance of from 20 to 40 cm from a thin (0.008 cm) mica window on the periphery through which the electrons were admitted. A brass tube limited the beam of electrons outside the window in such a way that the magnetic field excluded from the chamber many of the low energy electrons. The distribution as to initial kinetic energy of the tracks studied is that indicated in Table I, from which it will be seen that the measurements were confined to electrons with initial kinetic energies above 3 mc^2.

Besides rejecting tracks which apparently suffered deflections in the gas, tracks whose lengths for some reason (such as obliquity to the sensitive plane of the chamber) were less than 5 cm were not measured, it being felt that the absence of some such criterion would impair the accuracy of the curvature measurements. In comparing energies on both sides of the absorber, it is, of course, essential that one be as sure as possible that the tracks measured are really associated, i.e, belong to the same electron. Even when all tracks whose identities are rendered uncertain by virtue of the presence of other tracks are rejected from consideration, there remains the possibility that a Compton electron be ejected from the absorber close to the point at which another electron enters and is somehow scattered from view. From the number of apparently unaccompanied measurable electron tracks emerging from the absorber, we calculated that accidental coincidences would be expected to account for one-half of one per cent of the total number of "traversals." The number of pairs projected backward from the plate, which might be mistaken for reflected electrons, is altogether negligible.

Results

The results are shown in the histograms of Figs. 1 and 2. The scale of ordinates is such that in all the diagrams equal heights represent equal numbers of electrons *per measurable incident track*—the numbers appended at the side are, however, the true number of electrons. It will be noticed that a few negative energy losses are recorded. These may be the result of errors of measurement or of undetected deflections; in either case they should be included in the histogram, as they will tend to cancel similar positive errors when the average energy loss is calculated and so make the latter quantity more reliable.

TABLE I. *Distribution in initial kinetic energy of those tracks whose energy losses were measured.*

Initial kinetic energy	0–3	3–4	4–5	5–6	6–7	7–8	8–9	>9 mc^2
Number of tracks	0	30	29	21	19	6	3	0

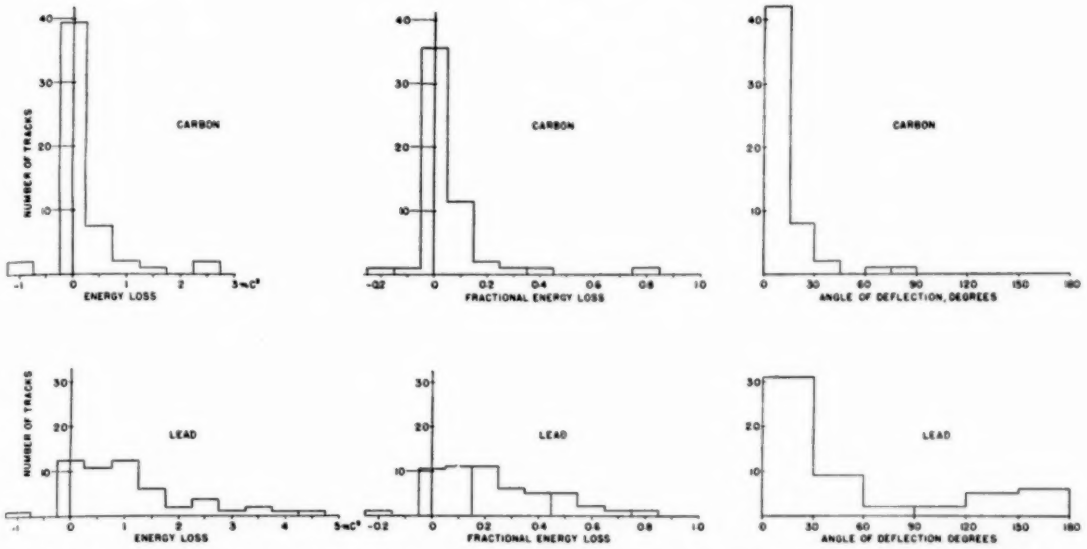

FIGS 1. AND 2. Histograms showing the energy losses, the fractional energy losses, and the angles of deflection in carbon and in lead of the electrons studied in this investigation. It is to be noted that, in the plots showing the distribution with respect to the angle of deflection, the histogram interval in carbon was taken as half that used in the case of lead. The total number of *incident* tracks in carbon = 210; in lead, 301.

In carbon one out of 3.9 measurable incoming tracks came out in such a way as to be measurable; in lead, one out of 5.5. These ratios do not differ greatly from what one might expect from the scattering of the incident electrons out of the sensitive region of the chamber, since it was required that an emerging track have a length of 5 cm to be "measurable."

The average energy losses were formed for those electrons whose curvatures could be measured on both sides of the absorber (or, in the case of reflections, whose curvatures could be measured before and after reflection.) These were then divided by what might be considered the *effective* thickness of the absorber when the obliquity of incidence and emergence is taken into account; for this quantity the attempt was made to find what might be regarded as upper and lower limits. As an estimate of the upper limit for the effective thickness, the average was taken of the thickness times the secant of the larger of the angles of incidence and emergence (for the few cases of reflections, the *sum* of the secants of the two angles was taken); as an estimate of the lower limit, the average was taken of the thickness times the secant of the smaller of the angles (in the case of reflections, *zero* was taken as the minimum thickness). The estimate of the mean effective thickness was simply the thickness times the average of the secants of all the angles of incidence and emergence. The spread in the energy loss per gram per square centimeter as calculated with these various values for the thickness of the absorber was not very great, as can be seen from Table II. The losses to be expected from inelastic collisions are 30 percent greater in the carbon than in the lead, the values, as given above, being 0.33 mc^2 and 0.44 mc^2 for the lead and carbon respectively. The expected radiative loss increases the theoretical average loss in the lead to 0.42 mc^2. Referring to Table II one sees that

TABLE II. *Average energy loss and fractional energy loss in carbon and lead. The figures give the average measured energy loss and fractional energy loss per gram per square centimeter calculated from the following figures: Av. energy loss in C = 0.233 mc^2, average fractional loss in C = 0.0515; Av. energy loss in Pb = 1.09 mc^2, average fractional loss in Pb = 0.225. The various columns have the following significance: a, from directly measured thickness; b, from estimate of lower limit of effective thickness; c, from estimate of upper limit of effective thickness; d, from estimate of the mean effective thickness.*

Element	Av. Energy Loss (mc^2/g·cm^{-2})				Av. Frac. Energy Loss (per g·cm^{-2})			
	a	*b*	*c*	*d*	*a*	*b*	*c*	*d*
Carbon 0.130 g·cm^2	1.79	1.74	1.64	1.69	0.396	0.384	0.363	0.374
Lead 0.158 g·cm^2	6.9	8.4	5.1	6.3	1.42	1.72	1.05	1.30

the carbon results are below the theoretical by 0.2 mc^2; a calculation of the probable error, taking into account fluctuations and errors of measurement leads to values close to 0.2 mc^2 for both the carbon and the lead. Hence the disagreement in the carbon can be explained on this basis, but if we apply a similar probable error to the energy loss found in lead, so that we have in the average *rate* of loss (expressed per $g \cdot cm^{-2}$) a probable error of 1.2 $mc^2/g \cdot cm^{-2}$, the experimental values (see Table II) indicate losses significantly greater than predicted by theory (2.7 $mc^2/g \cdot cm^{-2}$), even when the estimate of the upper limit for the effective thickness is used.[5]

A second comparison with theory—one which concerns itself with the *large* (radiative?) energy losses—may be made by calculating, for example, the theoretical probability of an incident electron experiencing in the lead strip a radiative loss between 0.45 and 0.55 of its initial kinetic energy. With the following notation:

$\mu = mc^2$ = the rest energy of the electron,
E_0 = initial total energy of the electron in units of mc^2,
k = energy of emitted quantum,
Ndl = number of atoms per cm^2 of the absorber,

Heitler[6] defines the probability of the emission of k in the range $dk/(E_0-\mu)$ by

$$\text{probability} = Ndl\phi_k dk/(E_0-\mu).$$

Substituting in the above $Ndl = 4.65 \times 10^{20}$, $dk/(E_0-\mu) = 0.1$, and the value of ϕ_k appropriate[7] to $k = 0.5(E_0-\mu)$ and $E_0 = 6\ mc^2$, one has for this probability the value 0.003. Thus the theory indicates the probability of a fractional (radiative) energy loss in the interval 0.45–0.55 to be 3 : 1000 for the thickness of lead used; actually, as can be obtained from the histogram shown in Fig. 2, we find experimentally that of the total 55 measured tracks, 5, or 91/1000, lost a fraction of their energy lying in this range. Since electrons which have suffered large losses should in any case not be less likely to be scattered, nor more likely to be "measurable," than those with small losses, our experimental value for the probability of practical losses in the range 0.45–0.55 is thirty times the theoretical.

Although the number of tracks in the histogram interval from which this experimental value was obtained is small, the fact that the distribution is fairly smooth in this region suggests that statistical fluctuations cannot account for a significant part of the discrepancy. Further, the marked difference between the distribution found for lead and that for the carbon absorber demonstrates that the large losses in the lead arise from processes other than those ascribable to electrons, i.e., they are due to interaction with nuclei. A possible resolution of the difficulty is to suppose that the path taken by the electron in the lead is very tortuous, and in some cases is so long that the resulting loss is many times that due to a straight traversal. Such deviations as are required to account for the long paths are caused by elastic scattering by nuclei. (The alternative of electronic scattering has been shown above to be untenable, while inelastic nuclear scatterings are, on current theory, almost exclusively radiative and these do not concern us at the moment.) A formula by Mott[8] gives the fraction of tracks deflected through an angle greater than some angle θ in terms of absorber, energy, etc. Employing this formula and Wentzel's criterion as stated by Rasetti,[9, 10] we find that single scattering only is effective for angles of deviation greater than 50°. This shows that elastic scattering cannot greatly increase the path.

Conclusion

As a result of this investigation, we feel that there are serious difficulties in fitting the energy losses—specifically, the large energy losses—observed for electrons traversing lead absorbers to those predicted on the basis of present theory. This difficulty has been encountered by the investigators,[1, 2] working with heavy gases in a cloud chamber; those results of Leprince-

[5] If electrons which have undergone reflection are excluded from the average, this latter quantity is reduced by 17 percent. However, there appears to be no convincing reason for excluding reflections, as is sometimes done.

[6] W. Heitler, *The Quantum Theory of Radiation* (Oxford, 1936), p. 165.

[7] Obtained from curves given by Heitler, reference 6, p. 170.

[8] F. C. Champion, Proc. Roy. Soc. **A153**, 353 (1936).

[9] G. Wentzel, Ann. d. Physik **69**, 335 (1922).

[10] F. Rasetti, *Elements of Nuclear Physics* (Prentice-Hall, 1936), p. 74.

Ringuet[2] which were concerned with the traversal of a lead lamina by electrons in the energy range we have investigated also indicate that the losses are above the theoretical. Similar discrepancies have been reported by Skobeltzyn and Stepanowa.[11]

In this connection it might be pointed out that a recent note by Jaeger[12] reports the result of calculating the theoretical radiative losses without having recourse to a Born approximation. For electrons of 1.5 Mev initial energy, Jaeger finds that the probability for a fractional loss of 0.5 is roughly thirty percent greater, in Pb, than that given by the approximate values we have used. For electrons of higher initial energy the corrections are presumably even smaller, except in those cases where the electron loses nearly the whole of its energy. These corrections therefore do not help to clear up the discrepancies that we have found.

Because of the difficulties mentioned above, it is planned that the experimental investigation of the subject will be continued by others in this laboratory.

ACKNOWLEDGMENTS

We are deeply grateful to Professor E. O. Lawrence for the privilege of working in his laboratory, to Dr. F. N. D. Kurie for his valuable help and advice throughout the course of the work, and to Professor J. R. Oppenheimer and Dr. A. Nordsieck for several helpful discussions of the theoretical features. The work was aided by grants to the laboratory from the Chemical Foundation and the Research Corporation. One of us (D. G. H.) thanks the Royal Commission for the Exhibition of 1851 for personal assistance.

[11] D. Skobeltzyn and E. Stepanowa, Nature **137**, 234, 456 (1936).
[12] J. C. Jaeger, Nature **140**, 108 (1937).

NOVEMBER 15, 1937 PHYSICAL REVIEW VOLUME 52

The Normal Energy Distribution of Photoelectrons from Sodium

CARL F. J. OVERHAGE
California Institute of Technology, Pasadena, California
(Received August 30, 1937)

The theory of the normal energy distribution of photoelectrons has been reformulated by including the effect of contact potential; if photoelectric currents are plotted against applied retarding potentials, the apparent stopping potential at 0°K is shown to be independent of the cathode work function. Apparatus has been constructed for the precise determination of the normal energy distributions of photoelectrons from sodium. Photoelectric currents emitted by monochromatic light were measured after passage through a retarding field. The results of such measurements were found to vary with changes of the anode potential barrier. Energy distribution curves taken at different frequencies exhibit satisfactory mutual consistency; when plotted logarithmically they are of identical shape. This shape does not agree with the theoretically predicted normal energy distribution. An explanation for this discrepancy is given in terms of the structure of the anode potential barrier. A method for the determination of h/e is suggested, which is based on the consistency in shape of the empirically determined curves.

INTRODUCTION

ON the basis of Fowler's[1] theory of photoelectric emission, the energy distribution of photoelectrons in the temperature dependent high energy region has first been discussed by DuBridge,[2, 3] who developed theoretical expressions for the distribution in "normal energy," i.e., in the energy associated with the momentum component normal to the surface, and for the total energy distribution. Shortly afterwards, DuBridge and Hergenrother[4] published the results of experimental work on the normal energy distribution of photoelectrons from molybdenum,

[1] R. H. Fowler, Phys. Rev. **38**, 45 (1931).
[2] L. A. DuBridge, Phys. Rev. **43**, 727 (1933).
[3] L. A. DuBridge, *New Theories of the Photoelectric Effect*, (Paris, 1935).
[4] L. A. DuBridge and R. C. Hergenrother, Phys. Rev. **44**, 861 (1933).

in which good agreement with the theory was obtained for a range of temperatures from 300° to 965°K, and for wave-lengths between 2400A and 2700A. Since that time, the attention of experimenters has generally been confined to determinations of the total energy distributions. For this case, however, the theoretical treatment[2, 3] involves additional approximations; moreover the experimental realization of a spherically symmetrical retarding field appears to be more difficult than that of the simple homogeneous field required for normal energy determinations. The author has therefore investigated the normal energy distribution of photoelectrons from sodium, in an attempt to gain further information on the validity of current photoelectric theory.

Theory

In an experiment of the type here considered, the dependence of the photoelectric current on the voltage of the homogeneous retarding field is determined for a number of frequencies. For each frequency, it is possible to ensure constant values of the intensity, of the illuminated area, and of the temperature of the cathode. Under those conditions, DuBridge[2, 3] obtains the following expression for the current:

$$I = C_\nu \varphi(y). \tag{1}$$

C_ν is a constant for each frequency; $\varphi(y)$ is Fowler's universal function,

$$\varphi(y) = \begin{cases} (e^{y} - e^{2y}/2^2 + e^{3y}/3^2 - e^{4y}/4^2 \pm \cdots), & y \leqslant 0 \\ (y^2/2 + \pi^2/6 - [e^{-y} - e^{-2y}/2^2 + e^{-3y}/3^2 \mp \cdots]), & y \geqslant 0 \end{cases} \tag{2}$$

of the argument

$$y = \frac{h\nu - (W_a^{(1)} - \mu^{(1)}) - Ve}{kT}. \tag{3}$$

The quantities $W_a^{(1)}$ and $\mu^{(1)}$ refer to the emitting surface; V is considered positive when retarding.

With certain changes in DuBridge's original treatment, it is possible to give an elementary derivation of Eq. (1) on the basis of three definite assumptions:

(1) The energy $h\nu$ of the photon is communicated to the electron in such a way that only its momentum normal to the surface is changed.

(2) The probability that an electron will be put into a state of higher energy by an incident quantum is proportional to the electron's initial velocity normal to the surface.

(3) The transmission coefficients at the boundary are

$$D(\epsilon_n, \nu) = 0, \quad \text{when} \quad (\epsilon_n + h\nu) < W_a,$$
$$D(\epsilon_n, \nu) = 1, \quad \text{when} \quad (\epsilon_n + h\nu) \geqslant W_a.$$

This derivation has since been supplemented by a more rigorous quantum-mechanical treatment. Assuming a free electron model with image field boundaries, Mitchell[5] has been able to derive substantially the same expression for the current voltage relation.

A retarding field V existing between two parallel electrodes arises, in general, from two contributions. In addition to the externally applied and measured potential difference V_p it is necessary to consider the contact potential difference V_c between the metals of anode and cathode. This contact potential difference can be re-expressed[6] as

$$V_c = -\frac{1}{e}[(W_a^{(2)} - \mu^{(2)}) - (W_a^{(1)} - \mu^{(1)})], \tag{4}$$

where the superscripts (1) and (2) refer to the cathode and anode, respectively. Since $V = V_p + V_c$, the argument y may now be written in the form

$$y = \frac{h\nu - (W_a^{(2)} - \mu^{(2)}) - V_p e}{kT}. \tag{5}$$

This substitution is of great convenience in the analysis of experimental curves in which the photoelectric currents are plotted as a function of the applied retarding potential; the comparison of such curves with the Fowler-DuBridge theory can be effected without determining the contact potential difference.

It has frequently been observed that curves of this type (current *vs.* applied potential), taken at different times with the same frequency, are displaced with respect to each other along the

[5] K. Mitchell, Proc. Camb. Phil. Soc. **31**, 416 (1935).
[6] C. Eckart, Zeits. f. Physik **47**, 38 (1928).

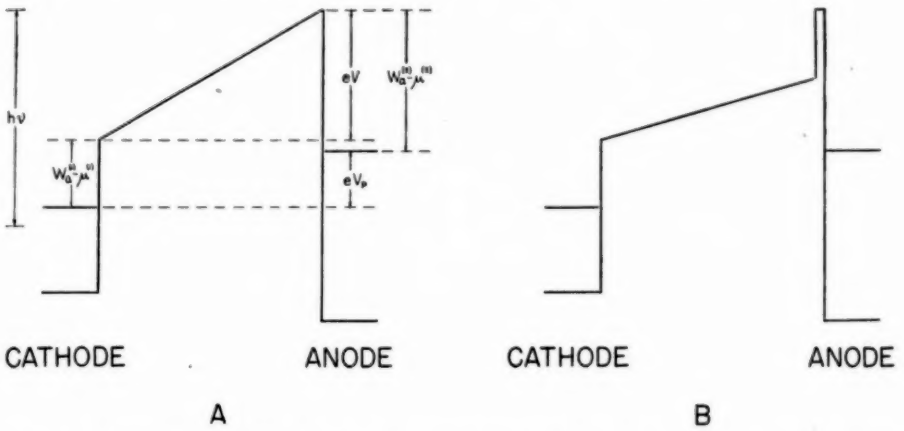

FIG. 1. Schematic representation of cathode and anode potential barriers. *A*, pure surfaces, *B*, anode barrier altered by adsorbed sodium. V, effective retarding potential, V_p, externally applied potential.

voltage axis. At 0°K, such displacements could be concisely described as changes in stopping potential. The present formulation brings out clearly that such shifts are to be attributed to changes in the work function of the anode. The underlying principle, as will be clear from the schematic representation of Fig. 1A, consists in the fact, long ago recognized by Millikan, that any change in the work function of the cathode is nullified by a corresponding change in the contact potential difference. In the case of experiments with alkalis, such changes of the anode work function can be plausibly explained as resulting from the gradual accretion on the anode of evaporated material from the cathode. Direct experimental evidence in support of this suggestion will be presented below.

EXPERIMENTAL ARRANGEMENT

The principal difficulties encountered in the construction of a satisfactory photoelectric tube for the present purpose arose from the gradual evaporation of sodium from the cathode. This necessitated, in the first place, extremely careful insulation of the anode, in order to circumvent the formation of leakage paths between anode and cathode. At the same time, provisions had to be made, by which the anode could be heated, and accumulated sodium atoms removed, without opening the apparatus, or interrupting any of its normal functions. Nickel was chosen as the anode material; its high work function permits the use of a large range of frequencies without interference from reverse currents. The supporting disk for the sodium cathode also consisted of nickel.

The general features of the tube will be clear from Fig. 2; its individual parts are represented in detail in Fig. 3. The central chamber contained the electrodes in their normal position. A quartz window, attached by means of a graded seal, provided for the illumination of the cathode at a large angle of incidence.

Two $2\frac{1}{2}$-inch tubes, whose axes enclosed an angle of 135°, were attached to the sides of this chamber. The electrodes were supported by glass tubes sliding in somewhat larger tubes, which, in turn, were rigidly attached to the outer walls. By means of glass enclosed iron armatures, the electrodes could be magnetically withdrawn from the central chamber into the side tubes, and rotated around the axes of the latter.

In the retracted position, the anode was located in the field of a high frequency furnace with which the electrode could be heated in order to eliminate adsorbed sodium. Fig. 3*A* shows the details of the anode support which provided a carefully baffled insulation path, over 18 inches long, between the electrode and the sliding Pyrex tube. This arrangement has been found entirely adequate to suppress internal leakage currents.

The cathode was mounted in such a way that its normal made an angle of 45° with the axis

of its side tube. In the retracted position, it could thus be rotated 90° around the latter axis, so that its surface was exposed to the opening of the sodium vapor inlet (Fig. 3*B*). The angular disposition of the side tube served the additional purpose of preventing evaporation of sodium by radiated heat from the anode.

The electrodes themselves were circular nickel disks, $1\frac{3}{4}$ inches in diameter, 0.008 inches thick, each with a cylindrical crimped edge $\frac{1}{8}$ inch wide. The separation of the electrodes, in the working position, was slightly less than $\frac{1}{2}$ inch. Electrical connections to the electrodes were made through helical tungsten springs of sufficient tension to prevent contact with the outer walls of the side tubes.

The apparatus was evacuated by a double mercury diffusion pump, backed by a Hyvac. Two liquid-air traps in series were inserted between pumps and tube, and a charcoal side tube was arranged directly below the central chamber of the tube.

During evacuation, the entire tube was surrounded by an electric furnace, and kept at a temperature of about 450°C for one week. The furnace was then temporarily removed, and each electrode heated for thirty minutes by induced high frequency currents. Then the tube furnace was reinstalled, and the tube baked for another week. After this second heating, the charcoal tube was kept immersed in liquid air. While this outgassing treatment would not be adequate for determinations of the characteristic photoelectric properties of pure metals, it has proven sufficient to ensure photoelectric surfaces which could be used for periods of over fifty days without perceptible decrease of sensitivity.

The sodium used as the photoelectrically active material was carefully predistilled, and transferred to the apparatus in an evacuated container with breakable tip. From this container, it was evaporated onto the cathode by means of an electric furnace. A visible deposit of matte white appearance was formed on the cathode.

Radiation from a quartz mercury arc, operated by a special voltage-regulated generator, was passed, in succession, through two Hilger quartz monochromators. The effective absence of stray light was indicated principally by the results of the energy distribution determinations, which will be discussed later on. The constancy of the illumination during the period required for the measurements at one particular frequency was established by the use of the resulting curve itself. The individual points on the curves were not taken in simple succession, but, beginning at the low current end, alternate points were determined, until the high current end was reached, whereupon the intermediate points were determined in the reverse order. If the points thus obtained were found to lie on smooth curves, it could be assumed that the required constancy of illumination prevailed throughout the time of measurement.

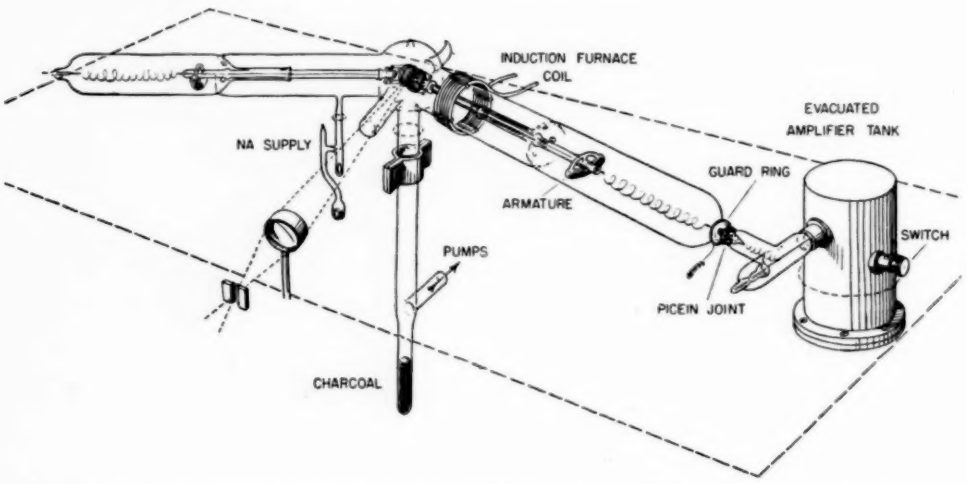

FIG. 2. General view of photoelectric tube (shielding removed). Amplifier tank and glass connecting piece form a separate vacuum system.

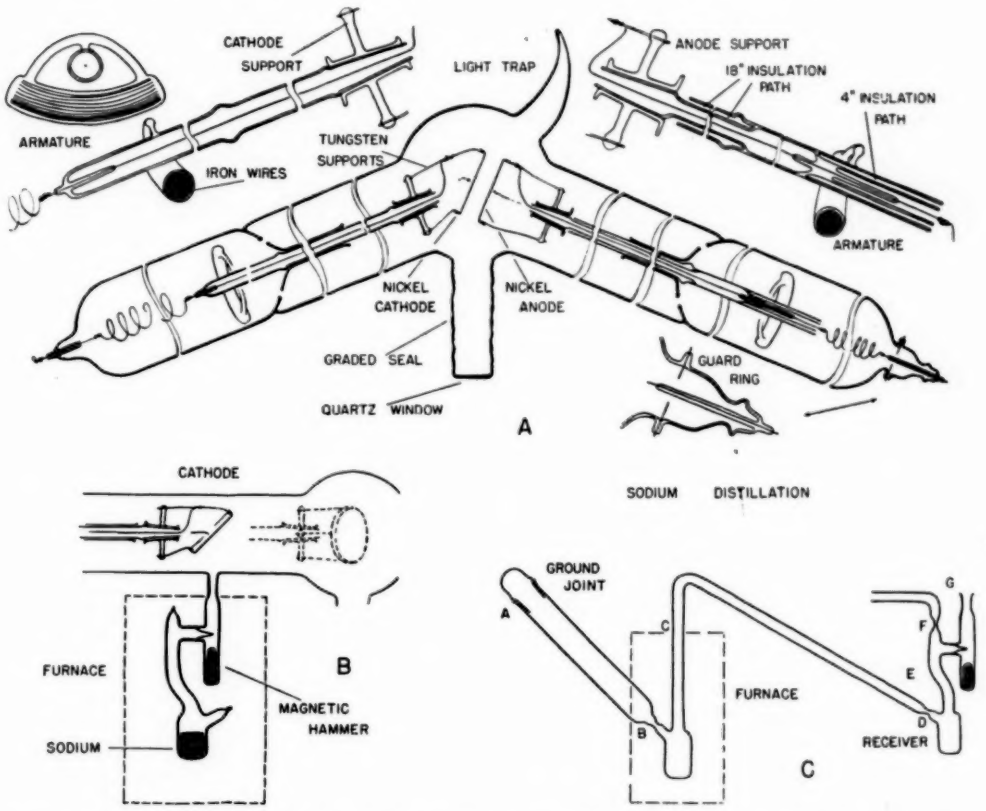

FIG. 3. Construction details of photoelectric tube. *A*, top view, *B*, side view, *C*, sodium distillation.

The essential features of the electrical apparatus for the production and measurement of the retarding field, and for the measurement of the photoelectric currents, are shown in Fig. 4. The potential for the retarding field was obtained from a six-volt storage battery by means of a potential divider. This potential was applied to the cathode, while the anode was connected to ground through the grid resistance of the amplifier system. The correction for the drop between anode and ground could be easily and accurately determined from the calibration curves of the amplifier.

The amplifying circuit was of the type designed by DuBridge and Brown,[7] operated at a maximum voltage sensitivity of 200,000 mm per volt. The amplifying tube itself, the grid resistance, and a calibration switch were contained in an evacuated brass chamber, which was directly attached to the end of the photoelectric tube. The circuit for the supply and measurement of the retarding field was also used for the calibration of the amplifier. Calibration potentials could be applied to the control grid of the pliotron by means of a cam-operated switch in the tube chamber. In determinations of complete sets of data, amplifier calibrations were performed both before and after the actual measurements.

Careful electrostatic shielding was applied to the photoelectric tubes, and to all parts of the electrical circuit.

MEASUREMENTS AND RESULTS

Almost immediately after deposition of the first coat of sodium, it became apparent that very considerable changes of the anode work function were taking place. These variations manifested themselves in displacements, along the voltage axis, of the entire set of current voltage curves. After introduction of the sodium, the curves shifted in the direction of decreasing retarding fields. This displacement was, in one

[7] L. A. DuBridge and H. Brown, R. S. I. **4**, 532 (1933).

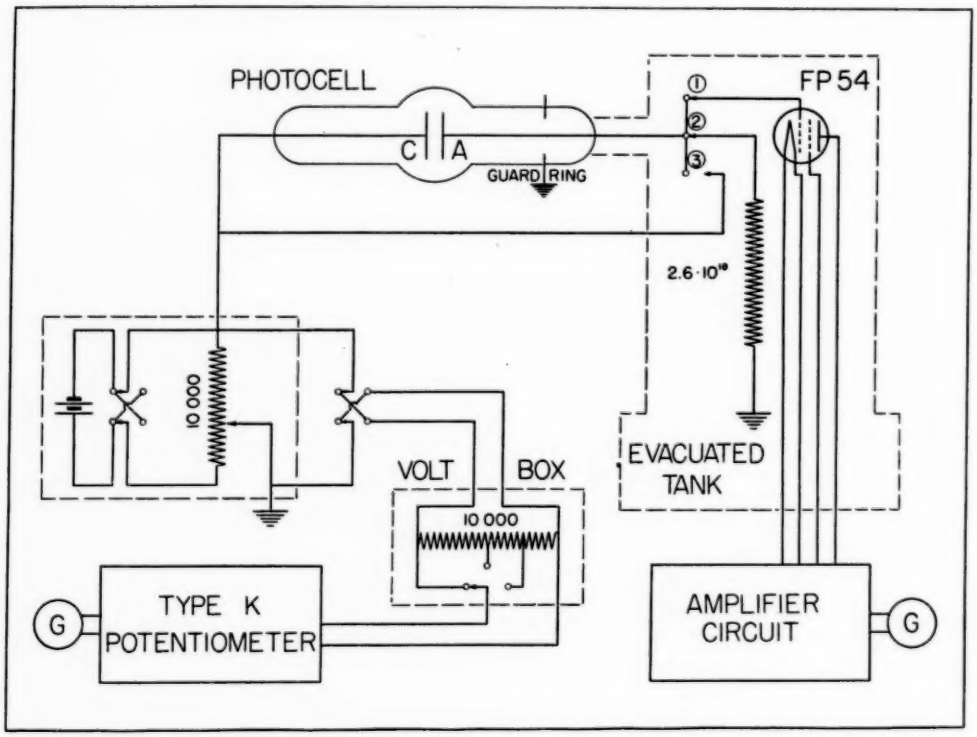

FIG. 4. Circuit diagram. For amplifier calibrations, switch (2) is opened, switch (3) is closed.

case, observed to amount to about 0.8 volts within the first twelve hours after deposition of the sodium. The process became gradually slower until, after four weeks, the displacement was only a few hundredths of a volt per week. The complete sets of energy distribution data, to be presented later, were taken at the end of this period.

Upon heating the anode to incandescence, the curves could be displaced back in the direction of increasing retarding fields by approximately the same amounts. After each such operation, the curves would resume their gradual shift toward lower retarding fields.

These variations are entirely consistent with the previously suggested interpretation of the anode work function. It is well known[8] that the presence of alkalis, even in layers of atomic dimensions, on ordinary metals involves a considerable decrease of the work function of such metals. Upon removal, by heating, of the adsorbed sodium, the opposite displacement of the current voltage curves indicated the expected increase of the anode work function. Further evidence in favor of this explanation was obtained from observations of the long wave-length limit of the anode.

Several weeks after deposition of a coat of sodium and repeated heating of the anode, conditions became sufficiently stable to permit the measurement of complete sets of current voltage curves, as shown in Figs. 5 and 6. When these curves were plotted logarithmically, in the manner suggested by Fowler[1] and DuBridge,[2] they exhibited very satisfactory agreement among each other. This is shown in the composite diagram, Fig. 7, which was obtained by selecting one curve, in this case λ4047, as standard, and displacing the curves horizontally and vertically, until their points fell along the standard curve. The amounts of the horizontal displacements are listed on the diagram.

With the exception of two high points originating from λ5461, the mutual consistency of the different curves appears to be well established. Regarding those two points, it should be realized that λ5461 is very close to the low frequency

[8] Cf., for example, R. Suhrmann, Ergeb. d. exakt. Naturwiss. **13**, 148 (1934).

limit of the cathode; the points in question represent the approach of current saturation.

The validity of the energy distribution represented by this composite curve is especially demonstrated by the fact that the points derived from different frequencies represent electrons which have left the sodium with quite different energies. While each curve represents a region of about 0.6 volts near the high energy end of the distribution, the total range of the energies, with which these electrons were emitted from the cathode material, is over two volts. The identical shapes of the corresponding curves not only show that the distributions are independent of the absolute energy of emission, but they also suggest the probable absence of disturbing effects dependent on emission energy. Again, the agreement obtained in the lower parts of these curves constitutes definite evidence for the absence of stray light of higher frequencies; for any distortions of the energy distribution curve as a consequence of scattered light from adjacent spectral lines would certainly not be identical for all five lines.

It thus appears unavoidable to conclude that the curve represented in Fig. 7 represents the normal energy distribution of the photoelectrons for the particular barriers which existed in the tube at that time. Curves obtained with the same sodium surface a week later show the same degree of mutual consistency; moreover, the distribution curves agree with the ones previously taken, in spite of an intervening small change in the anode work function.

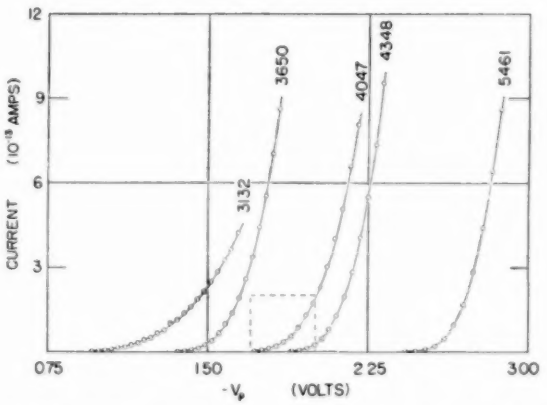

FIG. 5. Current voltage curves. V_p, externally applied and measured potential.

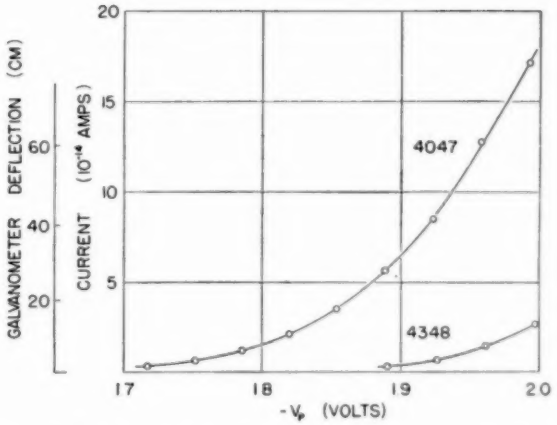

FIG. 6. Lower section of current voltage curves. Scale indicated by dashed rectangle in Fig. 5.

COMPARISON WITH THEORY

The disagreement of the observed distribution with the one theoretically predicted for a temperature of 300°K is shown in Fig. 8. It is of interest to mention here that, in 1936, Hill and DuBridge[9] reported a similar discrepancy in total energy distribution. Recently, another investigation by Mann and DuBridge[10] on absolute photoelectric yields revealed that also in this type of experiment the behavior of sodium does not agree with theoretical predictions. The very careful work by Brady and Jacobsmeyer[11] on total energy distribution also shows that definite agreement with the theoretical curve cannot be obtained (cf. especially Fig. 6 of their paper). In all these cases, the shapes of the observed curves were roughly similar to the theoretically predicted distribution at much higher temperatures. In order to examine this point more closely, a series of theoretical curves was drawn for different temperatures 50° apart. The curve which most nearly fits the observed data is that at 600°K; inspection of the two curves (Fig. 8) clearly shows, however, that systematic differences exist.

In order to explain the difference between observed and theoretical energy distributions, it has been suggested[9, 12] that gas contamination of

[9] A. G. Hill and L. A. DuBridge, Phys. Rev. **49**, 877 (1936).
[10] M. M. Mann and L. A. DuBridge, Phys. Rev. **51**, 120 (1937).
[11] J. J. Brady and V. P. Jacobsmeyer, Phys. Rev. **49**, 670 (1936).
[12] J. J. Brady, Phys. Rev. **46**, 768 (1934).

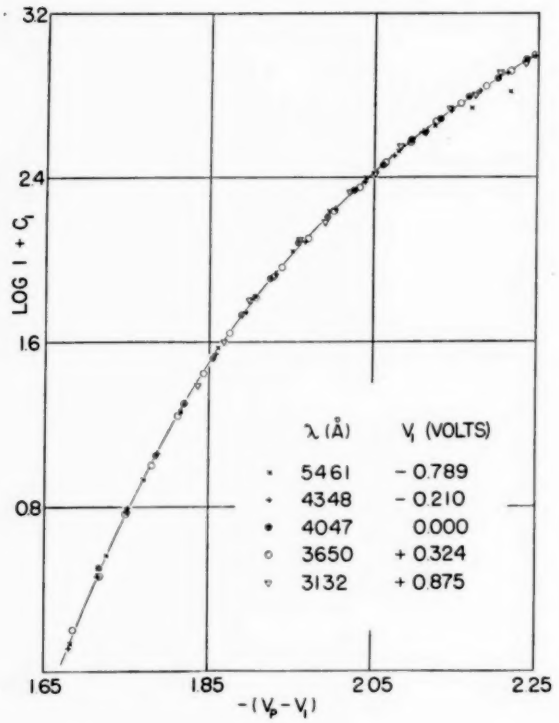

FIG. 7. Composite diagram showing mutual agreement of the shapes of the logarithmically plotted curves. V_i are the horizontal shifts required to bring the curves to coincidence.

the cathode is responsible for the altered shapes of the curves. In spectral distribution experiments, in which the total emission of the cathode is measured in accelerating fields as a function of frequency, such effects have often been observed. In experiments of that type, it is plausible, on a theoretical basis, that a cathode barrier of complicated shape, such as would be produced by gas contamination, would have a decided effect on the transmission of electrons.

In the present type of experiment, which deals with energy distributions at individual frequencies, the situation is, however, quite different. Here a retarding field is joined directly to the cathode potential barrier, and the effect of any change in the shape of the cathode barrier would presumably be restricted to the electrons in the low energy region. Furthermore, the theoretical treatment of Professor Houston[13] suggests that the interaction probabilities are approximately independent of the shape of the cathode potential barrier, provided that the highest point of this barrier is considerably lower than the energy of the slowest electrons which are considered, i.e. considerably lower than the top of the anode barrier. Thus, while it is not contended that the sodium surfaces used in the present investigation were absolutely pure, the explanation of the observed curves on the basis of cathode contamination is not applicable to the high energy region. It is just in the high energy region, however, that the present results, while mutually consistent, exhibit the most conspicuous disagreement with the theory.

On the other hand, under the conditions prevailing in this type of experiment, the nature of the anode potential barrier becomes an important factor. If this should be of a more complex type than the plain discontinuous barrier, and, more particularly, if it should be of the type shown in Fig. 1B, then theoretical considerations would certainly suggest an alteration in the shape of the current voltage curve. Moreover, this type of surface potential barrier is just the one which should be expected to result from the deposition of small quantities of sodium on the anode surface. In view of the experimental evidence for the existence of such adsorbed layers of sodium on the anode, this appears to be altogether the most satisfactory explanation of the shape of the observed distribution curves, although there are further possibilities of interference from surface roughness, small irregularities in the shape of the electric field, and from volume photoelectric phenomena.

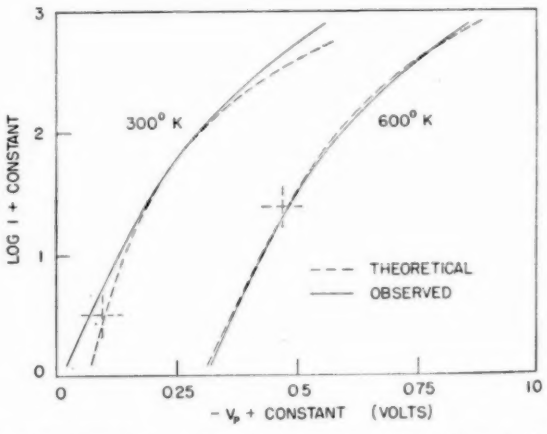

FIG. 8. Comparison of the composite curve of Fig. 7 with 300° and 600°K theoretical curves (Fowler-DuBridge).

[13] W. V. Houston, Phys. Rev., this issue.

One of the most interesting aspects of the mutual agreement of the logarithmic curves consists in the inference that the horizontal displacements necessary to bring the curves to coincidence are identical with the differences $(h/e)\Delta\nu$. On this basis, it appears possible to determine h/e from empirical energy distribution curves which are not in agreement with the Fowler-DuBridge theory. This procedure would, of course, be considerably strengthened by an adequate theoretical explanation of the shape of these curves. Meanwhile it may be of interest to note that an evaluation of the present data from this point of view gave h/e values within one percent of Birge's[14] weighted mean. A further increase in accuracy would thus open the possibility of using empirical curves of this type for a precise photoelectric redetermination of h/e.

ACKNOWLEDGMENTS

The author takes pleasure in acknowledging his indebtedness to Professor W. V. Houston, who suggested this investigation, and has always taken an active interest in its progress, and to all staff members of the Norman Bridge Laboratory who have generously contributed their advice on many technical problems.

[14] R. T. Birge, Nature **137**, 187 (1936).

NOVEMBER 15, 1937 PHYSICAL REVIEW VOLUME 52

The Surface Photoelectric Effect

W. V. HOUSTON
California Institute of Technology, Pasadena, California
(Received August 30, 1937)

The probability of ejection of an electron in the surface photo-effect is expressed in terms of a function of the potential barrier, the energy of the electron after ejection, and the frequency. This function is dominated, for low energies of ejection, by the transmission coefficient of the surface. It is then assumed that the function can be expanded in a power series in terms of the energy of the electron after ejection. In calculating the total emitted current it is shown that the power series development leads to a series of distinctive functions expressing the current in terms of the frequency and the stopping potential. Each of these functions has its own temperature dependence, so that from a complete knowledge of the energy distribution and the temperature dependence of the emitted current it would be possible to draw conclusions as to the nature of the potential barriers. By comparing the theoretical expressions with the observed curves of Overhage, and of Mann and DuBridge, it is possible to conclude that the transmission coefficient of Overhage's anode and of the sodium cathode used by Mann and DuBridge vanished linearly with the diminishing energy of the ejected electrons.

SINCE the development of the quantum theory of solids various attempts have been made to give a theoretical account of the photoelectric emission from metals. The general problem can be divided into two parts which have frequently been treated separately. The first part concerns the interaction of the light with the electrons in the metal and the computation of the probability of ejection. The second part concerns the effect of the statistical distribution of the electrons in the metal on the distribution in energy of those ejected, and the effect of the temperature on the photo-current.

Perhaps the outstanding conclusion from the study of the first problem was the recognition by Tamm and Schubin[1] of the distinction between the surface effect and the volume effect. They pointed out that it is the interaction of the free, or conduction electrons, with the surface potential barrier which makes possible the simultaneous conservation of energy and momentum in the interaction. This cleared up a difficulty of long standing which had been emphasized by

[1] I. Tamm and S. Schubin, Zeits. f. Physik **68**, 97 (1931). Also H. Frohlich, Ann. d. Physik **7**, 103 (1930).

Millikan.[2] The experimental evidence shows quite clearly that the photoelectrons have been free within the metal and have been bound by the surface work function only, and yet the theory also shows that truly free electrons can not absorb the radiation. The recognition that the surface potential barrier provides sufficient binding to satisfy the theoretical requirements, cleared up the difficulty. In the volume effect, on the other hand, the conservation of energy and momentum is made possible by the binding of the electrons to the atoms in the crystal lattice. Tamm and Schubin gave reasons for believing that the selection rules imposed by the periodic structure of the lattice, prevent the onset of the volume effect until a frequency is reached which is considerably higher than that required for the surface effect. Although this conclusion was based on considerations which it is very difficult to make precise, it seems probable that near the long wave-length limit, and in the high energies of the ejected electrons, the volume effect can be neglected entirely.

Mitchell[3] has criticized the work of Tamm and Schubin in some of its details without, however, changing the major conclusions. He also extended the treatment to the case of a potential barrier representing an image field. The first part of this paper will be devoted to the extension of Mitchell's treatment to the case in which the form of the potential barrier is not specifically given, and it will be shown that some conclusions about the barrier can be drawn from the observed currents.

The second part of the problem has been treated by Fowler and by DuBridge.[4] In these treatments various assumptions were made as to the probability of excitation of the electrons, and the assumptions were based to some extent on the possibility of integrating the resulting expressions. These assumptions have been analyzed and classified by Rudberg.[5] Mitchell also worked out this part of the problem on the basis of his results from the study of excitation probabilities, and showed a connection between the form of the transmission coefficient of the surface and the temperature dependence of the photo-current near the threshold. In the second part of this paper the distribution of energies normal to the surface will be calculated, and the dependence of this distribution on the form of the potential barrier will be discussed.

The third part will be concerned with the application of the theory to the experimental results, especially those described by Overhage in the accompanying paper. The fact that the distribution of normal energies measured by a retarding potential should, in the high energy region, be essentially independent of the cathode potential barrier makes it necessary to invoke some other factor to explain the observations. This factor is the potential barrier on the anode, and it is possible to draw some conclusions as to the transmission of this barrier from a consideration of the observed energy distribution.

Part I. Probability of Excitation

In treating the surface photo-effect it will be assumed that the problem is essentially one-dimensional. This is justified by the fact that a change in electron energy parallel to the surface is subject to the restrictions of the volume photo-effect, and may be expected to require frequencies considerably higher than the ordinary threshold. It is also true that an absorption of energy in the motion parallel to the surface reduces the energy available normal to the surface. For both of these reasons this possibility can be neglected near the threshold. In addition it will be assumed that the potential inside the metal is constant, and that the periodic structure is unimportant. This, also, is to be justified on the basis of the selection rules for the volume effect and the restriction of the results to apply to the surface effect.

Consider then a one-dimensional potential field in which three regions are to be distinguished:

Region I	$x<0$,	$V(x)=-W_a$,
Region II	$0<x<x_0$,	$V(x)$ arbitrary,
Region III	$x_0<x$,	$V(x)=0$.

For regions I and III the stationary state wave

[2] R. A. Millikan, Phys. Rev. **18**, 236 (1921).
[3] K. Mitchell, Proc. Roy. Soc. **A146**, 442 (1934); Proc. Camb. Phil. Soc. **31**, 416 (1935).
[4] R. H. Fowler, Phys. Rev. **38**, 45 (1931); L. A. DuBridge, Phys. Rev. **39**, 108 (1932).
[5] E. Rudberg, Phys. Rev. **48**, 811 (1935).

functions can be written down immediately. For $E_f>0$,

$$\psi_f^+=e^{igx}+a_fe^{-igx}, \quad \psi_f^+=b_fe^{ifx}$$
$$\text{and} \quad \psi_f^-=a_f^*e^{igx}+e^{-igx}, \quad \psi_f^-=b_f^*e^{-ifx} \tag{1}$$

form a set of independent solutions with

$$f^2=(2m/\hbar^2)E_f, \quad \text{and} \quad g^2=(2m/\hbar^2)(E_f+W_a).$$

The constants a_f and b_f could be evaluated for any specified form of the potential in region II. Also for $E_k<0$, in region I

$$\psi_k=\alpha_k\cos(kx+B_k), \tag{1a}$$

where $k^2=(2m/\hbar^2)(W_a+E_k)$ and B_k could be determined for a specified potential in region II.

The problem is now to find the perturbation of a given initial state u_k by a light wave whose vector potential is

$$\mathbf{A}=2\mathbf{a}\cos 2\pi\nu(t+x\cos\vartheta/c), \tag{2}$$

where ϑ is the angle of incidence. If the resulting wave function is $u=u_k+v$, with $u_k=\psi_ke^{-i(E_k/\hbar)t}$, v satisfies the equation[6]

$$(\hbar^2/2m)\partial^2v/\partial x^2-(\hbar/i)(\partial v/\partial t)-Vv=$$
$$-(he/imc)A_x\partial u_k/\partial x. \tag{3}$$

Following exactly the procedure of Mitchell leads to

$$v=(2\pi m/hr)(k|a_x|r)^+\psi_r^+e^{-(i/\hbar)(E_k+h\nu)t} \tag{4}$$

for large values of x and t. r is the value of f for which

$$E_r=E_k+h\nu.$$

Corresponding to this value of v is a current, when $x>x_0$, given by

$$j_x=(e\hbar/im)v^*\partial v/\partial x$$
$$=(4\pi^2me/hr)|(k|a_x|r)^+|^2|b_r^+|^2. \tag{5}$$

On the assumption that the wave-length of the light is long compared with the thickness of the potential barrier, so that the vector potential may be treated as constant in the region which contributes to the integral, the matrix element is given by

$$(k|a_x|r)^+=\frac{(e/mc)a_xr}{2\pi g(1-|a_r|^2)}\int_{-\infty}^{\infty}dx\frac{d\psi_k}{dx}$$
$$\times\{\psi_r^{+*}-a_r^*\psi_r^{-*}\}. \tag{6}$$

In region I from $x=-\infty$ to $x=0$ the functions are known, and with a convergence factor as used by Mitchell the integration gives

$$-\frac{(1-|a_r|^2)\hbar^2k\alpha_k}{2mh\nu}\{ig\sin B_k+k\cos B_k\}.$$

The remainder of the integral can be transformed by using the properties of the functions as expressed in the differential equation. Take the equation for ψ_r^{+*} and multiply it by $d\psi_k/dx$. Then differentiate the equation for ψ_k and multiply by ψ_r^{+*}. By subtracting the second from the first, integrating by parts, and using the original differential equation it can be shown that

$$(E_r-E_k)\int_0^{\infty}\psi_r^*\frac{d\psi_k}{dx}dx=\left\{(E_k+C)\psi_k\psi_r^*\right.$$
$$\left.+(\hbar^2/2m)\frac{d\psi_k}{dx}\frac{d\psi_r^*}{dx}\right\}_{x=0}.$$

The quantity C is a mean value of the potential in the barrier defined by

$$C\int_0^{\infty}\frac{d}{dx}(\psi_k\psi_r^*)dx=-\int_0^{\infty}V(x)\frac{d}{dx}(\psi_k\psi_r^*)dx.$$

With the known values of the functions at $x=0$ the matrix element is

$$(k|a_x|r)^+$$
$$=-(ea_xr/2\pi mch\nu g)(W_a-C)\cos B_k\alpha_k. \tag{7}$$

Inserting this value of the matrix element the current from this one initial state is

$$j_x=(e^2/\hbar c)(e/mc)(a_x/h\nu)^2|\alpha_k|^2$$
$$\times|W_a-C|^2\cos^2B_kD(r)/g, \tag{8}$$

where the transmission coefficient

$$D(r)=(r/g)|b_r|^2.$$

[6] The signs of this equation differ from those given by Mitchell because of the consistent use of the opposite convention for the sign of $\hbar/i$.

Let

$$|W_a-C|^2\cos^2 B_k D(r)/g=F(E_r,\nu)k(\hbar^2/2m). \quad (9)$$

The component parts of F are all functions of k and r, and so can be expressed as functions of E_r and ν.

The computation of $F(E_r,\nu)$ can always be carried out by suitable approximation methods if the potential is specified, although in using a W.K.B. approximation care must be taken not to neglect the reflection. For potential barriers made of discontinuities the function can be given exactly in relatively simple form. For a simple discontinuity region II shrinks to zero and

$$F(E_r,\nu)=4(W_a+E_r-h\nu)^{\frac{1}{2}}W_aE_r^{\frac{1}{2}}/\{(E_r+W_a)^{\frac{1}{2}}+E_r^{\frac{1}{2}}\}^2. \quad (9a)$$

For small values of E_r this varies as $E_r^{\frac{1}{2}}$ due to the form of the transmission coefficient. The variation of the other factors is of little importance.

In case the potential rises from $-W_a$ to $+B$ at $x=0$, and then drops to zero at $x=d$, the exact form of $F(E_r,\nu)$ is more complicated. In the important case in which the energy of the bound state is enough less than zero and the thickness of the barrier is not too small

$$F(E_r,\nu)=(W_a+B)^2(W-h\nu+E_r)^{\frac{1}{2}}D(E_r)/W_a(W_a+E_r)$$

with

$$D(E)=\frac{4(B-E)(E+W_a)^{\frac{1}{2}}E^{\frac{1}{2}}}{(B+W_a)B\cosh^2\{(2m/\hbar^2)(B-E)\}^{\frac{1}{2}}d-\{E^{\frac{1}{2}}(E+W_a)^{\frac{1}{2}}-B+E\}^2}. \quad (9b)$$

In each of these cases the behavior at $E_r=0$ is governed by the behavior of the transmission coefficient. In cases in which the potential does not vary too rapidly in the barrier the transmission coefficient will approach a finite value and the derivative will be finite. Under these circumstances the function $F(E_r,\nu)$ can be developed in a power series in E_r with coefficients which are functions of ν but can be expected not to vary too rapidly with it.

Part II. Calculation of Observed Current

Equation (8) gives the current due to the one initial state in which the electron density is $|\alpha_k|^2$. To determine the total photocurrent it is necessary to insert the value of this density, which is given by the Fermi statistics, and to integrate over all of the initial states.

The Fermi distribution function gives the electron density as a function of the energy, and for strictly free electrons this can be expressed in terms of the quantity k. The free electron approximation is certainly very good for the alkalis, but to make some allowance for possible deviations from it let

$$E(k,k_y,k_z)=E(k^2+k_y^2+k_z^2)$$

such that if $k^2+k_y^2+k_z^2=s^2$, and $E(s_0^2)=h\bar{\nu}$,

$$s^2-s_0^2=\beta(E-h\bar{\nu})+\gamma(E-h\bar{\nu})^2, \quad (10)$$

where $h\bar{\nu}$ is the energy for which the Fermi function gives a probability of $\frac{1}{2}$. With the potentials used here $\bar{\nu}<0$. Eq. (10) imposes a condition of spherical symmetry on the energy which is probably satisfied in the region of importance. It may be regarded as the first part of a series expansion in which s^2 is expressed as a function of E. s^2 is expressed as a series in E rather than E as a series in s^2 in order that the required derivatives shall have a simple form.

Let

$$A=(he^3/8m^2c^2)(a_z/h\nu)^2,$$
$$w=\{E(k^2+\rho^2)-h\bar{\nu}\}/\kappa T,$$
$$y=\{E(k^2)-h\bar{\nu}\}/\kappa T,$$
$$\rho^2=k_x^2+k_y^2.$$

Consider first the case in which the saturation current is observed. All of the electrons which penetrate the potential barrier of the cathode will be collected and the total current can be obtained by integrating over all of the electrons with positive E_r. Thus

$$J=2A\kappa T\int_0^\infty kdkF(E_r,\nu)\int_y^\infty\frac{(\beta+2\gamma\kappa Tw)dw}{(e^w+1)}. \quad (11)$$

The integration over k can be transformed to an integration over $E(k^2)$ by Eq. (10) and then to

one over E_r, so if

$$S_1(y)=\int_y^\infty wdw/(e^w+1),$$

$$J=A\kappa T\int_0^\infty dE_r F(E_r,\nu)(\beta+2\gamma\kappa Ty)$$
$$\times\{\beta\log(1+e^{-y})+2\gamma\kappa TS_1(y)\}. \quad (12)$$

The form of this integral will clearly depend upon the form of the function $F(E_r,\nu)$ which is not known and which depends upon the surface potential barrier, especially through the transmission coefficient D. In the case of an image field this transmission has a finite value at $E_r=0$. In the case of the discontinuous potentials mentioned above the transmission vanishes at $E=0$ and increases with $E_r^{\frac{1}{2}}$ above it until in the second case the exponential factor becomes dominant. It seems probable that the increase with $E^{\frac{1}{2}}$ is largely due to the nonphysical discontinuities introduced into the assumed potential, and that in most cases a form of $F(E_r,\nu)$ can be expected which can be expanded in a Taylor series above the point $E_r=0$. At least let us assume this to be the case and let

$$F(E_r,\nu)=F(0,\nu)+E_rF'(0,\nu)+\cdots. \quad (13)$$

From the conservation of energy

$$E_r/\kappa T=y+(h\nu+h\tilde{\nu})/\kappa T=y+x,$$

where $x=+(h\nu+h\tilde{\nu})/\kappa T.$

Eq. (12) then becomes

$$J=A(\kappa T)^2\int_{-x}^\infty dy\{F(0,\nu)+\kappa T(y+x)F'(0,\nu)$$
$$+\cdots\}(\beta+2\gamma\kappa Ty)\{\beta\log(1+e^{-y})+2\gamma\kappa TS(y)\}$$
$$=A(\kappa T)^2\{I_0+\kappa TI_1+\cdots\} \quad (14)$$

with $I_0=\beta^2F(0,\nu)\int_{-x}^\infty dy\log(1+e^{-y})$
$$=\beta^2F(0,\nu)\Phi_0(x),$$

$$I_1=\beta^2F'(0,\nu)(\Phi_1(x)+x\Phi_0(x)\}$$
$$+2\beta\gamma F(0,\nu)\{\Phi_1(x)+\Theta_1(x)\},$$

$$\Phi_1(x)=\int_{-x}^\infty ydy\log(1+e^{-y}),$$

$$\Theta_1(x)=\int_{-x}^\infty S_1(y)dy.$$

In the other case in which only part of the electrons are collected because of the use of a retarding field it is necessary to integrate not from $E_r=0$, but from the minimum value of E_r with which an electron can reach the anode. Let this minimum value be Ve. It is also necessary to take account of the reflection at the surface of the anode since its potential barrier also will, in general, transmit only a part of the electrons. Let $R(E_r-Ve)$ be the anode transmission coefficient, and assume that this can be expanded about the point $E_r=Ve$. Then the observed current will be

$$J=A(\kappa T)^2\int_{-x'}^\infty dy\{R(0)+R'(0)(y+x')+\cdots\}$$
$$\times\{F(0,\nu)+\kappa T(y+x)F'(0,\nu)+\cdots\}$$
$$\times(\beta+2\gamma\kappa Ty)\{\beta\log(1+e^{-y})+2\gamma\kappa TS_1(y)\}$$
$$=A(\kappa T)^2\{I_0'+\kappa TI_1'+\cdots\} \quad (15)$$

where $I_0'=\beta^2R(0)F(0,\nu)\Phi_0(x')$,

$$I_1'=\beta^2\{R(0)F'(0,\nu)+R'(0)F(0,\nu)\}$$
$$\times\{\Phi_1(x')+x'\Phi_0(x')\}$$
$$+\beta^2R(0)F'(0,\nu)(x-x')\Phi_0(x')$$
$$+2\beta\gamma R(0)F(0,\nu)\{\Phi_1(x')+\Theta_1(x')\},$$

and $x'=+(h\nu+h\tilde{\nu}-Ve).$

The various integrals in Eqs. (14) and (15) can be easily evaluated after expansion of the integrands in series. The function Φ_0 is just that given by Fowler. For $x<0$,

$$\Phi_1(x)=-x(e^x-e^{2x}/4+e^{3x}/9-\cdots)$$
$$+(e^x-e^{2x}/8+e^{3x}/27-\cdots)$$

and for $x>0$,

$$\Phi_1(x)=-x^3/3+x(e^{-x}-e^{-2x}/4+e^{-3x}/9-\cdots)$$
$$+(e^{-x}-e^{-2x}/8+e^{-3x}/27-\cdots).$$

TABLE I

x	$\Phi_0(x)$	$\Phi_1(x)$	$\Phi_1+x\Phi_0$	LOG $(\Phi_1+x\Phi_0)$
−5	0.00673	0.04039	0.00674	−2.171
0	0.8225	0.9014	0.9014	−0.045
5	14.138	−41.660	29.030	+1.463
10	51.645	−333.33	183.12	+2.263
15	114.15	−1125.00	587.3	+2.769
20	201.65	−2666.67	1366.3	+3.135
25	314.14	−5208.3	2645.2	+3.422
30	451.64	−9000.0	4549.2	+3.658

A few values of these functions are given in Table I.

PART III. APPLICATION TO EXPERIMENTAL RESULTS

Equations (14) and (15) indicate a number of possible forms of observed current as a function of the variable x. The form to be expected in any particular case depends upon the characteristics of the cathode and the anode as expressed in the functions $F(E_r, \nu)$ and $R(E_r - Ve)$. By comparison of the observed curves with the various theoretical functions one can attempt to draw some conclusions as to the surfaces.

The work of Overhage described in the accompanying paper is characterized by two facts. First, the observations are clearly not to be fitted to the curve $\Phi_0(x)$. Second, the curves for different frequencies can be superimposed with considerable accuracy. These two facts can both be accounted for on the assumption that $R(0)=0$. This leads to the equation

$$J=A(\kappa T)^3\beta^2R'(0)F(0,\nu) \times\{\Phi_1(x')+x'\Phi_0(x')\}. \quad (16)$$

In this expression all of the dependence upon ν is in A and $F(0, \nu)$ which occur in the multiplicative factor. When the logarithms of both sides are taken this dependence upon ν will affect the shift necessary for each frequency, but will not at all affect the shape of the curve. Fig. 1 shows the theoretical curve of $\log\{\Phi_1(x)+x\Phi_0(x)\}$ plotted against x. Superposed on it are points taken from Overhage's composite curve of $\log I$ against $Ve/\kappa T$ after the necessary horizontal and vertical displacements have been made. The agreement is sufficiently good to give one some confidence in the correctness of the suggested explanation. Furthermore, in view of the fact that the anode work function was apparently considerably reduced by a very thin layer of sodium on it, it is not surprising that the transmission coefficient of the barrier should approach zero gradually rather than stopping suddenly.

If it were possible to keep the surfaces of the electrodes, and the work functions, unchanged during a change of temperature, the temperature dependence at the threshold should show a variation with T^3 rather than with T^2. Although an observation of this point would be very interesting it probably presents grave experimental difficulties because of the tendency of a complex surface to change with the temperature.[7] Mitchell indicated that the temperature dependence might be expressible in terms of $T^{\frac{1}{2}}$ on the ground that the transmission coefficient should be expressed as a series in r rather than E. Investigation of this point would certainly throw some light upon the nature of the surface.

Although the agreement between the experimental points and the theoretical curve in Fig. 1 is quite good, there is a definite systematic

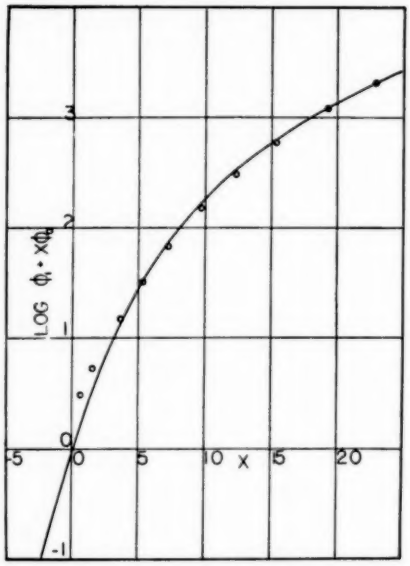

FIG. 1. The solid curve is $\log\{\Phi_1(x)+x\Phi_0(x)\}$ plotted against x. The points are taken from the composite curve given by Overhage in the accompanying paper.

[7] In a paper which has just appeared, Cashman has shown that the observed temperature variation of the photo-current at the threshold is not of the type required by any theory, and has attributed the difference to a temperature dependence of the work function. Whether or not this is a complete explanation, it is a factor which must certainly be considered, and which will complicate the interpretation of the observed currents. Phys. Rev. **52**, 512 (1937).

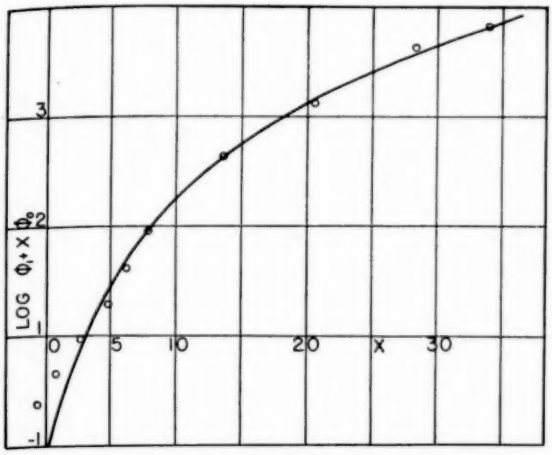

FIG. 2. The curve is log $\{\Phi_1(x)+x\Phi_0(x)\}$ plotted against x. The points are taken from those published by Mann and DuBridge for sodium.

discrepancy, especially at the lower end. This is, of course, the region in which the measured currents are very small and where some experimental error is to be expected. If, however, this discrepancy is regarded as significant, it indicates that the terms in the next power of κT are important. In fact, if to the function $\{\Phi_1(x)+x\Phi_0(x)\}$ there is added $(1/10)\int_{-x}^{\infty}(y+x)\ \log\ (1-e^{-y})dy$, the agreement can be made almost perfect. It is questionable, however, whether the data is such as to justify so detailed a treatment.

Other observations on the photocurrent from sodium which show a lack of agreement with the simple theory have been published by Mann and DuBridge.[8] Since they were observing the saturation current as a function of frequency Eq. (14) should apply. Fig. 2 shows log $\{\Phi_1+x\Phi_0\}$ plotted against x and compared with some points taken from their published curve. The agreement is very similar to that in Fig. 1 and would indicate that the transmission coefficient of the sodium surface which they were using increased from zero with the first, and possibly a small contribution from the second, power of the energy. Correspondingly the current at the threshold should have been roughly proportional to T^3.

In these two cases it is unnecessary to invoke the constant γ to satisfy the observations. This is certainly what was to be expected in the case of the alkalis, although for some other substances it may be necessary. The value of β must then be $(2m)^{\frac{1}{2}}/\hbar$. One can also conclude that in the considerable number of substances for which the observed currents have been shown to follow the Fowler curve, the transmission coefficient is roughly constant above the threshold. This seems to be true rather generally for the heavy metals in very pure condition.

It thus seems possible to determine from the energy distribution of the photoelectrons and from the spectral distribution of the photocurrent something about the nature of the potential barriers on the cathode and on the anode. It may also be possible to study the effect of alkalis, or of oxides, on the surfaces of pure metals by observing the change of the distributions with time.

[8] Mann and DuBridge, Phys. Rev. **51**, 120 (1937).

The Electric Spectrum of Liquid Water from Five to Twenty Centimeters*

HENRY W. KNERR†
University of Michigan, Ann Arbor, Michigan

(Received August 12, 1937)

A magnetron generator was used in the production of continuous electromagnetic radiation with wave-lengths ranging from five to twenty centimeters. The refractive index and absorption index of liquid water were determined for nineteen wave-lengths distributed over this region, by using two completely different methods of investigation. The conventional free wave method was studied and an expression for the energy transmitted through an absorption cell derived. This equation was experimentally verified but it is concluded that one must be very careful to exclude undesirable diffraction effects if satisfactory results are to be secured. It is also shown that several methods of calculation frequently applied are incorrect. A wire wave method suggested by the experiments of Seeberger is presented and discussed. This method is analyzed in detail and a simplified procedure is given in which the determinations of absorption index and refractive index are separated. The two methods were compared at a wave-length of 10.20 cm and an agreement between results to within one percent was secured. The wire wave method has a great advantage because of the high reproducibility of its results while the free wave method is laborious to use and its results are difficult to duplicate. The absorption index was observed to increase steadily from 0.048 at 20.44 cm to 0.153 at 4.80 cm. The average refractive index was 8.80 with only one point differing from the mean by more than 0.6 percent. Although there was no clear evidence of dispersion, reasons are given for expecting a slight variation of refractive index. The expected variation however lies within the limits of experimental error. A very complete comparison is given between the data presented in this paper and the abundant but discordant results previously published.

INTRODUCTION

THE absorption and dispersion of electromagnetic waves by different substances, particularly in the liquid state, has been a subject of study since the classical experiments of Hertz in 1888 and a prodigious number of data has been accumulated. Unfortunately much of this work was done with highly damped sources of radiation and provides us with but little qualitative and practically no quantitative information. Subsequent work with continuous radiation has clarified many of the early experiments and now the long wave spectra of many polar liquids are fairly well established. However, great confusion is still encountered in the very short wave spectrum, which is usually the most interesting because here occurs the region of dispersion in which the refractive index decreases from a high value (square root of the static dielectric constant) to the much smaller value observed in the infrared.

Probably the most extensive investigation in the electric spectrum to be carried out before the advent of modern continuous wave generators was the study of liquid water. Observers with damped waves traced the spectrum of water for wave-lengths ranging from 10^6 down to 0.4 cm and found a very complex structure.[1,2] For wave-lengths greater than 300 cm absorption was found to be very slight and no dispersion was observed, the refractive index being, within the limits of experimental error, equal to the square root of the static dielectric constant. However below 300 cm many bands of dispersion were apparently located, although different observers did not agree upon the location. At the very short wave-lengths an increase of absorption and a sharp decrease of refractive index was indicated but here also flagrant discrepancies exist between different investigators.

With the aid of continuous wave sources and better controlled experiments, these investigations have been repeated in part. For wave-lengths greater than 300 cm continuous wave measurements have confirmed the data of earlier observers. Thus for $\lambda = 391.8$–2547 cm Drake, Pierce and Dow[3] found the refractive index, n,

* Presented in part at the Washington meeting of the American Physical Society, April 29, 1937.

† Now at Pennsylvania State College, State College, Pennsylvania.

[1] Romanoff, "Die Dispersion und Absorption elektrischer Wellen," Geiger u. Scheel, *Handbuch der Physik*, Vol. 15 (1927), p. 491.

[2] Ziegler, Physik. Zeits. **35**, 476 (1934).

[3] Drake, Pierce and Dow, Phys. Rev. **35**, 613 (1930).

at 22°C to be 8.925 while Wyman[4] by a wholly different method found $n_{22}=8.924$ for $\lambda=368.2$–8112 cm. These are in good agreement with $n_{22}=8.899$ for wave-lengths greater than 300 cm as given in the *International Critical Tables*[5] and based largely upon damped wave data. This agreement is not surprising because one would expect the influence of damping to be most marked in a region of dispersion. In the region below 300 cm the complex structure observed by the early experimenters has not been confirmed. Only part of this region has been systematically investigated but no bands of dispersion have ever been found by continuous wave experiments. The more recent results down to 28 cm are summarized in Table I. While there is need for more experiments below 200 cm it is highly probable that there is no dispersion in liquid water for λ greater than 28 cm. There are no continuous wave absorption measurements in this range but the absorption is known to be very slight.

In the region of still shorter wave-lengths the experimental difficulties increase and the disagreement between different observers is great. In addition to the many observations with damped waves, Seeberger[6] and Goldsmith[7] have published results for continuous waves. However these two observers do not agree so that we still have no satisfactory information about the electric spectrum of water below 28 cm. Acceptable results in this region have been greatly delayed by the absence of suitable sources of radiation and by experimental difficulties. The calculations of Malsch[8] have emphasized the necessity of using continuous wave sources. However it is now possible to produce continuous waves in this region by means of the magnetron generator, so the difficulty of securing a proper source is largely removed. While it is questionable whether the radiation from the magnetron is strictly monochromatic,[9] it is unlikely, under proper adjustment, that the band of frequencies would be wide enough to introduce any variation outside the limits of experimental error. The absence of very rapid changes of refractive index in the electric spectrum of polar liquids minimizes the possible effect of such a frequency band.

TABLE I.[1] *Index of refraction of water as determined by various observers.*

WAVE-LENGTHS	NUMBER OF DIFFERENT WAVE-LENGTHS	n_{22}	OBSERVER
267.8–271.14 cm	14	8.89	Deubner[2]
266.1–268.8	2	8.93	Holborn[3]
220–300	141	8.90	Novosilzew[4]
91.24–93.92	3	8.89	Devoto[5]
68.76	1	8.92	Scheremetzinskja[6]
49.13–63.56	20	8.89	Girard and Abadie[7]
36.75–321.44	11	8.88	Heim[8]
28.4–56.7	34	8.85	v. Ardenne, Groos and Otterbein[9]

[1] In his summary of work in this field Ziegler erroneously reported a value of refractive index at 150 cm by Akerlof. Akerlof worked at 150 meters with a comparison method in which he took water as his standard liquid assuming its refractive index from Wyman's work.
[2] Deubner, Ann. d. Physik **84**, 429 (1927).
[3] Holborn, Zeits. f. Physik **6**, 328 (1921).
[4] Novosilzew, Ann. d. Physik **2**, 515 (1929).
[5] Devoto, Gazz. Chim. Italiana **60**, 208 (1930).
[6] Scheremetzinskja, Russ. fiziko-khim. obsh. Zhurnal **59**, 499 (1927.)
[7] Girard and Abadie, Comptes rendus **191**, 1300 (1930).
[8] Heim, Jahrb. d. drahtl. Telegr. **30**, 176 (1927).
[9] v. Ardenne, Groos and Otterbein, Physik. Zeits. **37**, 533 (1936).

The method of investigation most commonly used in the ultra-short wave region is the free wave method in which a beam of radiation, directed by mirrors, is passed through a cell and the reflected or transmitted beam is studied. Since the wave-length in many such experiments is comparable to the dimensions of the apparatus, one must expect serious difficulty due to diffraction. A second general method of directing these waves is the wire wave method in which the waves are guided by a Lecher system so that the energy is largely concentrated between the wires and diffraction is minimized. While there are many variations of the method their use has been confined to the longer wave-lengths.

It is the purpose of the present paper to present a wire wave method which can be used below 10 cm and to report a study of both methods in the ultra-short wave region where they were applied to the investigation of liquid water in the wave-length range 5–20 cm.

FREE WAVE OR OPTICAL METHOD

1. Production of radiation

Conventional split anode magnetron tubes were used in the generator built by Cleeton and Williams.[10] To concentrate the radiation into a

[4] Wyman, Phys. Rev. **35**, 623 (1930).
[5] *International Critical Tables*, Vol. 6 (1929), p. 78.
[6] Seeberger, Ann. d. Physik **16**, 77 (1933).
[7] Goldsmith, Phys. Rev. **51**, 245 (1937).
[8] Malsch, Ann. d. Physik **19**, 707 (1934).
[9] Cleeton, Physics **6**, 207 (1935).
[10] Cleeton and Williams, Phys. Rev. **45**, 234 (1934).

beam, a parabolic brass mirror (diameter 90 cm) was set up in a vertical position with the magnetron tube at its principal focus. The parallel beam of radiation was directed to an echelette grating, the angle of incidence being about $6\frac{1}{2}°$. The paper of Cleeton and Williams gives the details of construction of this grating by means of which wave-lengths up to 12 cm can be measured directly. From the grating the beam of radiation was reflected to a second parabolic mirror at the focus of which was located the detector.

2. Detection

A detector composed of an iron pyrite crystal and a tungsten wire was found to be very satisfactory and was used for all final observations. A thermal detector of the Klemencic type with an Advance-Chromel *C* cross and a tungsten heater wire was used in some of the preliminary work but was abandoned because of ambiguity in the experimental determination of the law of response.

The absorption index of a material is defined as

$$\kappa = (\lambda/4\pi nx) \log (I_0/I_x)$$

where the intensity of radiation of wave-length λ decreases from I_0 to I_x when the thickness of the material in the beam is increased by an amount x. The refractive index of the material is designated by n. The rectified current through the detector is a measure of the energy incident upon it but the precise relation between rectified current and energy must be known before I_0/I_x, and hence κ, can be calculated. Experiments at lower frequencies[6, 11, 12] indicate that the pyrite crystal detector responds linearly to energy but it seemed desirable to verify this at higher frequency inasmuch as the exponent in the law of response enters directly into the calculated absorption index as a multiplicative factor. Thus if the rectified current varies with the β power of intensity and one has assumed linearity, the calculated value of absorption index will be $\beta\kappa$ instead of the true value κ. The law of response can be determined experimentally by controlling the energy incident upon the detector through the use of Hertzian grids. One of these grids consists of a set of suitably spaced parallel wires. That such a grid acts as an analyzer for electromagnetic waves is shown by the experimental work of Hertz[13] and the analysis of Gans[14] and Ignatowsky.[15] When a beam of radiation strikes such a grid it is resolved into two component fields; the one having its electric vector parallel to the wires is largely reflected or absorbed, and the other having its electric vector perpendicular to the wires is largely transmitted. Blake and Fountain [16] found the wire spacing must be of the order of a fortieth of a wave-length for no transmission to occur when the wires are parallel to the electric vector.

The grids used in this experiment were made by fastening copper wires (diameter 0.25 mm) onto wooden frames about 110 cm square. Uniform spacing was secured by winding the wires over threaded rods, two rods being permanently attached to each frame. Since this work was done with approximately 10 cm radiation a wire spacing of 2.5 mm was used. Each frame was mounted so it could be rotated about an axis perpendicular to the plane of the frame. One frame was provided with a graduated circle for reading inclinations. One of these grids was placed about one meter from the detector mirror so as to receive the beam of radiation at normal incidence. When a second grid was used it was placed directly in front of, or behind, the first one and parallel to it. A cylindrical shield of sheet metal one meter long and 90 cm in diameter was attached to the detector mirror and reached to the nearer grid so there was no possibility of diffracted waves passing around the grids and reaching the detector.

When only one grid was used it was found that the radiation from the magnetron generator is plane polarized with the electric vector in the plane of the Lecher wires and perpendicular to them. When the grid wires were set up perpendicular to this electric vector the presence of the grid did not appreciably reduce the intensity; but when the grid wires were parallel to the

[11] Bergmann, Ann. d. Physik **67**, 13 (1922).
[12] Zakrzewski, Bull. Int. Acad. Polon. Sciences Lettres Serie A, 489 (1927).
[13] Hertz, *Electric Waves* (MacMillan, 1893), p. 177.
[14] Gans, Ann. d. Physik **61**, 447 (1920).
[15] Ignatowsky, Ann. d. Physik **44**, 369 (1914).
[16] Blake and Fountain, Phys. Rev. **23**, 276 (1906).

electric vector no measurable energy was transmitted.

When a single grid is used the electric and magnetic field amplitudes transmitted by the grid will vary with cos θ where θ is the angle of inclination of the grid wires measured from the position of optimum response. The energy reaching the detector will vary with $\cos^2\theta$ and the fields will rotate with the grid, the electric field vector remaining perpendicular to the grid wires. By plotting rectified current, as measured by the galvanometer deflection, as a function of the inclination of the grid wires one can determine β, where it is assumed that the rectified current varies with the β power of the incident energy. With one grid this function is $\cos^{2\beta}\theta$ and the calculated value of β is 1.01. Since the fields at the detector rotate, the question of a preferred direction at the detector and the possibility of a second resolution of fields arises. When the detector itself was rotated there was no evidence of a preferred direction, but this test is rather crude since there is considerable danger of shifting the detector slightly away from the focus of the mirror. This question is eliminated by the use of two grids. The one next to the detector is left fixed while the one in front of it is rotated. There is now a resolution of field amplitudes at each grid so the energy transmitted by the grids will vary with $\cos^4\theta$ but the fields at the detector will be constant in direction. Fig. 1 shows a plot of galvanometer deflection as a function of inclination of the rotating grid. For two grids this function is $\cos^{4\beta}\theta$ where

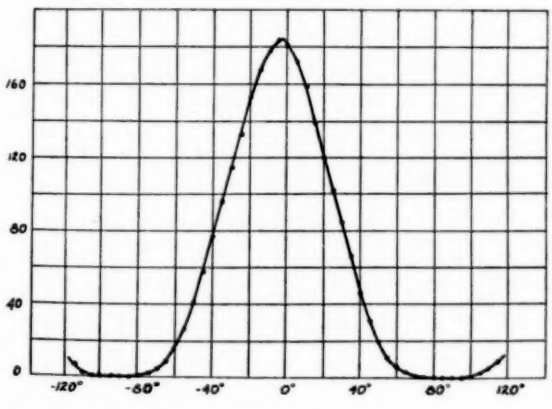

FIG. 1. Calibration curve for an iron pyrite crystal detector. The ordinate is galvanometer deflection in cm; the abscissa the inclination of grid wires measured from an arbitrary position.

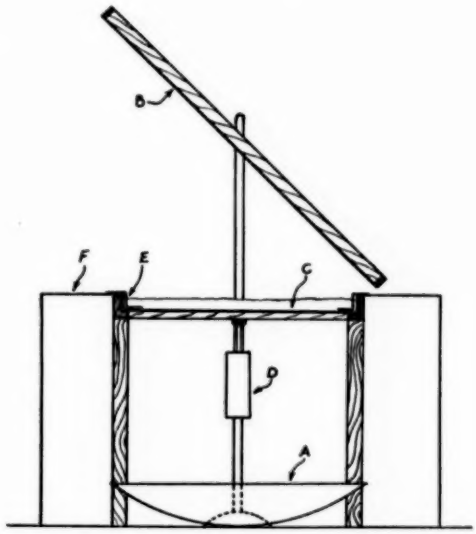

FIG. 2. Diagram of a section through the free wave absorption cell and receiving unit.

β is calculated to be 0.99. If the fields which are not transmitted by the fixed grid should be largely reflected instead of absorbed, there is the possibility of additional energy reaching the detector after multiple reflection between the grids. No evidence of such additional energy was found. From these calibrations it appears that to within about one percent, at most, the crystal detector responds linearly to energy.

3. Absorption cell

A vertical section through the absorption cell is shown in Fig. 2. A horizontal beam of radiation was reflected from the grating to the inclined mirror *B*. This mirror (90×120 cm) was built of 5 mm sheet aluminum attached to a wooden frame. After passing through the cell *C*, the radiation was focused by the parabolic mirror *A* upon the detector *D*. The detector, which was shielded on five sides by a metal box, was connected through a shielding cable to a high sensitivity Leeds and Northrup galvanometer.

The cell (76.2×91.4×4.5 cm) was constructed of plate glass supported by a wooden frame, the glass joints being sealed with a special aquarium cement and paraffin. A guard strip *E* of sheet tin, built to reach completely around the cell, had the effect of placing the cell aperture within the liquid where the wave-length was much reduced. It was hoped that this might minimize diffraction

at the aperture. The guard strip reached out over the heavy sheet metal shield F which completely enclosed the receiving unit except for the cell aperture. When the shield and guard strips were in place it was impossible for any radiation to reach the detector without passing through the cell. A large sheet of metal shielded the cell from any direct rays from the tube. The cell supports were set back from the aperture so that no obstruction was presented to the beam except a narrow soft wood bar which supported the detector.

4. Preliminary experiments

The obvious method of determining the absorption index of a liquid is to vary the thickness of the liquid layer in the beam and observe the transmission. An annoyance immediately arises, however, in the case of liquids of high refractive index because of the high reflectivity of liquid surfaces. The direct beam through the cell is augmented, unless the absorption is very great, by other beams arising from multiple reflection between the liquid surfaces; and the net result is such a curve as is shown in Fig. 3.

It is frequently assumed that one can determine the absorption index from such a curve by drawing a sort of average curve through the middle of the interference maxima and minima. This amounts to assuming that the energy transmitted by the cell can be written as the sum of a simple exponential and one or more periodic terms. On this assumption one calculates values of κ which cannot be verified by other methods. Analysis of the free wave method shows this assumption to be too simple. Moreover there seems to be no satisfactory way of eliminating these troublesome secondary beams. Since they are absorbed more rapidly than the direct beam one can begin observations with enough liquid in the cell to quite completely absorb all but the direct beam. To do so however is to greatly reduce the energy available for observations and to probably endanger the cell bottom since about 20 liters of water is required for 10 cm radiation.

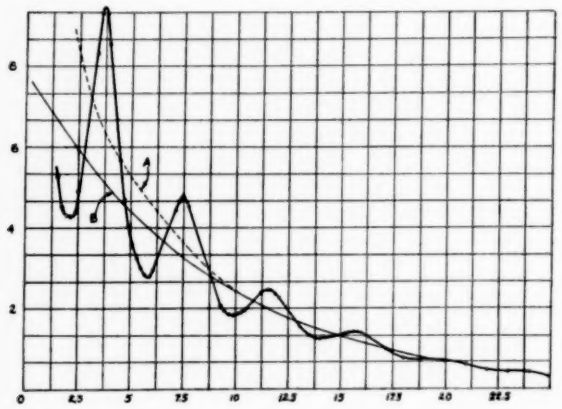

FIG. 3. Interference curve with the free wave method for water at 24°C and for $\lambda = 10.20$ cm. The ordinate is galvanometer deflection in meters (ordinates above three result from reduction to no shunt values); the abscissa is liters of water in the cell (6.95 liters produce a layer of liquid one cm thick).

There is also the possibility of isolating the direct beam by refraction. If one edge of the cell is elevated a bit the liquid layer is converted into a prism surmounted by a uniformly thick layer of liquid which still receives the radiation at normal incidence. Since the direct and multiply reflected beams have different angles of incidence at the lower liquid surface they are separated by refraction. An angular separation of 20° between the direct and twice reflected beam is easily obtained. By tilting the detector mirror these two distinct beams can be picked up. Moreover when the mirror is set to receive the direct beam there is no possibility of the twice reflected beam entering the detector for one can show by rotating the mirror that a beam 10° off the axis has practically no effect. However, when the mirror is set on the direct beam and the thickness of the liquid layer is varied interference peaks are still found. Their spacing is related to twice the layer thickness, so they are evidently due to double reflection within the liquid. The origin of this interfering beam is apparently oblique radiation produced by diffraction at the inclined mirror and the cell aperture. Evidently one must be very careful to avoid undesirable diffraction effects when doing free wave experiments at these wave-lengths.

5. Analysis of the free wave method

Consider a horizontal layer of liquid of uniform but variable thickness x bounded above by air and below by glass. A plane wave strikes the upper surface at normal incidence. Let the electric component of this wave be $E_0 e^{i\omega t}$ where E_0 is the amplitude and ω is the angular frequency. The transmission factor at the air-liquid surface

may be written $Te^{-i\tau}$ where T represents the ratio of transmitted amplitude to incident amplitude and τ gives the retardation in phase upon transmission. Similarly $T'e^{-i\tau'}$ will be the transmission factor at the liquid-glass surface. $Re^{-i\rho}$ and $R'e^{-i\rho'}$ are the internal reflection factors at the upper and lower surfaces, respectively.

The amplitude of the electric vector after direct transmission through the liquid layer will evidently be:

$$E_1=E_0TT'\exp\left[-\alpha x+i(\omega t-\tau-\tau'-2\pi x/\lambda')\right]$$

where λ' is the wave-length in the liquid and α is an abbreviation for $2\pi n\kappa/\lambda$. A wave which is twice reflected internally before entering the glass will have an amplitude: $E_2=E_0TT'RR'\times\exp\left[-3\alpha x+i(\omega t-\tau-\tau'-\rho-\rho'-6\pi x/\lambda')\right]$. In the case of four internal reflections the electric amplitude becomes: $E_3=E_0TT'R^2R'^2\exp\left[-5\alpha x+i(\omega t-\tau-\tau'-2\rho-2\rho'-10\pi x/\lambda')\right]$. No more than four internal reflections need be considered for a liquid which absorbs as strongly as does water, although one can continue and treat an infinite number of internal reflections. Neglecting all internal reflections beyond the fourth we can represent by $E'=E_1+E_2+E_3$ the net amplitude transmitted through the liquid layer into the glass.

The glass-air surface reflects but little because of the low refractive index of glass while the glass-liquid surface will reflect strongly because of the high refractive index of the liquid. Hence no appreciable part of the wave which once enters the glass will ever get back into the liquid and then reenter the glass. In passing from within the glass to the detector, changes of phase and amplitude will occur; but all terms of E will be equally affected and there will be no dependence upon x. If A represents the fraction of amplitude transmitted and θ the retardation in phase in passing from within the glass to the detector, the electric field at the detector may be written $E=E'Ae^{-i\theta}$. The average energy reaching the detector may be written aEE^* where a is a constant and E^* is the complex conjugate of E. Computing we have:

$$\begin{aligned}\text{Energy}=B(&e^{-2\alpha x}+2RR'e^{-4\alpha x}\cos\phi\\&+R^2R'^2e^{-6\alpha x}+2R^2R'^2e^{-6\alpha x}\cos 2\phi\\&+2R^3R'^3e^{-8\alpha x}\cos\phi+R^4R'^4e^{-10\alpha x}),\end{aligned}\quad(1)$$

where $B=aA^2E_0^2T^2T'^2$ is a constant and $\phi=2\pi(2x/\lambda')+\rho+\rho'$. Additional terms of higher order in $RR'e^{-2\alpha x}$ would occur had we not neglected internal reflections beyond the fourth. If $RR'e^{-2\alpha x}$ is very small this equation indicates the usual exponential decrease of transmission with increasing thickness. When this condition is not met it may be that Eq. (1) can be approximated by its first two terms. This will be the case for liquids with a low refractive index, high absorption index or for any liquid after a certain thickness is reached. Under these circumstances, and only then, is the calculation of absorption index from an average curve drawn through the experimental curve permissible. For water at 10 cm a layer of water about 15 mm thick is necessary to meet these requirements. For thinner layers additional terms must be taken into account. At a wave-length of 10 cm, RR' is approximately 0.5 and $e^{-2\alpha x}$ varies in value from about 0.8 to 0.3 over the first half of the experimental curve, so we can safely omit the last two terms of Eq. (1) for water at 10 cm or less.

We have then finally:

$$\begin{aligned}\text{Energy}=B\{&e^{-2\alpha x}+2RR'e^{-4\alpha x}\\&\times\cos\left[2\pi(2x/\lambda')+\rho+\rho'\right]+R^2R'^2e^{-6\alpha x}\\&+2R^2R'^2e^{-6\alpha x}\cos 2\left[2\pi(2x/\lambda')+\rho+\rho'\right]\}\end{aligned}\quad(2)$$

where $$\alpha=2\pi n\kappa/\lambda.$$

It is possible to determine κ and also n from an experimental curve without completely isolating any of these four terms. We note that the last term has a maximum value whenever the second term has either a maximum or minimum value so that its effect is to shift all of the maxima and minima of Eq. (2) up by an amount which depends upon x. If, by trial and error, we draw a curve through the interference maxima and minima in such a fashion that the successive maximum deviations of this curve from the experimental curve decrease exponentially we effectively isolate the extremes of the second term. Such a curve, illustrated by curve A, Fig. 3, would constitute an average curve in the sense in which that term is used in this work. The maximum deviations of the experimental curve from the average curve are the extreme values of the second term in Eq. (2). Since the

spacing of these maximum deviations is $\lambda'/4$ we can calculate the refractive index from their spacing. Also the ratio of successive extreme values is $e^{-2\pi\kappa}$ from which κ can be calculated. At the points where this second energy term is an extreme, curve A represents the sum of the other three energy terms. Having calculated n and κ we can also plot the first term of Eq. (2) which is represented by curve B in Fig. 3. The ordinate difference $A-B$ is due to the second and third terms of Eq. (2) and therefore should decrease with $e^{-6\alpha}$.

6. Discussion

The conclusions drawn from this analysis are experimentally verified. Fig. 3 was obtained for a wave-length of 10.20 cm and at a temperature 24.0°C. From the analysis of the second term in Eq. (2) we have $n=8.85$ and $\kappa=0.078$. If we calculate κ from the ordinate difference $A-B$ we find 0.075. These results may be compared with $n=8.80$ and $\kappa=0.077$ obtained by wire wave methods. It is obvious that if we assume the average curve A to be a simple exponential and calculate κ from it we will get a value which is too large. This fact was observed many times in the course of this work. Unfortunately it is not possible to check on this point from other work in this region because too many other uncertainties enter. Thus if diffraction around the cell is not prevented, this will operate to make the absorption index calculated from the average curve too small, so that a partial compensation may occur.

We may note that the refractive index must be determined from the periodic term and not from the total curve. The spacing of the maxima and minima of the periodic term gives the true wave-length in the liquid because the spacing of the extremals of the function $e^{-\alpha x}\cos\beta x$ is the same as the spacing for the cosine function alone. Multiplication by the exponential shifts the maxima and minima but by a constant amount. When the function $e^{-\alpha x}\cos\beta x$ is added to another exponential, however, the maxima are shifted toward smaller values of x and the minima are shifted toward larger values of x by an amount which depends upon x. If one determines the wave-length in the liquid from the total curve by measuring from the first minimum to the first maximum he obtains values which are too small. The calculated refractive index then becomes too large. This accounts for the unusually large values of refractive index found by Zakrzewski[12] and by Miesowicz.[17] It also explains the curious observation of Miesowicz that at about 7 cm the refractive index of water increased with decreasing wave-length, inasmuch as the error pointed out will increase with increasing absorption, i.e., with decreasing wave-length.

Wire Wave Method

1. Apparatus

The design of the horizontal Lecher system and the absorption cell (Fig. 4) was suggested by the work of Seeberger.[6] The cell C (18.5×18.5×15.0 cm) was built of soft wood 13 mm thick and lined with rubberized cloth. The Lecher wires L were copper (dia. 1.9 mm) and were spaced one centimeter apart. They were sealed into the front cell wall but the length outside the cell could be varied from 73 to 83 cm by means of the trombone arrangement T which consisted of a 15 cm section of brass tubing (3.3 mm outside dia.) into which the movable end section of the Lecher system fitted. This end section was inductively coupled to the magnetron tube. The Lecher system was supported at the trombone by a pin of soft wood. The open end of the Lecher system came within the cell. The reflecting bridge B (8×13×0.3 cm) was made of brass. The wires passed through the bridge by means of two small holes which fitted the wires closely. By means of the micrometer screw M, the displacement of the bridge could be controlled to within about 0.005 mm.

The detector D was held in a wooden mounting which permitted adjustment in any direction. The detector was a fixed iron pyrite-tungsten crystal detector and was connected in series with a microammeter. The pick-up wires of the detector were spaced at about 8 mm and their tips were brought up to about one or two millimeters from the Lecher wires. At this distance there was no evidence that their presence influenced the oscillation of the wire system. The

[17] Miesowicz, Bull. Int. Acad. Polon. Sciences Lettres Serie A, 95 (1934).

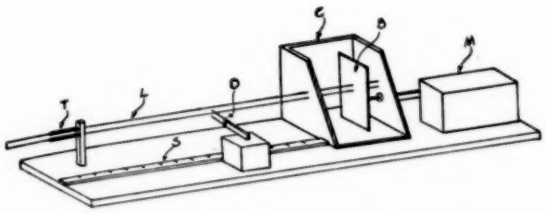

FIG. 4. Diagram of the wire wave apparatus.

meter stick S served as a guide for the detector mounting and provided an easy means of measuring the distance between electric field loops or nodes and hence the wave-length. The measured wave-length corresponds to the wave-length of a free wave, however, only if the waves propagate along the wires with the velocity of light. It is well known[18] that on account of the resistance of the wires the velocity of propagation along a wire system is less than the velocity of light by an amount which depends upon the frequency, resistance, and geometry of the system. The dependence upon frequency is inverse and at these frequencies the correction is negligibly small for copper wires. An alternate method of measuring wave-lengths less than 12 cm was to withdraw the wire wave apparatus from the oscillator and set up a parabolic mirror. The free wave apparatus was then complete and the grating could be used.

To adjust the system one first places the reflecting bridge well back in the liquid so that the portion of a wave transmitted into the cell will be very largely absorbed by the liquid before getting out into the external circuit again. Then by adjusting the Lecher system to the most favorable length one can get a system of standing waves between the liquid surface and the tube end of the wire system. The detector is now adjusted to a position of maximum response, i.e., to an electric loop. By varying the coupling with the tube the energy of oscillation of the system is controlled. As the reflecting bridge is moved toward the front cell wall increasing amounts of energy will be transmitted back into the external circuit. The combination of these waves and the standing wave system of the external circuit will yield an interference pattern from which the optical constants of the liquid in the cell can be determined.

[18] Hund, Scientific Papers of the National Bureau of Standards, No. 491 (1924).

2. Analysis of the wire wave interference curve

For a similar wire wave system Seeberger has given an equation for the energy reaching the detector which involves only one term dependent upon the thickness of the liquid layer. But, because of the complexity of the free wave interference pattern, one suspects that Seeberger's equation is no more than a first approximation and that, therefore, a more complete analysis is desirable.

Let l be the distance of the detector from the cell wall and L its distance from the tube end of the Lecher system. Denote by x the distance of the reflecting plate from the front cell wall. The length of the external Lecher system $L+l$, the position of the detector as given by l, and the thickness x of the liquid layer are all variable. Consider first the case of x so large that a wave entering the cell will be almost completely absorbed by the liquid layer and no appreciable part of it will reenter the external Lecher system. For water at a wave-length of ten centimeters, $x=10$ cm is sufficient to meet this requirement. A plane wave set up by the oscillator and propagating toward the cell from the tube end of the external circuit may have its electric component at the detector represented by $E_0e^{i\omega t}$. The energy of the wave is largely concentrated in the space between the two wires and in this small region the assumption of a plane wave is a justified approximation.

After one complete passage around the external circuit the electric amplitude of this wave may be written: $E_0R_1R_2 \exp\{-2\beta(L+l)+i[\omega t-\rho_1-\rho_2-4\pi(L+l)/\lambda]\}$ where β is the attenuation constant for the external wire system, λ is the wave-length in air, and $R_1e^{-i\rho_1}$ and $R_2e^{-i\rho_2}$ are the reflection factors at the tube end of the circuit and at the cell wall respectively. The R gives the fraction of amplitude reflected and the ρ gives the retardation in phase upon reflection. The preliminary adjustment of the length $L+l$ of the external Lecher system for a maximum response of the detector is such that this twice reflected wave will be in phase with the wave being set up by the oscillator, i.e., $2\pi[2(L+l)/\lambda]+\rho_1+\rho_2$ is an integral multiple of

2π. Under this adjustment all waves moving toward the cell after any number of reflections will be in phase and can be represented by a single wave. Similarly the sum of all waves moving away from the cell can be represented by a single wave. The preliminary adjustment of the detector location for a maximum response places it at one of the positions where the electric components of these two net waves are in phase, i.e., at an electric antinode of the standing wave system. The total electric amplitude at the detector may then be written as $\mathcal{E}=Ee^{i\omega t}=(E_1+E_2)e^{i\omega t}$ where E_1 is connected with the wave moving toward the cell and E_2 with the wave moving away from the cell. Since E_1 is always greater than E_2 there will be no true electric nodes but antinodes will appear. The difference E_1-E_2 is very small compared with E_1+E_2, however, for liquids of high refractive index. This is verified for water by shifting the detector along the Lecher wires. The average energy at the detector is given by $a\mathcal{E}\mathcal{E}^*$ where a is a constant depending upon units and $\mathcal{E}^*$ is the complex conjugate of $\mathcal{E}$. This becomes aE^2 which is constant as long as the output of the oscillator remains unchanged.

As a next step we consider the layer thickness to be reduced to such an extent that a wave entering the cell may be only partially absorbed and will reenter the external circuit with considerable amplitude. We will however require the thickness to be great enough to quite completely absorb a wave which passes through the liquid layer a second time. In terms of the previous notation the wave represented by $E_1e^{i\omega t}$ at the detector will move to the cell and be partially transmitted. After passing through the liquid layer and again reaching the detector the electric component may be written:

$$E_1T_1T_2R_3\exp[-2\beta l-2\alpha x+i(\omega t-\tau_1-\tau_2-\rho_3-4\pi l/\lambda-4\pi x/\lambda')],$$

where λ' is the wave-length in the liquid, $R_3e^{-i\rho_3}$ is the reflection factor at the reflecting bridge within the cell, $T_1e^{-i\tau_1}$ and $T_2e^{-i\tau_2}$ are the transmission factors upon entering the cell and upon leaving respectively and α is the attenuation constant for the wire system within the cell. The attenuation within the cell due to absorption by the liquid is so much greater than losses due to radiation and ohmic heat that we may neglect these latter two and set $\alpha=2\pi n\kappa/\lambda$. Because of the length adjustment of the external circuit all waves which have gone through the liquid layer once will be in phase with all other waves going in the same direction, i.e., a second system of quasi-standing waves will be set up. Moreover this second system of standing waves will have its antinodes coincident with the antinodes of the system composed of waves which have not entered the cell at all. This is also a consequence of the length adjustment of the external circuit. Of course the two standing wave systems will be in phase with each other only for definite values of layer thickness. Since all the waves of this second system will have the same phase at the detector as did the wave written out explicitly above, the total electric amplitude at the detector due to the two systems of waves may be written: $\mathcal{E}_1=E\exp[i\omega t]+B\exp[-2\alpha x+i(\omega t-\tau_1-\tau_2-\rho_3-4\pi l/\lambda-4\pi x/\lambda')]$ where B is a constant. Calculating the average energy we find:

$$\text{Energy}=aE^2+aB^2e^{-4\alpha x}+2aEBe^{-2\alpha x}\cos[(4\pi x/\lambda'+\delta)], \quad (3)$$

where $\delta=\tau_1+\tau_2+\rho_3+4\pi l/\lambda$. The second term will be relatively small if α is large, if x is large, or if B is very small. We will then have an oscillating term added to a constant. If we plot energy as a function of x we have the third term oscillating about a horizontal line. If the second term enters, as it may at small x, we have an oscillation about an average curve which rises exponentially as x decreases. The presence of this second term is obvious in all experimental curves for water (see Fig. 5). This exponential rise was also observed by Seeberger but he did not explain its origin.

Because of the relatively high absorption this energy equation must be essentially correct and any additional terms due to additional passages through the cell must be very small terms except at a small layer thickness. However, to see something of the influence of these correction terms, we shall consider the effect of those waves which go through the cell a second time. The second passage of a wave through the cell may occur as a result of an internal reflection at the front cell wall or by a reentry into the cell after having

passed through once. The amplitude of these waves will be small and not particularly interesting but their phases will be very significant. For simplicity we shall not write out these amplitudes in terms of the amplitudes of the waves treated above but we shall write out the phase retardations of these waves, referring the phase when the wave first reaches the detector after its double passage, to the phase of the original wave $E_0e^{i\omega t}$. The angular retardation of a wave which reenters the cell and passes through the liquid layer twice will be $2\pi(4l+2L)/\lambda+8\pi x/\lambda'+2\tau_1+2\tau_2+2\rho_3+\rho_1$, while the retardation for a wave which is reflected internally at the front cell wall will be $4\pi l/\lambda+8\pi x/\lambda'+\tau_1+\tau_2+2\rho_3+\rho_4$ where ρ_4 is the phase retardation upon internal reflection at the front cell wall. Because of the condition on L and l any complete transits around the outside circuit do not introduce any phase displacements and so are omitted here. Also because of this condition $2\pi(2L+2l)/\lambda+\rho_1$ may be replaced by $-\rho_2$. These two waves will be in phase provided $\tau_1+\tau_2-\rho_2$ and ρ_4 are equal. These angles can be calculated from the optical constants of the liquid and the electromagnetic theory.

It follows from the boundary conditions that upon entering a medium, characterized by n and κ, from free space the reflected electric field is retarded in phase by $\pi+\gamma$ and the transmitted field is advanced in phase by α. While upon entering free space from the denser medium the reflected electric field is retarded in phase by γ and the transmitted field is retarded by β where

$$\tan\alpha=\frac{n\kappa}{n+1},\quad \tan\beta=\frac{\kappa}{n\kappa^2+n+1}$$

and

$$\tan\gamma=\frac{2n\kappa}{n^2+n^2\kappa^2-1}.$$

For water at 10 cm $\gamma=1.5°$, $\alpha=4°$, and $\beta=0.5°$ so that the two waves above lack only about 7° of being completely out of phase. This is considering a liquid-free space boundary but this is a satisfactory approximation because of the very low reflecting and absorbing power of the cell wall. For most polar liquids these two waves will be essentially out of phase and will eliminate each other if the two amplitudes are approximately equal. In the case of water the amplitude of the

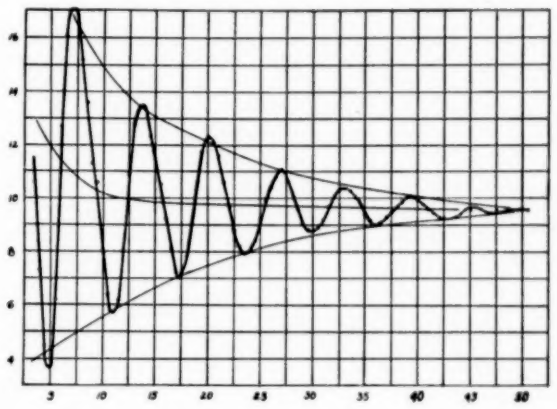

FIG. 5. Interference curve with the wire wave method for water at 22°C and for $\lambda=10.87$ cm. The ordinate is rectified current in microamperes; the abscissa bridge displacement in mm.

wave reflected internally is much the greater and a contribution from these waves is to be expected. Since $4\pi l/\lambda+\rho_1$ is an integral multiple of 2π as a result of the adjustment of the detector, we may write the resultant electric field as $\pm C\exp[-4\alpha x+i(\omega t-2\delta-8\pi x/\lambda')]$ where C is a constant and δ has the meaning given above. The alternate sign occurs because either of the component waves may predominate, the negative sign indicating predominance of the wave reflected internally. Combining this with the previous expression for total electric amplitude at the detector we have:

$$\mathcal{E}_2=E\exp[i\omega t]+B\exp[-2\alpha x+i(\omega t-\delta-4\pi x/\lambda')]\pm C\exp[-4\alpha x+i(\omega t-2\delta-8\pi x/\lambda')]$$

and

$$\text{Energy}=a[E^2+B^2e^{-4\alpha z}+2EBe^{-2\alpha z}\cos(4\pi x/\lambda'+\delta)+C^2e^{-8\alpha z}\pm 2BCe^{-6\alpha z}\cos(4\pi x/\lambda'+\delta)\pm 2ECe^{-4\alpha z}\cos 2(4\pi x/\lambda'+\delta)] \quad (4)$$

where $\alpha=2\pi n\kappa/\lambda$.

The last three terms are new but because of the smallness of C and the rapid absorption, the fourth and fifth could have an effect only with very thin liquid layers. The last term may be appreciable because of the large value of E and

less rapid absorption. But due to the double angle the periodic term will be a maximum when the main periodic term (third term) is either a maximum or a minimum. Hence its effect will be to shift the extremes of the main periodic term up or down depending upon the sign of C. In either case it is still easy to isolate the main periodic term by simply drawing an average curve about which the periodic term oscillates symmetrically. From this periodic term, $2aEBe^{-4\pi n\kappa z/\lambda}\cos(4\pi x/\lambda'+\delta)$, the optical constants of the liquid can be determined.

3. Experimental procedure

In practice it is more convenient to separate the determination of n and κ because it is very tedious to make the hundred or more observations necessary to plot a curve such as Fig. 5 and the time required is so great that there is some chance for change in the output of the oscillator. This separation can be satisfactorily made only in that region where the average curve is essentially horizontal so that the spacing of the extremals of the periodic term become the same as for the total function represented by Eq. (4). The usual experimental curve shows a considerable region where this method is applicable. The spacing of the maxima and minima is very easily and quickly determined by means of the micrometer screw. By taking ten to twenty observations consistent averages for λ' can be obtained.

To determine κ we note that the displacement from one extremal to the next one is $\lambda'/4$ and hence the ratio of amplitudes of the periodic term at adjacent extremals is $e^{-\pi\kappa}$. Therefore we do not need the value of n nor the value of x in centimeters but we simply record the series of maximum and minimum microammeter readings. By plotting these with an equal but arbitrary spacing on the abscissa axis we can draw two curves, one connecting the maxima and the other the minima of Eq. (4). These two curves will mark the limit of the main periodic term and their ordinate difference will decrease with $e^{-\pi\kappa}$ from one extremal to the next. From a series of five to ten such runs one easily obtains fifty or more values of κ from which consistent averages can be obtained. Fig. 5 shows two of these auxiliary curves as calculated from the data shown in the figure.

4. Comparison of methods

Because of the wide discrepancies existing between the published results of different observers in this region of the spectrum, a satisfactory investigation must cover a region of the spectrum systematically and be checked as thoroughly as is practical. It is particularly desirable to secure a check between essentially different methods of measurement. On this account considerable work was done at about 10 cm with both the free wave and the wire wave method in an attempt to establish the validity of these methods. The results given under the discussion of the free wave method show the data obtained by these two methods to agree to within about one percent, which is within the limits of experimental error for the free wave method. This certainly indicates the possibility of securing trustworthy data at these frequencies.

The wire wave method has one great advantage over the free wave method in regard to the reproducibility of data. The results of the wire wave method can be reproduced very closely under the most favorable conditions. For example, at 11.12 cm three measurements distributed over an interval of three hours gave $\lambda'=1.259$, 1.260 and 1.257 cm, respectively. When the experiment is repeated after several days the agreement is naturally not as good, but careful work secures agreement between individual observations to within about one percent. On the other hand it is very difficult to obtain consistent free wave data. This is probably partly due to the necessity of taking a complete curve and then isolating the periodic term by trial and error methods, but it is also difficult to secure good experimental curves. The time required for taking a complete experimental curve, the clumsy method of varying the layer thickness (pouring liquid into the cell), and diffraction effects probably all contribute to this difficulty.

Since the essential experimental points for the wire wave method are $\lambda'/4$ cm apart and at least six points are required for a calculation of absorption index, this method will finally be limited by the absorption. In the free wave method the

interference effect will disappear at high absorption so that the refractive index cannot be obtained but it will still be possible to investigate the absorption. Thus at 4.80 cm the refractive index of water could not be determined but the absorption could still be measured by the free wave method.

Experimental Results and Discussion

A summary of the data obtained for water is presented in Table II and the wave-length dependence of κ is shown in Fig. 6. The wire wave method was successfully applied to the determination of both λ' and κ from 20.44 to 6.48 cm. Beyond the range of this method the free wave apparatus was used but not enough of the interference curve could be obtained to secure a measure of λ'. Consequently the interference was eliminated by the use of thick liquid layers and $n\kappa$ was calculated from the exponential graph of transmitted energy. For comparison with the remainder of the absorption curve it was assumed that $n=8.80$, and κ was calculated. For some of the wave-lengths only the one item of data was obtained because of experimental difficulties which cut short the work. Difficulties are occasionally experienced in securing satisfactory adjustments and the danger of burning out tube filaments is always present.

Although that part of the absorption index which is due to conductivity of the water can be calculated from Maxwell theory and is known to be completely insignificant in comparison with the dipole absorption in this region, the conductivity of the distilled water used was measured. It was of the order of 10^{-6} ohm^{-1} cm^{-1} when the water came from the still but increased about tenfold during exposure to the air and the cell during the course of an experiment. This increase had no appreciable effect but fresh water was regularly used as a safeguard against the influence of impurities.

Table II. *Summary of data on index of refraction and index of absorption.*

λ (cm)	λ' (cm)	κ	n
4.80 (free wave)	—	0.153*	—
5.34 " "	—	.141*	—
6.48	0.732	.123	8.85
8.05	0.917	.097	8.78
8.16 (free wave)	—	.097*	—
8.80	1.004	.093	8.77
9.55	1.095	.086	8.72
9.85	1.119	—	8.80
10.10	—	.082	—
10.20	1.160	—	8.79
10.87	—	.075	—
11.12	1.259	.074	8.83
11.80	1.333	.071	8.85
13.41	—	.068	—
14.48	1.642	.062	8.82
15.29	1.746	.062	8.76
16.83	1.902	—	8.85
18.41	—	.052	—
20.44	2.327	.048	8.78

* Calculated from the measured value of $n\kappa$, assuming $n=8.80$.

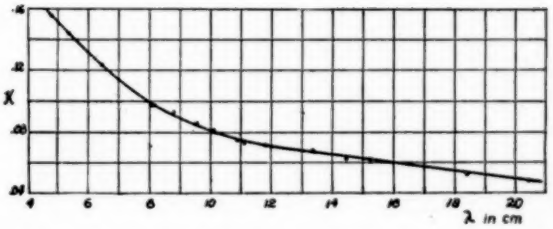

Fig. 6. Absorption index of water at 22°C as a function of wave-length. Legend: open circle, wire wave method; closed circle, free wave method.

Since the temperature coefficients of the indices of refraction and absorption are unknown at these wave-lengths it is necessary to work at a single temperature, 22.0°C having been chosen as the most convenient one.

The monotonic increase of absorption with decreasing wave-length shown by Fig. 6 is to be expected on the basis of the Debye theory if one is here approaching the dispersion region in which the refractive index decreases sharply. While no systematic investigation of absorption has been previously attmpted, the data that do exist are scattered about the present curve as shown in Fig. 7. The only continuous wave results here are recorded by Seeberger who used both wire wave and free wave methods but the results are not consistent and show no definite trend. The observation of Zakrzewski,[19] made with slightly damped radiation and using a free wave method, shows a great displacement from the present curve and leads one to suspect an error of the type discussed under Section 6 of the "Free Wave Method." The data of Eckert[20]

[19] Zakrzewski uses a peculiar notation in which κ has the meaning usually attached to $n\kappa$ so that his result $\kappa=0.62$ means $n\kappa=0.62$ in the usual notation. Because of this fact errors have crept into the literature in connection with Zakrzewski's data.

[20] Eckert, Ber. d. D. Phys. Ges. **15**, 307 (1913).

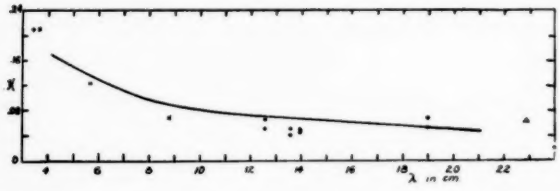

FIG. 7. Comparison of observed absorption index with previous data. Legend: open circle, Seeberger (wire waves); closed circle, Seeberger (free waves); △, Zakrzewski; +, Mobius; ×, Eckert.

and Mobius[21] were obtained by free wave methods but with very highly damped radiation so that these points give us no reliable quantitative information. However they do indicate the general trend of the absorption. At still shorter wave-lengths (2.7–0.42 cm) we have the results of Tear[22] but these were secured with highly damped waves and are of little present significance. While all of these earlier results are unsatisfactory they confirm the present data in a general way.

The average value of refractive index for the twelve wave-lengths shown in Table II is 8.80 with only one point departing more than 0.6 percent from the mean. While this result indicates no dispersion over the region 6.48–20.44 cm there are several lines of evidence which support the conclusion that probably a very slight dispersion occurs: (*a*) The average refractive index as reported over the interval 6.48–20.44 cm is 1.4 percent smaller than the square root of the static dielectric constant, 1.1 percent smaller than n as observed by Novosilzew for 141 wave-lengths between 220 and 300 cm, and 0.6 percent smaller than the value given by v. Ardenne, Groos and Otterbein for 34 wave-lengths between 28 and 57 cm. Moreover, in the results of Table II the average n for the six observations below 11 cm is 0.3 percent smaller than the average n for the six observations above 11 cm. All of these results suggest a small decrease of n over the entire short wave region. (*b*) The data of Merczyng,[23] Mobius, Tear, and some further data of Eckert below 5 cm, while very unsatisfactory and for the most part contradictory, do consistently show a marked decrease of refractive index in the region 1–5 cm which leads one to expect some slight dispersion over the lower part of the present region. (*c*) The observed increase of absorption index with decreasing wave-length implies, on the basis of the Debye dipole theory, an accompanying dispersion. Although these facts indicate the existence of a slight dispersion, the expected variation of refractive index is of the order of one percent and it is very doubtful if present methods could detect so small a variation over an interval of two octaves.

In comparing the present results with the discordant data already existing in this region one naturally considers first the continuous wave data. This comparison is shown in Fig. 8. Seeberger has $n=8.80$, 8.84, 8.57, 9.10 and 8.76 at $\lambda=12.6$, 13.6, 14.0, 19.0 and 24 cm, respectively. While these points do not show a definite trend the average value, 8.81, agrees well with the present results. It seems more reasonable to attribute the variation in the results at 14 and 19 cm to experimental error than to dispersion because of the lack of any other points to support these two departures from the average value. Moreover the sharp break in refractive index over the interval 13.6–14.0 cm is hardly plausible because of the absence of a corresponding break in the absorption index which would be expected if marked dispersion occurred at this point.

The recent investigation of Goldsmith[7] indicates a linear decrease of refractive index from 9.73 at 23.82 cm to 8.36 at 8.53 cm but this investigation is open to the criticism that the method of measuring the wave-length is very unsatisfactory, particularly for the longer waves. These results as they stand are not consistent with those of the present report nor with the data of Seeberger. Moreover they conflict with established long wave data above 28 cm inasmuch as the curve of Goldsmith indicates an increase of n as one goes to longer wave-lengths in spite of the fact that his value at 23.82 cm is already over 10 percent above the value found in the region 28–60 cm by v. Ardenne, Groos and Otterbein, Girard and Abadie, and Heim. Frankenberger[24] has investigated the region from 23 to 73 cm with slightly damped radiation and

[21] Mobius, Ann. d. Physik **62**, 293 (1920).
[22] Tear, Phys. Rev. **21**, 611 (1923).
[23] Merczyng, Ann. d. Physik **34**, 1015 (1911).
[24] Frankenberger, Ann. d. Physik **1**, 948 (1929).

found $n=8.91$ with no evidence of dispersion so it seems unlikely that a marked decrease of refractive index occurs between 23 and 28 cm as would be required to bring Goldsmith's data into harmony with the long wave results.

From the paper of v. Ardenne, Groos and Otterbein there are four observations with continuous waves at the single wave-length 13.45 cm which give $n=8.72$. This result is 1.5 percent smaller than the value reported by these writers at 28–57 cm and hence indicates dispersion but unfortunately only the one point was secured in the region of suspected dispersion so the evidence is not very conclusive.

The refractive index as measured for slightly damped waves by Zakrzewski and by Miesowicz is rather high but this is evidently due to the method of measurement as was pointed out in Section 6 under the "Free Wave Method." If this is correct it brings their data into closer agreement with the present result. Frankenberger's data from 10.6 to 24.9 cm were obtained with slightly damped waves but are tentative. They were not regarded by the author as satisfactory because of the evident influence of bridge diameter upon the results. Further experiments were indicated but no results have been published so far. The average of the data presented is 8.89.

The remaining results due to Wildermuth,[25]

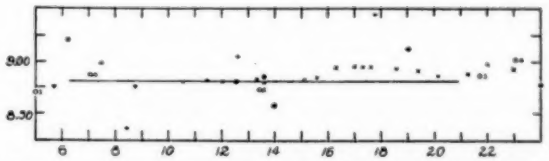

FIG. 8. Comparison of observed refractive index of water with previous data. The ordinate is refractive index at 22°C; the abscissa wave-length in cm. The solid line represents the present data. Legend: ⊕, Seeberger; +, Goldsmith; ×, Frankenberger; □, Miesowicz; ▽, Eckert; △, Becker; ⊙1, Cole; ⊙2, v. Ardenne, Groos and Otterbein; ⊙3, Wildermuth; ⊙4, Zakrzewski.

Eckert, Becker[26] and Cole[27] lie within about one percent of the present data but all of these were obtained with highly damped waves and consequently are of doubtful significance.

While it is apparent that none of these earlier reports (when the criticisms pointed out are considered) contradict the present results, it is also true that none of them are complete or precise enough to verify the small dispersion which is suspected.

In conclusion I wish to acknowledge my indebtedness to Professor D. M. Dennison and Professor N. H. Williams for many helpful discussions of the problem, and to Dr. C. E. Cleeton, who assembled the detectors, for many suggestions on the production and detection of ultra-short waves. I also wish to express my thanks to the University of Michigan for financial aid during the course of this research.

[25] Wildermuth, Ann. d. Physik **8**, 212 (1902).

[26] Becker, Ann. d. Physik **8**, 22 (1902).
[27] Cole, Wied. Ann. **57**, 290 (1896).

NOVEMBER 15, 1937 PHYSICAL REVIEW VOLUME 52

Accommodation Coefficients of the Noble Gases and the Specific Heat of Tungsten

WALTER C. MICHELS
Department of Physics, Bryn Mawr College, Bryn Mawr, Pennsylvania

(Received August 13, 1937)

By the use of the specific heat theory developed by A. H. Compton and a simple one-dimensional model, a semi-classical treatment of the problem of the thermal accommodation coefficients for monatomic gases against solid surfaces has been obtained. Application of this theory to the data of Roberts gives a satisfactory fit if the heats of adsorption of helium and neon on tungsten are taken as 50 cal. per gram atom and 278 cal. per gram atom, respectively. The Compton characteristic temperature for tungsten is found to be 148°K, which leads to the conclusion that the excess specific heat of tungsten above the classical value is partially due to anharmonic terms in the potential energy of the atomic oscillators, as suggested by Born and Brody.

FOLLOWING the work in which Roberts[1–3] showed that the thermal accommodation coefficients of the noble gases against metals have much lower values than indicated by earlier work and that they show a distinct dependence upon temperature, several attempts have been made to give a satisfactory theoretical account of the transfer of energy between monatomic gases and solid surfaces.[4–7] While the various theories have agreed, at least roughly, in predicting the order of magnitude of the accommodation coefficients and have shown that the temperature variation is dependent upon the binding energy of the solid and the heat of adsorption of the gas upon the surface, they either have done so only by the introduction of parameters which could not be checked against other data or have been limited, by the approximations used, to very low temperature ranges for possible combinations of gases and metals. The difficulties which have been encountered in attempts to carry through a rigorous quantum-mechanical treatment of the problem make it seem desirable to attempt a semi-classical treatment. Such a theory is given in this paper and seems to lead to results which are consistent both among themselves and with the data on specific heats and adsorption, in spite of the fact that it is based on a model which cannot correspond very closely to reality.

We shall treat the problem as one-dimensional, since previous treatments have shown that the simplicity gained by such a method does not lead to any great divergence from experimental facts. As a first approximation we shall consider a head-on collision between an atom of the one-dimensional gas and a solid atom, which is behaving as an independent harmonic oscillator of characteristic frequency ν. The following simplifying assumptions, some of which will later be removed, will also be used in this approximation: (1) that the temperature is sufficiently high so that a classical Boltzmann distribution may be used for the energies of both the gas and the solid, (2) that there are no long range attractive forces in operation, and (3) that the collision is perfectly elastic and that the time during which collision forces are appreciable is small compared with the time of oscillation of a solid atom, so that negligible energies are transferred to the crystal as a whole. If one assumes conservation of momentum and energy in the collision, the energy transferred to the gas from the solid, per collision, is found to be:

$$\Delta E=\{2Mm/(M+m)^2\}(mv+MV)(v-V), \quad (1)$$

where M and m are the masses of the gas and solid atoms, respectively, and V and v are their respective velocities before impact. This result must be averaged over all possible values of V and v in order to find the average energy transferred per collision. For a one-dimensional gas the Boltzmann distribution gives a probability function, while for the oscillator the probability of an amplitude between A and $A+dA$ is:

$$P_A=Ae^{-\alpha A^2}dA,$$

where $\alpha=2\pi^2\nu^2m/kT_s$, T_s being the temperature of the solid. In order to adapt this expression to the necessary averaging process we can express v as a function of the amplitude and the time, t. If we assume that the collision is equally probably in any time interval dt, the averaging operator becomes:

$$P=Ae^{-\alpha A^2}e^{-\beta V^2}dAdtdV, \quad (2)$$

where $\beta=M/2kT_g$, T_g being the gas temperature. In carrying out the averaging process it is necessary to consider four cases, corresponding to the possible signs of v and V and, in each of these, to limit the range of V to those values which make collision possible. When this is done we have:

$$(\Delta E)_{Av}=\frac{\left\{\frac{2Mm}{(M+m)^2}\right\}\int_0^\infty Ae^{-\alpha A^2}\int_0^{1/4\nu}dt\left\{\int_0^\infty(MV+mv)(v-V)e^{-\beta V^2}dV+\int_0^\infty(mv-MV)(V+v)e^{-\beta V^2}dV\right\}}{2\int_0^\infty Ae^{-\alpha A^2}dA\int_0^{1/4\nu}dt\int_0^\infty e^{-\beta V^2}dV},$$

[1] Roberts, Proc. Roy. Soc. Lond. **A129**, 146 (1930).
[2] Roberts, Proc. Roy. Soc. Lond. **A135**, 192 (1932).
[3] Roberts, Proc. Roy. Soc. Lond. **A142**, 518 (1933).
[4] Jackson, Proc. Camb. Phil. Soc. **28**, 136 (1932).
[5] Zener, Phys. Rev. **40**, 335 (1932).
[6] Jackson and Mott, Proc. Roy. Soc. Lond. **A137**, 703 (1932).
[7] Landau, Physik. Zeits. Sowjetunion **8**, 489 (1935).

which gives:

$$(\Delta E)_{Av}=2Mmk(T_s-T_g)/(M+m)^2. \quad (3)$$

If the gas were to come to complete equilibrium with the solid in a single collision, the average energy transfer would be:

$$(\Delta E')_{Av}=(k/2)(T_s-T_g),$$

so the accommodation coefficient is:

$$a_2=(\Delta E)_{Av}/(\Delta E')_{Av}=4Mm/(M+m)^2. \quad (4)$$

As would be expected from the purely classical treatment used, this result is independent of temperature. It agrees with that obtained by Baule[8] for the similar problem of the mixing of two gases. He used a detailed three-dimensional treatment and the agreement may therefore give us an added confidence in the one-dimensional model used here.

The most important limiting assumption which has entered into the classical result is that of a Boltzmann distribution of energies in the solid. In order to correct for the breakdown of this distribution law at low temperatures an appeal to specific heat theory is necessary. In view of the difficulties which have arisen when attempts were made to treat the problem on the Einstein and Debye models,[5-7] it would seem that a more mechanistic thory, even if not too well grounded, may be preferable. Such a treatment of specific heats was proposed by A. H. Compton in 1915.[9] Although Compton developed this theory as a classical one, it is really only semi-classical in nature, since the ratio of the "critical energy" which is characteristic of a solid to the characteristic frequency, as determined by other means, has a value equal to Planck's constant. Compton considers a solid made up of a set of independent harmonic oscillators with a fixed critical frequency, as used in the Einstein theory. At high temperatures there are $3N$ degrees of freedom. He then assumes that, "if the relative energy between two neighboring atoms in a solid falls below a certain critical value, the two atoms become agglomerated so that the degree of freedom between them vanishes; but as soon as the energy increases again above the critical value, the degree of freedom reappears." The Compton solid, in other words, has a classical distribution of energies, except for a sharp cut-off of the population below some critical energy E_0 and therefore corresponds to an Einstein solid in which a distinction is made only between the zero quantum state and a group consisting of all other states. Ordinary statistical methods show that the probability that a state be unagglomerated is:

$$P=e^{-\tau/T}, \quad (5)$$

so that the resultant specific heat is:

$$C_v=3Nke^{-\tau/T}(\tau/T+1), \quad (6)$$

where τ is the Compton characteristic temperature and N and k are Avagadro's number and the Boltzmann constant, respectively. As Compton shows in his paper, the fit of Eq. (6) to the experimental results is distinctly better than that obtained with the Einstein equation, and as good as with the equation of Debye.

To apply the Compton theory to the problem of thermal accommodation, we shall assume that the energy transfer takes place between the solid and gas atom as would be predicted classically if the former is unagglomerated but that, if it is agglomerated, the collision is effectively one with a body of infinite mass, so that only momentum transfer takes place. Using Eqs. (4) and (5) and averaging the energy gained by the gas over all molecules in the surface, we find for the resultant accommodation coefficient:

$$a_1=4Mme^{-\tau/T_s}/(M+m)^2. \quad (7)$$

In the case for which the most complete experimental data exists, the accommodation of helium atoms on a tungsten surface, Eq. (7) gives a good agreement with the observations. This pair of atoms, however, come very close to satisfying the second and third simplifying assumptions used in the treatment thus far, and before we can expect an agreement for most cases it will be necessary that these assumptions be removed as far as possible. A first-order correction for the effect of attractive forces is easily made. As Jackson and Mott have shown,[6] the effect of such forces is to introduce a potential energy well, of maximum depth ϕ (the heat of adsorption) near the surface of the metal. Atoms of the gas are speeded up as they enter this well

[8] Baule, Ann. d. Physik **44**, 145 (1914).
[9] A. H. Compton, Phys. Rev. **6**, 377 (1915).

and retarded as they leave it. These interactions with the solid, however, take place at distances of many times the atomic diameters and, therefore, the interaction forces act upon many atoms of the solid, rather than a single one, so that the net effect of the two processes taking place is a zero transfer of energy. Some of the impinging atoms, however, will lose energy to the solid between their two approaches to the outer well wall, and will not have sufficient energy to escape. Since the time required to traverse the well is much shorter than the mean time between collisions among gas atoms, these captured atoms will be reflected from the side of the well and will again strike the solid, before coming to equilibrium with the gas. After their second collision, part of them will have gained sufficient energy to escape to the gas, while a fraction will again be reflected and will make a third collision, and so on.

Roberts[1] has shown that, in the case of multiple collisions, the apparent accommodation coefficient, a, is related to the accommodation coefficient, a_1, for a single collision, by the expression:

$$a=1-(1-a_1)^n, \tag{8}$$

where n is the number of collisions. In our case, let x be the fraction of atoms which are reflected on each approach to the outer well wall, then application of Eq. (8) gives, for the apparent accommodation coefficient:

$$\begin{aligned} a&=(1-x)a_1+x(1-x)\{1-(1-a_1)^2\}+\cdots \\ &\qquad +x^n(1-x)\{1-(1-a_1)^{n+1}\}+\cdots \\ &=a_1(1-x)\sum_0^\infty {}_nx^n\left\{(n+1)-\frac{(n+1)(n)}{2}a_1\right. \\ &\qquad \left.+\frac{(n+1)(n)(n-1)}{6}a_1^2-\cdots+(-a_1)^n\right\}. \end{aligned}$$

The summation for each term in the brackets may be reduced to a series of sums of the form:

$$1+2x+3x^2+4x^3+\cdots,$$

giving for the whole series:

$$\begin{aligned} a&=\{a_1/(1-x)\}\left\{1-\frac{a_1x}{1-x}+\frac{a_1^2x^2}{(1-x)^2}-\cdots\right\} \\ &=a_1/(1-x+a_1x). \end{aligned} \tag{9}$$

It now remains to evaluate x. Unless either the temperature difference between the gas and the solid or the heat of adsorption is too large, the gas atoms after collision with the solid will be characterized by a temperature which approximates T_s and, by the use of the distribution function used for a one-dimensional gas in Eq. (2), we find:

$$x=K\int_0^{(2\phi/M)^{\frac{1}{2}}} e^{-\beta V^2}dV,$$

K being a normalization factor. By a change of variable and the replacement of ϕ by a characteristic adsorption temperature:

$$\psi=2\phi/k,$$

this expression may be transformed to:

$$x=\frac{2}{(\pi)^{\frac{1}{2}}}\int_0^{(\psi/2T)^{\frac{1}{2}}} e^{-y^2}dy, \tag{10}$$

the normalization having been accomplished by setting $x=1$ when $\psi=\infty$.

Thus far, no quantitative treatment based on this model has been found to remove the requirement of short impact times. It is evident that the ratio of impact time to oscillation period will, in general, become small as the ratio M/m decreases, hence we can expect the present treatment to be most nearly correct as this ratio approaches zero. As the ratio increases and the time of collision becomes more nearly comparable with the period of the oscillators, binding forces will come into play during the collision, momentum will be transferred to neighboring atoms of the solid, and the effective value of m will increase, lowering the accommodation coefficient. It might be expected that the temperature, as well as the mass ratio, would influence the ratio of these times, but an analysis of the existing published data and of measurements made in this laboratory seem to indicate that such is not the case.

Insofar as the Compton specific heat theory is valid and the classical analysis used here is legitimate, then, the thermal accommodation coefficient can be expected to be:

$$a=Fa_1/(1-x+a_1x), \tag{11}$$

where a_1 and x have the values given in Eqs. (7) and (10) and F is an undetermined function of

M/m (and possibly T) which approaches unity as M/m approaches zero and asymptotically approaches zero as this ratio becomes large.

Before any comparison of this result with the experimental data is possible, we must remember that the theoretical value applies only to a smooth, clean surface, while the surfaces actually used are, as has been pointed out by Roberts,[1-3] both roughened and contaminated. The procedure used in most measurements has been to clean the surface by flashing to high temperatures and then to observe the values of the accommodation coefficient as a function of time after the flashing current was stopped. A general upward drift of a has been found, corresponding to the deposition of impurities of low atomic weight, loosely bound to the surface. Roberts, and later Mann,[10] found the value for a clean surface by extrapolating the measured values of a to zero time, but their procedure is open to objection on the grounds that the first part of the observed curve is affected by the heat capacity of the filament, and that the extrapolation is made over the period of time during which the most rapid changes in a are taking place. Some of the uncertainties of the extrapolation may be removed by considering the process by which impurities build up an adsorbed surface layer. Since the pressure of the contaminating gases can be expected to remain essentially constant over the short times (20–30 minutes) required to obtain the data, we can assume that the probability of capture of a gas atom in unit time is proportional to A_1, the proportion of the total surface uncovered at any time t. We therefore have, as the differential equation governing the proportion of uncovered surface:

$$dA_1/dt = -K'A_1. \tag{12}$$

Suppose that the accommodation coefficient for a clean surface is a_0 and that for a completely covered surface, such as will be observed after a long time, is a_∞, then the accommodation coefficient at any time can be obtained by the integration of Eq. (12) and an averaging of the energy losses over the covered and uncovered parts of the surface. This yields the relation:

$$\log (a_\infty - a) = \log (a_\infty - a_0) - K't. \tag{13}$$

[10] Mann, Proc. Roy. Soc. Lond. **A146**, 776 (1934).

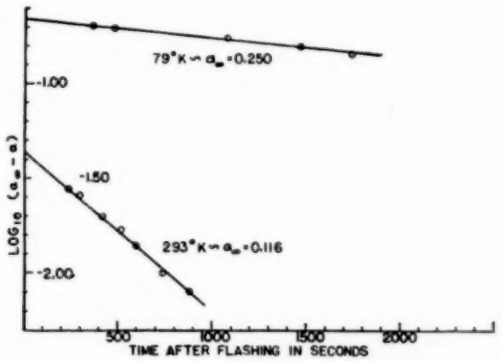

FIG. 1. Correction for contamination of tungsten surface in presence of helium. (Data from Roberts).

Since a_∞ may be obtained by direct measurement, this expression enables one to use a linear extrapolation to obtain the value for a clean surface. In practice, the linearity of the curve is extremely sensitive to the value of a_∞, and small adjustments of this quantity are sometimes necessary, but in no case thus far tried has it been necessary to use a value which departs by more than two or three percent from that obtained after the heat losses seem reasonably steady,—a limit well within the experimental error. Two plots from data given by Roberts for He−W are shown in Fig. 1. The linear extrapolations obtained give striking verification of the guessed extrapolations of Roberts, using the same data, as the values of a_0 here obtained are 0.072 for 295°K and 0.026 for 79°K, while he gives 0.07 and 0.025, respectively. The extremely low value of K' indicated by the plot for 79°K may mean that the principal impurity may not be oxygen, as has usually been believed, but rather some gas which is largely condensed on the walls at this temperature.

There finally remains the problem of correction for the roughness of a surface. It has been shown repeatedly that the heat treatment of a tungsten wire, under ordinary vacuum conditions, results in an etching of the surface to reveal the dodecahedral crystal faces.[1, 11, 12] This leads to the possibility that a gas atom will make two or more collisions with the wire before returning to the body of the gas, so that the accommodation coefficient for the roughened surface will be

[11] Compton and Langmuir, Rev. Mod. Phys. **2**, 157 (1930).
[12] Tonks, Phys. Rev. **38**, 1030 (1931).

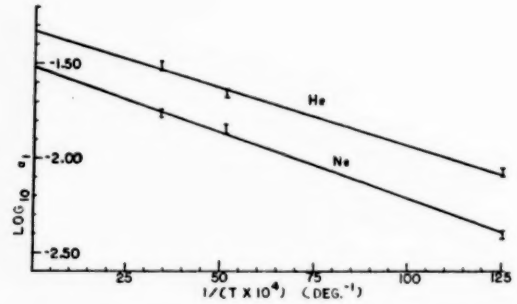

FIG. 2. The temperature variation of the accommodation coefficients of helium and neon on tungsten, corrected for adsorption. (Data from Roberts.)

related to that for a smooth surface by Eq. (8). The evaluation of the average number of collisions, n, has offered considerable difficulty and Roberts has repeatedly remarked that the values which he has obtained can only be taken as an upper limit for the accommodation coefficients on a smooth surface. In the case of tungsten, fortunately, it is possible to evaluate n from other data. By measurements of the thermionic emission of caesium covered tungsten surfaces, Taylor and Langmuir have shown[13] that the ratio of the exposed surface for a thoroughly heat treated tungsten wire to that for a smooth wire is 1.34 : 1. Now consider such a roughened wire, inscribed in a cylinder. At a given temperature and pressure, N molecules of the gas will cross the surface of this cylinder per second. But, since the number of collisions per unit area in unit time must be the same for the real and imaginary surfaces, the number of collisions of these gas atoms with the actual surface per second must be $N'=1.34N$. Hence the average number of collisions per atom is $n=1.34$. Since Roberts, like Taylor and Langmuir, heat treated his tungsten until a stable surface was obtained, we can take the surface excess ratio to be the same for the two sets of measurements. For small values of the accomodation coefficient, the first term of the expansion of the parenthesis of Eq. (8) will be all that is justified by the experimental accuracy, hence all of Roberts' values for stable surfaces should be reduced by the factor 1.34 before being compared with the theoretical values. For He—W at room temperature, this treatment gives a mean of $a=0.043$, and the lowest value which Roberts has reported for any condition of the tungsten surface is 0.05. The values of the accommodation coefficients of helium and neon on tungsten, have been determined from Roberts' data and are given in Table I. In this determination the correction for the roughness of the surface and the linear extrapolation for contamination correction have been used whenever the published papers give the requisite information.

The simplest way of comparing these results with the deduced equation is to pass to logarithms in Eq. (7). Inserting the function F in the right-hand side we have:

$$\log a_1=\log F+\log\{4Mm/(M+m)^2\}-\tau/T_s. \quad (14)$$

A plot of $\log a_1$ against $1/T_s$ should therefore give a straight line, the negative slope of which is equal to the Compton characteristic temperature of the metal. If we solve Eq. (9) for a_1, we have:

$$a_1=a(1-x)/(1-ax), \quad (15)$$

and, if the treatment given above is justified, it should be possible to choose a value of ψ such as to give the required straight line logarithmic plot, within the experimental uncertainty, which has here been estimated as five percent. Fig. 2 shows the best fitting logarithmic plots which have been obtained in this manner, obtained by choosing the characteristic adsorption temperatures for helium and neon on tungsten as 50°K and 280°K, respectively. These values of ψ correspond to heats of adsorption of 50 and 278 cal. per gram atom. While I have been unable to find other measurements of the heats of adsorption of the noble gases on metals, these values seem inherently reasonable for closed shell structures and are in agreement with the fact that neon and helium, particularly the latter, are not easily adsorbed on tungsten unless the temperature is appreciably below room temperature. In this connection, it is rather interesting to note that the interpretation of the same data

TABLE I. *The thermal accommodation coefficients for neon and helium against a smooth, clean tungsten surface.*

TEMPERATURE (°K)	NEON	HELIUM
79	0.06	0.019
195	0.06	0.034
295	0.05	0.043

[13] Taylor and Langmuir, Phys. Rev. **44**, 423 (1933).

as was used here, in accordance with the theoretical treatment of Jackson and Mott, requires a heat of adsorption of 2460 cal. per gram atom for neon on tungsten,[3] a value which seems to be unreasonably high.

The slopes of the two curves give values of the Compton characteristic temperature for tungsten equal to 144° and 160°. Since the accommodation coefficient data on helium are better than those on neon, we may take a weighted mean of 148° as being representative. In Fig. 3 the circles show the observed values of C_v for tungsten,[14] and the lower curve shows the Compton specific heat curve, calculated by using $\tau=148°$ and the asymptotic value of C_v as $3R$, or 25.05 joules per deg. It will be noticed that the curve falls below the observed data everywhere. But it is known that tungsten, in common with most of the metals, has a specific heat which rises above $3R$ at high temperatures.[15] Two possibilities have been proposed to account for these excess specific heats. In any of the metals there will be an electronic contribution, but this would be expected to be small at reasonable temperatures in any except the transition metals. On the other hand, Born and Brody have suggested[16] that the assignment of $kT/2$ of potential energy per degree of freedom may be in error, due to nonharmonic terms in the potential of the oscillators. The present treatment gives a possibility of distinguishing between these two effects, for the characteristic temperature obtained from accommodation coefficient data must be characteristic of the crystal oscillations only, since energy exchange between colliding atoms and conduction electrons will be negligible. If the specific heat curve can be fitted using the accommodation coefficient value of τ but adjusting the asymptotic value of C_v, the evidence will be in favor of Born and Brody's explanation, but, if the shape of the curve is wrong, we shall need to use an alternative explanation, presumably that of electronic contributions. The upper curve of Fig. 3 is based on an asymptotic value of C_v equal to 26.9 joules per deg., and will be seen to give a good fit to the specific heat data. We may therefore conclude that an appreciable portion of the excess specific heat of tungsten arises in the crystalline oscillations, rather than from conduction electrons.

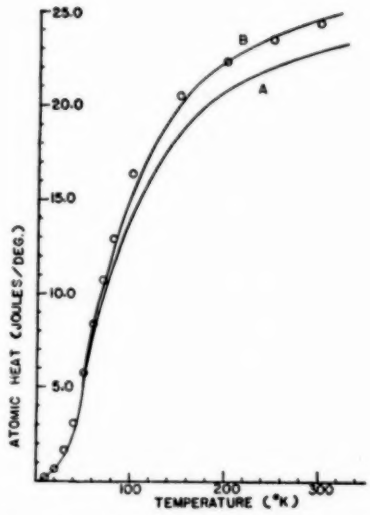

FIG. 3. The specific heat of tungsten. Curve A, $\tau=148°$, $C_{v_{00}}=25.05$ joules/deg.: curve B, $\tau=148$, $C_{v_{00}}=26.9$ joules/deg.

Experimental work to test further the validity of Eqs. (7), (10) and (11) and to extend the analysis of the specific heats to the transition metals is now under way in this laboratory. I wish to express my thanks to Dr. Melba Phillips for many helpful discussions during the course of this work.

[14] *International Critical Tables*, Vol. 5, p. 86.
[15] Magnus and Danz, Ann. d. Physik **81**, 407 (1926).
[16] Born and Brody, Zeits. f. Physik **6**, 132 (1921).

LETTERS TO THE EDITOR

Prompt publication of brief reports of important discoveries in physics may be secured by addressing them to this department. Closing dates for this department are, for the first issue of the month, the eighteenth of the preceding month, for the second issue, the third of the month. Because of the late closing dates for the section no proof can be shown to authors. The Board of Editors does not hold itself responsible for the opinions expressed by the correspondents.

Communications should not in general exceed 600 words in length.

Interpretive Remarks Bearing on the Metrical Field Associated with Heavy Particles

A detailed balance of energy and angular momentum in the process of beta-decay has for some years appeared to demand the existence of a neutrino body. The beta-ray theory involving the simplest assumptions as to the form of the neutrino interaction with the particles known to participate in the process has at least qualitative success in predicting the form of the beta-ray distribution. The saturation properties of the nuclear forces suggest likewise an exchange interaction between the heavy particles lending further support to the neutrino postulate. There is as yet, however, no evidence from direct observation substantiating the hypothesis; presumably because the neutrino does not make itself evident by a large interaction with the matter it traverses. To the neutrino, if it exists, have been ascribed the following characteristics:[1]

No charge,
Mass very small compared to electron mass, probably zero,
Spin $\frac{1}{2}\hbar$,
Fermi statistics,
Magnetic moment less than 1/7000 Bohr magneton, if any,
No detectable effects in free space.

We thus know a considerable amount about the neutrino, sufficient indeed to construct a usable model of this entity.

It is the purpose of this note to suggest the identification of the neutrino model with certain solutions of the field equations of the general relativity theory. As a particular component of the (nonstatic) metrical field of a disintegrating nucleus the neutrino finds a mode of description which is not in contradiction with any of the above requirements. Einstein and Rosen,[2] particularly, have described such solutions, but heretofore no physical identification has been provided for them. The form of the solutions imply the radiation of energy (and possibly also angular momentum) from a system whose internal configuration is changing rapidly.

The question of the *intensity* of these "gravitational waves" is, however, a critical one as energies of millions of electron volts are involved. One is forcibly inclined in meeting this apparent difficulty to suppose that the large nuclear forces extend into asymptotic interactions at great distances, which there become recognized as forces of gravitation! The change in the energy configuration within the nucleus on the conversion of a neutron into a proton would on this basis be accompanied by the appearance of a negatron and a large perturbation of the metrical field corresponding to the neutrino. The problem of the interaction thus seems to go back to a correct formalizing of the field equations for the interacting particles, where quantum and electromagnetic properties are not neglected as in the usual macroscopic theory. When and if such a unified field theory becomes available we may anticipate answers to such important questions as the origin of the "extra" magnetic moment of the proton and the spin dependence of the heavy particle interaction.

Finally the remark may be made that if it should be demonstrated that the neutrino is actually nonexistent this knowledge would render logically inapplicable to nuclear phenomena not only quantum mechanics in its present form, but also the general theory of relativity.

WALTER H. BARKAS

Columbia University,
New York, N. Y.,
October 12, 1937.

[1] H. A. Bethe and R. F. Bacher, Rev. Mod. Phys. **8**, 189 (1936).
[2] A. Einstein and N. Rosen, J. Frank. Inst. **223**, 43–54 (1937) have described the solutions of the field equations corresponding to a "damped" physical system and have given them rigorous form for the case of cylindrical waves. It is to be noted that the equations provide solutions corresponding to both receding and approaching waves which may be interpreted respectively as neutrinos and antineutrinos.

The Isotopic Constitution of Tungsten

Over a year ago, the ions from a spark between tungsten electrodes were analyzed by the mass spectrograph, and it was found that on seven photographs with long exposures a faint isotope at mass 180 appeared in addition to the four strong ones at 182, 183, 184 and 186 observed by Dr. Aston. The tungsten used, however, had several of the light elements as impurities and also showed faint lines at 185 and 187 which were probably due to a trace of rhenium. On this account it was thought desirable to examine other samples of tungsten to confirm the existence of the isotope at 180. This has now been done, at the urging of Dr. L. Alvarez, who inquired as to the possibility of an isotope at 180. With pure tungsten electrodes, six photographs have been made showing the isotope at 180, and by varying the time of exposure, its intensity was estimated as approximately one one-hundredth of that of the isotope at 183. In the earlier photographs, the faint isotope was also found on two photographs of doubly charged ions, on two of triply charged ions, and on one of quadruply charged ions. Thus there can be no doubt that tungsten has a fifth faint stable isotope at mass 180.

A. J. DEMPSTER

Ryerson Physical Laboratory,
University of Chicago,
Chicago, Illinois,
November 2, 1937.

The Infrared Absorption of HCl in Oxygenated Solvents

The absorption of HCl in certain non-ionizing solvents has been observed in both the infrared[1] and the Raman spectra.[2] However, Raman spectra measurements of electrically conducting solutions of HCl in oxygenated solvents[3] have failed to show any lines which could be attributed to HCl. That the power of dissociation does not depend wholly on the internal electrostatic field is evidenced by the fact that some of the non-ionizing solvents have much higher dielectric constants than certain of the solvents in which HCl forms conducting solutions. It is now generally believed that the dissociation is produced as a result of the combination of the proton with an oxygen or some other highly electronegative atom of the solvent. According to the hydrogen bond theory[3] it would be possible for the proton to become attached to an oxygen of the solvent without becoming completely detached from the Cl, thus forming the additive compound, R−O−H−Cl. If such a complex is formed, it should still be possible to observe the HCl vibrational band in the infrared, although this would certainly be expected to occur at wave-lengths longer than those for the unassociated HCl. Walkenstein and Syrkin[4] have suggested that the absence of the HCl line in the Raman spectra of HCl solutions in ether may indicate the strengthening of the heteropolarity of HCl, which can make the line forbidden in the Raman spectra. These observers recorded variations in the ether spectrum which support the theory that the HCl is linked to the ether oxygen through a hydrogen bridge.

The present investigation was undertaken to ascertain whether in solutions of HCl in oxygenated solvents, there is absorption which can be attributed to the HCl. In Fig. 1 are given results obtained from a study of concentrated solutions of HCl in dioxane, in di-ethyl ether, and in ethyl acetate for the region 2.6μ to 5.8μ. The curves represent the ratio of the transmission of the solution to an approximately equal thickness of the pure solvent. They were obtained by the use of a 60 degree rocksalt prism of 7 cm face, through which the light was made to pass twice.

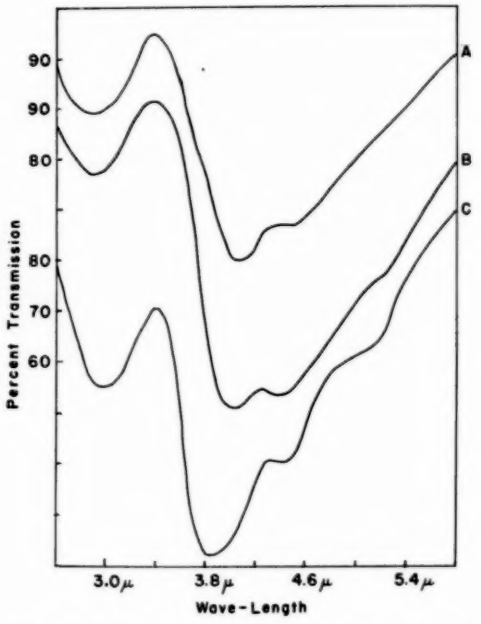

FIG. 1. The ratios of the transmission of HCl solution to that of the pure solvent, cell thickness 0.004 cm. *A*. HCl in ethyl ether; *B*, HCl in dioxane; *C*, HCl in ethyl acetate.

For each of the solutions there is a broad intense band in the region of 4μ. When the solvent is ethyl acetate the maximum of absorption appears at 3.88μ; when it is ethyl ether or dioxane, the maximum appears at 4.08μ approximately. In each case the band is unsymmetrical, being very diffuse on the long wave-length side. There is a small rise in each curve at about 4.28μ which makes the band appear double. It may be that this is a falsification caused by the very intense absorption of atmospheric CO_2 in this region. Also, the less intense band in the region of 3μ may not be real. The solvents have bands in the region of 3.4μ which are due to the CH group. Hence a smaller number of CH absorbers in the solution cell than in that of the pure solvent would cause an abnormal rise at about 3.4μ in the curve representing the ratio of their transmission and may thus produce a minimum at about 3μ. There is no question, however, as to the absorption in the region of 4μ. A curve for HCl in ethyl alcohol, which is not included, shows similar but slightly more diffuse absorption in this region.

The vibrational band in gaseous HCl appears at 3.46μ. The formation of strong hydrogen bonds between the HCl and solvent molecules would probably cause a very pronounced shift to the longer wave-lengths as well as an increase in intensity and a broadening of the HCl band. In view of these facts it seems quite possible that the band observed near 4μ in these solvents is the HCl fundamental, the variations from the corresponding band of gaseous HCl being a result of hydrogen bonding. The absorption in the 3μ region, if it is real, may arise from the OH resulting from this linkage.

West and Edwards[1] using the infrared spectra studied concentrated solutions of HCl in ether and in alcohol in the region of 1.7μ. They found no maximum which could be attributed to the HCl harmonic. Their results, however, do not necessarily conflict with the results given here, for the effect of the hydrogen bonding may be so to broaden and weaken the harmonic that it would escape detection. This seems to be the effect of hydrogen bonding upon the OH harmonic of alcohol.[5]

The experimental results reported here were obtained in the Mendenhall Laboratory of Physics, Ohio State University, and the writers wish to express their thanks to Dr. Alpheus W. Smith and to Dr. H. H. Neilsen for their support and interest in this work.

WALTER GORDY

Mary Hardin-Baylor College,
Belton, Texas.

PHILIP C. MARTIN

Mendenhall Laboratory of Physics,
Ohio State University,
Columbus, Ohio,
October 29, 1937.

[1] E. K. Plyler and D. Williams, Phys. Rev. **49**, 215 (1936); D. Williams, Phys. Rev. **50**, 719 (1936); W. West and R. T. Edwards, J. Chem Phys. **5**, 14 (1937).
[2] W. West and P. Arthur, J. Chem. Phys. **5**, 10 (1937).
[3] M. L. Huggins, J. Organic Chem. **1**, 407 (1936).
[4] M. Walkenstein and J. K. Syrkin, Nature **139**, 288 (1937).
[5] E. L. Kinsey and J. W. Ellis, J. Chem. Phys. **5**, 399 (1937); A. M. Buswell, V. Dietz and W. H. Rodebush, J. Chem. Phys. **5**, 50 (1937).

The Interaction of Neutrons with Normal and Parahydrogen

Teller[1] and Schwinger and Teller[2] have shown that (1) the spin dependence of proton-neutron forces and (2) the real or virtual character of the singlet level of the deuteron can be investigated by the scattering of slow neutrons by *o*- and *p*-H_2. The preliminary report of Halpern, Estermann, Simpson, and Stern[3] indicates that the cross sections of *o*- and *p*-H_2 differ. We have performed a series of scattering experiments using a beam of slow neutrons emerging from a "howitzer"[4] which could be cooled to 90°K by circulating liquid air. The neutrons emerging at ~100°K are absorbed in boron 1.6 times as strongly as those emerging at room temperature, thus indicating considerably better cooling than heretofore obtained (the simple $1/v$ law gives $(300°/100°)^{\frac{1}{2}}$ for complete equilibrium at both temperatures). After being defined by Cd cylinders and diaphragms the neutron beam passed through two thin walled "cerium" glass cells enclosed in the vacuum space of a Dewar and into each of which *n*-H_2 or *p*-H_2 could be condensed independently. The transmitted neutrons were detected by a BF_3 pressure ion chamber connected to a linear amplifier. Absorption by the glass Dewar system was approximately 6 percent. The *ortho-para* composition of the hydrogen from any cell was determined upon removal by comparison of its vapor pressure with that of freshly condensed *n*-H_2. Corrections were made for the self-conversion of the *n*-H_2 during the measurements.[5] The observations and results are summarized in Tables I and II, and also in Fig. 1, each transmission being the average of several measurements. Table II indicates qualitatively that filtration of the neutron beam through *p*-H_2 increases the transmission for *p*-H_2 and decreases it for *n*-H_2. The trend of the transmissions with decreasing neutron temperature indicates that the average neutron energy of the unscattered beam is further reduced by filtration through liquid *p*-H_2. The cross section for *p*-H_2 then is $\sim 14\times10^{-24}$ cm², and for *n*-H_2 is $\sim 75\times10^{-24}$ cm².

TABLE I. *Transmission data and calculated neutron scattering cross sections per hydrogen molecule.*

Composition % *o*-H_2	Neutron temperature °K	Cell thickness cm	Transmission	Cross section per molecule $\times10^{24}$ cm^{-2}
74.2	~300	0.234	0.780	48.6
73.9	"	.35	.695	47.4
74.0	"	.58	.538	48.7
73.3	"	.93	.371	48.6
74.5	~100	.234	.720	64.2
72.6	"	.58	.449	63.0
74.0	"	.814	.34	60.6
1.7	~300	.234	.871	27.1
3.0	"	.58	.671	31.4
2.5 est.	"	.814	.593	29.3
1.4	~100	.234	.911	18.0
6.5	"	.58	.740	23.6
5.0	"	.814	.690	20.8

Transmission values apply to the slow neutrons absorbed by Cd, and have a calculated precision of ±2 percent.

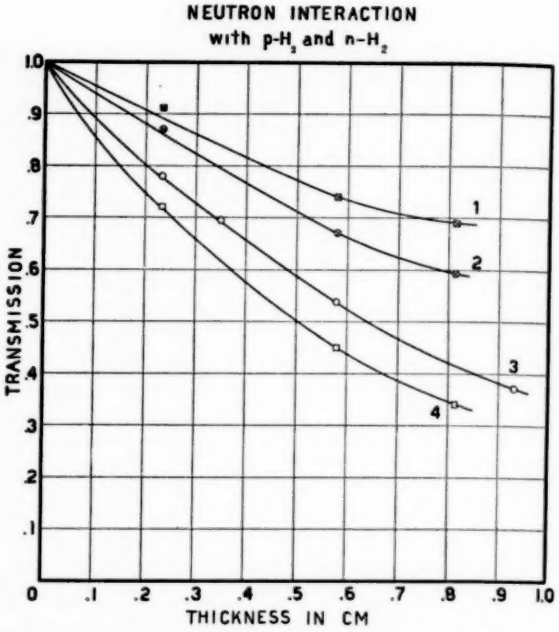

FIG. 1. Transmission of neutrons through liquid *n*- and *p*-H_2. 1, *p*-H_2, ~100°K neutrons; 2, *p*-H_2 ~300°K neutrons; 3, *n*-H_2, ~300°K neutrons; 4, *n*-H_2, ~100°K neutrons.

Several factors warrant further consideration before final conclusions are drawn. Temperature distributions of the neutrons are only roughly Maxwellian. The effect of a long "tail" of high energy neutrons becomes more important at low temperatures. However, on the basis of the theory, the trend of the cross sections as the neutron temperature is lowered (downward for *p*-H_2, upward for *n*-H_2) proves conclusively that spin dependent forces exist. Also the magnitude of the effect shows definitely that the singlet state of the deuteron is virtual. A preliminary reduction of the data for ~300°K neutrons shows the *ortho* cross section to be 2.5 to 3 times the *para* cross section, which is in agreement with the values calculated

TABLE II. *"Filtration" experiments making use of two cells: Passage through the cells was in the order indicated. Neutron temperature ~100°K.*

Composition % *o*-H_2	Cell thickness in cm	Transmission of 2 cell unit	Transmission of 2nd cell for filtered beam from 1st cell	Transmission of 2nd cell alone
6.5 1.4	0.58 0.234	0.690	0.932	0.911
5.9 74.3	0.58 0.234	0.50	0.68	0.72
73.7 16.2	0.58 0.234	0.39	0.87	0.87*
74.2 73.4	0.58 0.234	0.34	0.76	0.72

* Calculated from transmission of 0.014 *o*-H_2.

by Schwinger and Teller on the assumption of a virtual singlet state of the deuteron. The theory predicts p-H_2 to be practically transparent to slow neutrons, although fast ones are strongly scattered. Consequently filtering through liquid p-H_2 should be quite effective in eliminating the high energy tail of a neutron beam. The filtration experiments are in qualitative agreement with this prediction of the theory.

A series of measurements of the neutron-proton cross section, using H_2O, gives an average of 42.2×10^{-24} cm² for 300°K neutrons, and 56.0×10^{-24} cm² for ~100°K neutrons, a ratio of 1.325. Measurements of O and N cross sections using liquid O_2 and N_2, give average values of 4.05 and 12.7×10^{-24} cm², respectively, for 300°K neutrons. A complete description of the experiment and interpretation of the results will appear in a future issue of the *Physical Review*.

The writers desire to express their appreciation to Mr. Julian Schwinger and Professor E. Teller for their cooperation and many helpful suggestions.

J. R. DUNNING
J. H. MANLEY*

Columbia University,
New York, N. Y.

H. J. HOGE
F. G. BRICKWEDDE

National Bureau of Standards,
Washington, D. C.

* Now at the University of Illinois.

[1] Teller, Phys. Rev. **49**, 420 (1936).
[2] Schwinger and Teller, Phys. Rev. **52**, 286 (1937).
[3] Halpern, Estermann, Simpson and Stern, Phys. Rev. **52**, 142 (1937).
[4] Powers, Carroll and Dunning, Phys. Rev. **51**, 1112 (1937).
[5] Scott, Brickwedde, Urey and Wahl, J. Chem. Phys. **3**, 653 (1935).

Diffraction Patterns of Silicon Iron Crystals Oscillating Magnetostrictionally

The question as to whether magnetostriction oscillation of single crystals of magnetic substances would produce effects in their Laue diffraction patterns similar to those observed when crystals such as quartz and tourmaline are excited by piezoelectric oscillation has recently been investigated. Through the courtesy of Dr. S. Dushman of the General Electric Company, we were able to obtain some specimens of silicon iron in the form of strips, approximately 1.5 cm wide, 30 cm long, and of thickness 0.0095, each of which contained several large single crystals of silicon iron. A special holder was built which allowed placing a properly clamped strip in any orientation so that symmetrical Laue pictures could be obtained. Radiation from a broad focus universal tube run at 60 kv and 4 ma produced satisfactory blackening after exposures of ten hours.

The oscillator, which covered quite a range of frequencies in order to match the resonances of strips of different lengths, was of the Hartley type and utilized a type 10 tube. The test strip was coupled to a push-pull amplifier driven by the oscillator through the use of suitable coupling coils. Resonance was indicated by observing the motion of a few grains of sand placed on a small mica plate affixed to one end of the specimen.

Nine sets of corresponding Laue pictures were obtained under conditions as nearly identical as possible. In one picture of each set, the strip was at rest and in the other it was driven magnetostrictionally.

The results, though not as decisive as one might wish, indicate that magnetostriction oscillation acts similar to piezoelectric oscillation. The nine sets of photographs were submitted to the independent judgment of ten persons about the laboratory with the result that eighty percent of the choices indicated the pattern of the oscillating crystal as the more intense.

We tried also the same procedure with some single iron crystals furnished by Dr. P. P. Cioffi of the Bell Laboratories. These were in the form of small wires but of such short lengths that, with the available equipment, it proved impossible to drive them.

G. W. FOX
H. T. HURLEY

Iowa State College,
Ames, Iowa,
October 25, 1937.

The First USSR Cyclotron

By aid of the cyclotron apparatus of the State Radium Institute the first beams of protons (energy 0.5–2.1 Mev) and of hydrogen ions (0.1–1.0 Mev) have been obtained.

The excellent field homogeneity of the especially constructed electromagnet permitted the construction of a chamber with thin bottoms, tightly compressed in vertical position between the poles, and with vacuum between the poles' faces and the bottoms. No corrections of the field by use of shims were required. The chamber's internal diameter is 600 mm, protonic exit radius is 256 mm. In our first experiments it appeared, that the chamber had an accessory ion source, besides that of the glowing filaments. The intensity of proton beam obtained without electron emission of the filament attains some 10^{-9}A. This phenomenon is to be attributed to the hydrogen ionization by the high frequency at maximum voltages, approximately equal to those required for a glow discharge. Our suggestions are supported by a letter to the Editor of your journal by P. Gerald Kruger, G. K. Green, and F. W. Stallmann[1] who also have observed analogous effects, and who suggest a similar explanation.

Of great interest is also the deflection system of our cyclotron. By means of an especially constructed filter system (condensers and RF chokes) there is obtained a shift of the voltage phase between the deflecting plate and the accelerator and a decrease of the gradient arising between them.

In the future the deflecting plate will be placed in the interior of the accelerator. The deflecting potential will be applied with aid of a water-cooled RF resistor. Theoretically this method will be most advantageous because of the partiole beam getting into the deflector exit when the accelerator and the deflecting plate are at equal potentials.

V. N. RUKAVICHNIKOV

The State Radium Institute,
Leningrad, USSR,
October 5, 1937.

[1] P. Gerald Kruger, G. K. Green and F. W. Stallmann, Phys. Rev. **51**, 291 (1937).

Electromagnetic Waves in Conducting Tubes

Leigh Page and N. I. Adams[1] have recently discussed a paper by Carson, Mead and Schelkunoff,[2] and have interpreted the results from an optical point of view. They thus explain the high phase velocity of these waves by regarding them as bundles of a finite or infinite number of "elementary" plane waves traveling with normal phase velocity and bouncing back and forth between the walls of the tube. This interpretation will be illuminating to many physicists.

During the early stages of the investigation I was privileged to discuss such optical analogies with Dr. Thornton C. Fry, whose papers relating to plane waves of light are very well known. These conversations, which followed the line of thought presented by Page and Adams, were helpful at that time, but this method of approach became prohibitively laborious when more complicated problems were taken up. Because of this disadvantage, and also because we had come to believe that the optical ideas were less fundamental than we at first supposed, we adopted the more direct attack presented in the paper referred to above.

This letter records a few observations in addition to those made by Page and Adams. These observations detract somewhat from the *importance* of the optical analogy, but not from its *interest*.

(1) Guided waves in perfectly conducting metal tubes are "plane waves." They differ from the "elementary plane waves" into which Page and Adams resolve them in that the latter have identical intensity and polarization at all points of the wave front, whereas the former do not. As these "elementary" waves cannot be produced in a pure form physically, their importance lies primarily in their mathematical simplicity. We agree that they are "fundamental physically," but not in the sense in which such radiation entities as quanta are. Moreover, an engineer would remark that the generators used by Southworth do not produce elementary waves and then subject them to multiple reflection in the tubes.

(2) Page and Adams confine their discussion to frequencies above the critical frequency. For lower frequencies the guided waves are of such a character that it seems impossible to interpret them as a result of interference between the waves which they call "elementary." This is also true at all frequencies when the guide is dissipative. In such cases it seems necessary to introduce the kind of plane waves which Fry has called "hybrid."[3] These occur in nature on the dark side of a prism within which "elementary plane waves" are being subjected to total internal reflection—a situation in which an interpretation of the hybrid wave as the interference product of elementary waves would be physically artificial. Moreover, since these hybrid waves are already differentiated from elementary waves by the same characteristics as are the waves in tubes (i.e., by an abnormal velocity and an amplitude which is not the same at all points of the wave front) nothing fundamental is achieved by decomposing guided into hybrid waves.

(3) One statement by Page and Adams seems questionable. They state that among tubes of polygonal cross section only those with square, triangular, and hexagonal shapes can transmit guided waves; and that only square tubes can transmit all waves, while the others transmit only waves in which the electric intensity is perpendicular to the axis of the tube but not those in which the magnetic intensity is so disposed. Our method of approach does not suggest that this is so. On the contrary, waves with H perpendicular to the axis of the tube can be transmitted in triangular tubes at least; the appropriate solution was found by Lamé[4] in 1852.

SERGEI A. SCHELKUNOFF

Bell Telephone Laboratories, Inc.,
New York, N. Y.
October 15, 1937.

[1] Leigh Page and N. I. Adams, Jr., Phys. Rev. **52**, 647–651 (1937). See also L. Brillouin, Revue Générale de l'Électricité **40**, 227–239 (1936).
[2] John R. Carson, Sallie P. Mead and S. A. Schelkunoff, Bell Syst. Tech. J. **15**, 310–333 (1936).
[3] Thornton C. Fry, J. O. S. A. and Rev. Sci. Inst. **15**, 137–161 (1927).
[4] M. G. Lamé, *Leçons sur la Théorie Mathématique de L'élasticité des Corps Solides* (1852).